NOTE TO USERS

This reproduction is the best copy available.

UMI®

uOttawa

L'Université canadienne
Canada's university

FACULTÉ DES ÉTUDES SUPÉRIEURES ET POSTDOCTORALES

uOttawa

L'Université canadienne
Canada's university

FACULTY OF GRADUATE AND POSTDOCTORAL STUDIES

Sean Crawford
AUTEUR DE LA THÈSE / AUTHOR OF THESIS

M.Sc. (Biochemistry)
GRADE / DEGREE

Department of Biochemistry, Microbiology and Immunology
FACULTÉ, ÉCOLE, DÉPARTEMENT / FACULTY, SCHOOL, DEPARTMENT

Obsesity-Associated Diabetes, the Human AMPKy3 R225W Mutation and Skeletal Muscle Metabolism

TITRE DE LA THÈSE / TITLE OF THESIS

M-E. Harper
DIRECTEUR (DIRECTRICE) DE LA THÈSE / THESIS SUPERVISOR

CO-DIRECTEUR (CO-DIRECTRICE) DE LA THÈSE / THESIS CO-SUPERVISOR

EXAMINATEURS (EXAMINATRICES) DE LA THÈSE / THESIS EXAMINERS

T. Moon

R. Milne

Gary W. Slater
Le Doyen de la Faculté des études supérieures et postdoctorales / Dean of the Faculty of Graduate and Postdoctoral Studies

Obesity-Associated Diabetes, the Human AMPKγ_3 R225W Mutation and Skeletal Muscle Metabolism

M.Sc. Thesis of Sean A. Crawford

Supervisor: Mary-Ellen Harper, Ph.D.

A thesis submitted to the Faculty of Graduate and

Postdoctoral Studies in partial fulfillment of the

requirements for the degree of Masters of Science, Biochemistry

Department of Biochemistry, Microbiology, and Immunology

University of Ottawa

Ottawa, ON, Canada

© Sean A. Crawford, June 2009

Library and Archives Canada

Published Heritage Branch

395 Wellington Street
Ottawa ON K1A 0N4
Canada

Bibliothèque et Archives Canada

Direction du Patrimoine de l'édition

395, rue Wellington
Ottawa ON K1A 0N4
Canada

Your file Votre référence
ISBN: 978-0-494-59468-1
Our file Notre référence
ISBN: 978-0-494-59468-1

NOTICE:

The author has granted a non-exclusive license allowing Library and Archives Canada to reproduce, publish, archive, preserve, conserve, communicate to the public by telecommunication or on the Internet, loan, distribute and sell theses worldwide, for commercial or non-commercial purposes, in microform, paper, electronic and/or any other formats.

The author retains copyright ownership and moral rights in this thesis. Neither the thesis nor substantial extracts from it may be printed or otherwise reproduced without the author's permission.

AVIS:

L'auteur a accordé une licence non exclusive permettant à la Bibliothèque et Archives Canada de reproduire, publier, archiver, sauvegarder, conserver, transmettre au public par télécommunication ou par l'Internet, prêter, distribuer et vendre des thèses partout dans le monde, à des fins commerciales ou autres, sur support microforme, papier, électronique et/ou autres formats.

L'auteur conserve la propriété du droit d'auteur et des droits moraux qui protège cette thèse. Ni la thèse ni des extraits substantiels de celle-ci ne doivent être imprimés ou autrement reproduits sans son autorisation.

In compliance with the Canadian Privacy Act some supporting forms may have been removed from this thesis.

While these forms may be included in the document page count, their removal does not represent any loss of content from the thesis.

Conformément à la loi canadienne sur la protection de la vie privée, quelques formulaires secondaires ont été enlevés de cette thèse.

Bien que ces formulaires aient inclus dans la pagination, il n'y aura aucun contenu manquant.

Canada

ABSTRACT

The prevalence of obesity and type 2 diabetes mellitus (T2DM) is increasing worldwide at an unprecedented pace. The fundamental understanding of the molecular mechanisms underlying the pathogenesis of these diseases is essential for the development of novel therapeutics. The objective of this work was to characterize skeletal muscle metabolism of obese subjects with a history of T2DM and that of subjects carrying the AMP-activated protein kinase (AMPK) γ_3 R225W mutation. Primary myotubes from obese subjects with a history of T2DM showed defects in mitochondrial biogenesis, oxidative capacity and in mechanisms known to mitigate oxidative stress. Conversely, primary myotubes from subjects carrying the AMPKγ_3 R225W mutation had elevated mitochondrial content and oxidative capacity relative to matched controls. R225W carriers also showed evidence of increased muscle glucose uptake *in vivo* and *in vitro,* leading to the conclusion that AMPKγ_3 may represent an effective novel pharmaceutical target for treatment of T2DM.

ACKNOWLEDGEMENTS

I would like to thank my supervisor, Dr. Mary-Ellen Harper, for her fantastic support and guidance throughout my time here at the University of Ottawa. She has provided me with enormous research opportunities and instilled in me a passion for research that I will always hold. I would also like to thank Dr. Sheila Costford for the tremendous amount of work that she has contributed to this project as well as for her excellent mentorship and guidance throughout my graduate studies. Finally, I would like to thank everyone in the Mitochondrial Bioenergetics Laboratory for their support, especially Mahmoud Salkhordeh, Linda Jui and Jian Xuan for their remarkable technical support throughout my studies.

MITOCHONDRIAL BIOENERGETICS LABORATORY

SUPERVISOR

Dr. Mary-Ellen Harper

CURRENT LABORATORY MEMBERS

Cyril Adjeitey
Dr. Céline Aguer
Mark Bastianelli
Brittany Beauchamp
Carmen Estey
Adrienne Gowing
Linda Jui
Dr. Ryan Mailloux
Cynthia Moffat
Marisa Rossi
Mahmoud Salkhordeh
Dr. Erin Seifert
Jian Xuan

PREVIOUS LABORATORY MEMBERS

Shehla Chaudhry
Dr. Sheila Costford
Meredith Evans
Benny Hill
Samantha Prevost
Neha Sarna

I would also like to thank all of our collaborators at the University of Ottawa Heart Institute, the Ottawa Hospital Weight Management Clinic and the School of Human Kinetics at the University of Ottawa. Without all of the time and effort these individuals contributed, these studies would not have been possible.

University of Ottawa Heart Institute

Dr. Robert Beanlands
Dr. Jean da Silva
Dr. Rob deKemp
Dr. Ruth McPherson
Heather Doelle
Ed Gannon
Kimberly Gardner
Michaela Garkisch
Sybil Hebert
Linda Garrard
Stephanie Thorn

Ottawa Hospital Weight Management Clinic

Dr. Robert Dent
Brenda Bradley

University of Ottawa – School of Human Kinetics

Dr. Marshall Kendall
Dr. Dany Lafontiane
Dr. Mario Lamontagne
Stéfanie Pagé

Pennington Biomedical Research Center

Dr. Sheila Costford
Dr. Steve Smith
Shantele Thomas

Chapter 1 - TABLE OF CONTENTS

LIST OF ABBREVIATIONS

ACC – acetyl-CoA carboxylase
ADA – American Diabetes Association
AICAR – aminoimidazole carboxamide ribonucleotide
AMPK – adenosine monophospate-activated protein kinase
aPKC – atypical protein kinase
BCA – bicinchoninic acid
BMI – body mass index
CBM – glycogen binding domain
CDA – Canadian Diabetes Association
CNTF – ciliary neurotrophic factor
CoA – coenzyme A
COX-1 – cytochrome c oxidase, subunit 1
CPT-1 – carnitinepalmitoyl-transferase-1
CRE – cAMP-responsive element
CRTC2 – CRE-binding protein transcription coactivator 2
CytC – cytochrome c
DAG – diacylglycerol
EMG – electromyography
ETC - electron transport chain
ETC – electron transport chain
FAO – fatty acid oxidation
FFA – free fatty acids
FOXO1 – fork-head box O1
FU – fluorescent units
G6Pase – glucose-6-phosphatase
GLUT3 – glucose transporter 4
HGI – high glucose and insulin
HNE – 4-hydroxy-2-nonenal
HPLC – high performance liquid chromatography
HSL – hormone sensitive lipase
IDV – integrated density value
IMTG – intramuscular triglyceride
IR – insulin receptor
IRS-1 – insulin receptor substrate-1
LGI – low glucose and insulin
mnSOD – manganese superoxide dismutase
mTFA – mitochondrial transcription factor A
mTFA – mitochondrial transcription factor A
NRF-1 – nuclear respiratory factor 1
NRF-1 – nuclear respiratory factor 1
NS – not significant

p-AMPK – phospho-AMP-activated protein kinase
PDK1 – phosphoinositide dependent kinase-1
PEPCK – phosphoenolpyruvate carboxykinase
PET – positron emission tomography
PGC-1α – peroxisome proliferator gamma coactivator1α
$PI(3,4,5)P_3$ – phosphatidylinositol (3,4,5)-triphosphate
PI3K – phosphoinositide 3-kinase
PKCζ – protein kinase C-zeta
PKCθ – protein kinase C-theta
Post-DM – post-diabetes mellitus
PP2A – protein phosphatase 2A
ROS - reactive oxygen species
RPLP0 – ribosomal protein large, P0
SDH – succinate dehydrogenase
SUV – standard uptake value
T1DM – type 1 diabetes mellitus
T2DM – type 2 diabetes mellitus
TAG – triglyceride
TCA – tricarboxylic acid
TMRE – tetramethylrhodamine, ethyl ester, perchlorate
UCP3 – uncoupling protein-3
WHO – World Health Organization
WPW – Wolff-Parkinson White

Chapter 2 - LIST OF FIGURES

Chapter 3 - LIST OF TABLES

General Introduction

Obesity

The World Health Organization (WHO) defines obesity as an "abnormal or excessive fat accumulation that presents a risk to health" (1). Obesity is now reported to be the sixth most important risk factor contributing to the overall burden of disease worldwide (2, 3), and the WHO has predicted that in the next few years, non-communicable diseases such as obesity will become the leading cause of mortality (4). At the most fundamental level, obesity is an imbalance between caloric intake and energy expenditure. While this imbalance primarily stems from energy dense diets and a lack of physical activity, numerous genetic and environmental factors contribute to the regulation of energy intake and expenditure. The WHO defines obesity in terms of the Body Mass Index (BMI), or an individual's weight (kg) divided by their height squared (m^2). An individual is considered obese with a BMI of ≥ 30 kg/m^2, overweight with a BMI of 25-29.9, normal with a BMI of 18.5-24.9, and underweight with a BMI of <18.5.

In the most recent Canadian survey (2004), 59% of Canadian adults aged 24-60 and 28% of Canadian children aged 7-13 were either overweight or obese (5). The prevalence of obesity in Canada has progressively increased since 1972, and has more than doubled in the last two decades (6). The increasing prevalence of obesity however is not unique to Canada: more than 1.7 billion individuals world-wide are either overweight or obese (7).

Obesity is a major risk factor for many chronic diseases including cardiovascular disease, colon cancer, post menopausal breast cancer, osteoarthritis, and type 2 diabetes mellitus (T2DM) (reviewed in (8)). The resulting economic burden of this growing obesity 'epidemic' has been estimated at upwards of 5.3 billion dollars annually in Canada, which is 2.6% of our total health care costs (9, 10).

DIABETES MELLITUS

The incidence of diabetes mellitus (type 1 or type 2, see below) is rapidly increasing worldwide. It is estimated that in 1985, 30 million people were afflicted with diabetes. Today the WHO estimates that 176 million people worldwide have diabetes. Indeed, diabetes is quickly becoming one of the greatest health challenges facing our society: the WHO predicts that by the year 2030, 366 million people worldwide will be suffering from the disease (11). Over 2 million Canadians currently have diabetes and this number is expected to surpass 3 million by 2010 (Canadian Diabetes Association; CDA).

Diabetes mellitus is a disease characterized primarily by hyperglycemia resulting from either a lack of insulin secretion (type 1) or from the development of insulin resistance followed by pancreatic β-cell failure (type 2). Type 1 diabetes mellitus (T1DM), an autoimmune disorder, represents approximately 10% of diabetes mellitus cases; whereas type 2 diabetes mellitus (T2DM), often developed in association with obesity, represents 90% of diabetes mellitus cases (WHO).

T2DM is a metabolic disorder characterized by insulin resistance (the inability of insulin to suppress hepatic glucose production and promote peripheral glucose uptake) and

subsequently the inability of the pancreatic β-cell to secrete sufficient insulin to counteract the insulin resistance. Obesity is the primary risk factor for T2DM; among adults diagnosed with T2DM, 54% are obese (BMI ≥ 30), 31% are overweight (25 ≤ BMI < 30), and only 15% have a normal BMI (18.5 ≤ BMI < 25) (9). Failure to maintain normal glycemic control in individuals with diabetes mellitus eventually results in a deleterious decline of organ function causing retinopathy, neuropathy, kidney failure, heart disease and stroke. The annual economic cost of diabetes related health care in Canada is estimated to be 6.5 billion dollars, and is expected to increase to 8.1 billion dollars with the increasing prevalence of T2DM (12).

Molecular Pathology of Type 2 Diabetes Mellitus

The primary cause of T2DM is unknown; however, insulin resistance has been demonstrated in nearly all cases of T2DM (13, 14). Insulin resistance has been shown to be the best predictor of the development of the disease (15), and prospective studies have been able to identify insulin resistance up to two decades prior to the onset of T2DM (16).

The major insulin resistant organs involved the pathogenesis of T2DM are liver, skeletal muscle, and adipose tissue. Skeletal muscle makes up on average 42% of the human body weight and accounts for ~20% total body energy expenditure at rest, which increases dramatically with exercise (17). Skeletal muscle is the primary source of peripheral glucose disposal in humans, accounting for 80% of postprandial glucose disposal (18). As a result, skeletal muscle is considered the primary site of insulin resistance in T2DM and plays a

tremendous role in maintenance of normoglycemia. However, the mechanism(s) underlying the development of insulin resistance have yet to be fully elucidated.

In the healthy insulin-sensitive state, the action of insulin binding to the insulin receptor in skeletal muscle initiates a signaling cascade that ultimately results in the translocation of glucose transporter 4 (GLUT4) to the plasma membrane, allowing for increased glucose uptake (Figure 0-1). While insulin signaling is a complex process with many levels of regulation, the best characterized pathway begins with insulin inducing a conformational change in the insulin receptor (IR), activating its intrinsic tyrosine kinase activity (19). The activated IR then phosphorylates and activates insulin receptor substrate-1 (IRS-1) (20), which complexes to phosphoinositide 3-kinase (PI3K) via an SH2 domain and catalyzes the formation of phosphatidylinositol (3,4,5)-triphosphate ($PI(3,4,5)P_3$) (21, 22). The formation of the $PI(3,4,5)P_3$ within the plasma membrane results in recruitment and activation of Akt and atypical protein kinase C (aPKC) by phosphoinositide dependent kinase-1 (PDK1)(23, 24). While it has been demonstrated that the activation of Akt and aPKC is required for the translocation of GLUT4 to the plasma membrane, the mechanism by which this is accomplished is not well understood (25, 26).

In healthy individuals, when caloric intake exceeds energy expenditure, excess energy is stored primarily in the form of triglycerides (TAG) within adipocytes. Adipose tissue plays a crucial role in buffering energy levels between the fed and fasted state; however, a chronic positive energy balance results in weight gain and ultimately obesity. In the case of obesity, adipose storage nears maximal capacity and its ability to continue to store excess

Figure 0-1: Insulin signaling pathway. IRS-1 (insulin receptor substrate-1); PI3K (phosphoinositol-3-kinase); PIP3 (phosphoinositol (3,4,5)-triphosphate); PDK1 (phosphoinositide dependent kinase-1); DAG (Diacylglycerol); GLUT (glucose transporter-4)

Figure 0-1: Insulin signaling pathway

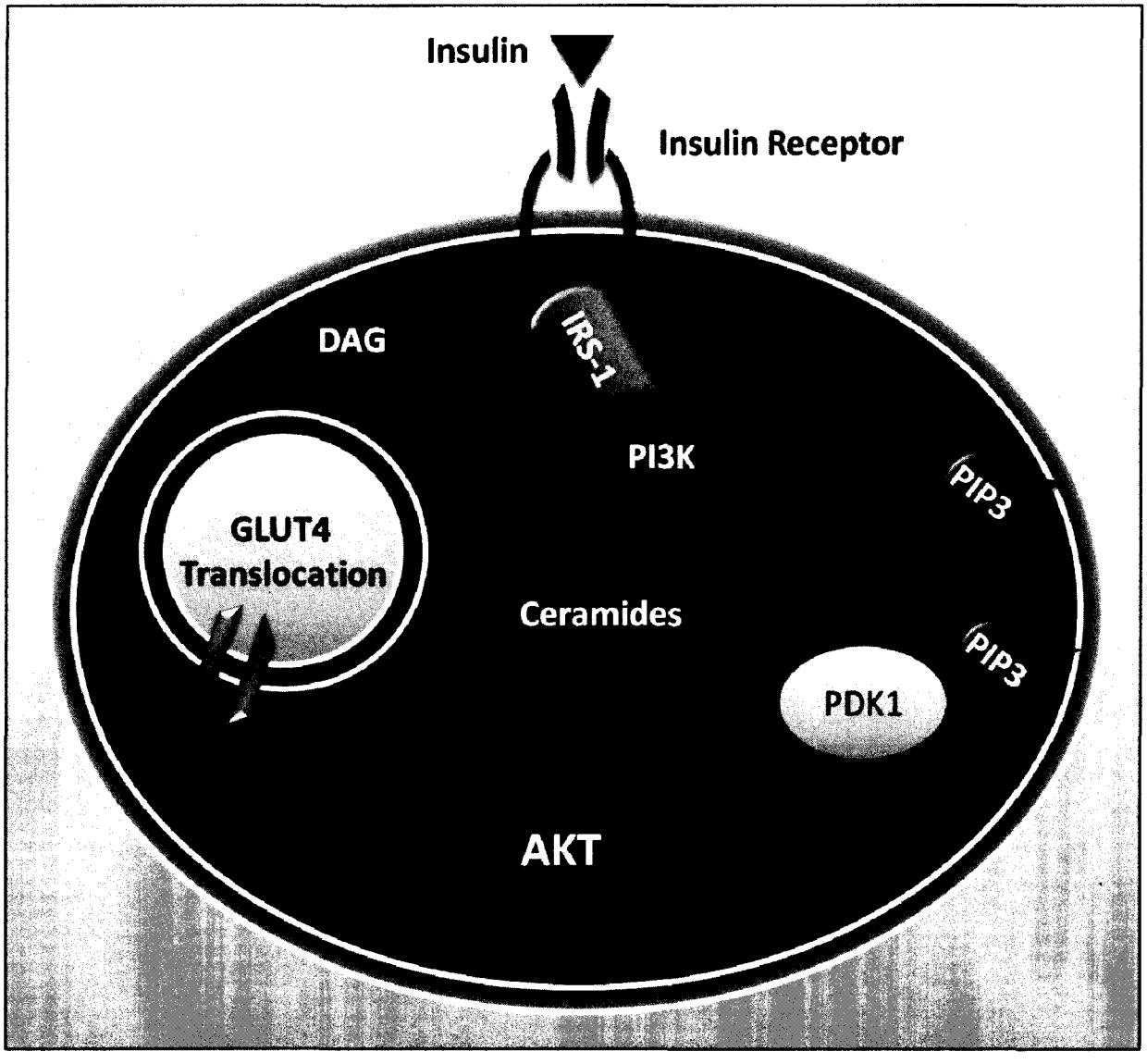

triglycerides is reduced (reviewed in (27)). The resulting overflow of TAG, especially in the post-prandial state, exposes other organs and tissues to a surplus of fatty acids (FA), which can lead to ectopic lipid storage (28). Several studies have linked ectopic lipid accumulation in non-adipose tissues such as skeletal muscle (29-31), pancreas (32), and liver (33) to insulin-resistance.

Lipid accumulation in skeletal muscle, referred to as intramuscular triglyceride (IMTG), is highly correlated with the development of insulin resistance (34-36). However, whether this increase in IMTG is related to increases in fatty acid uptake or the impairment of fatty acid oxidation remains controversial. Kelley *et al.* reported that obese subjects had reduced fatty acid oxidation but similar free fatty acid (FFA) uptake levels, suggesting that it may in fact be the impairment of fatty acid oxidation that leads to IMTG accumulation and not elevated FA uptake (37). Interestingly, elevated IMTG levels are also observed in insulin-sensitive endurance trained athletes; therefore, it is likely not the accumulation of IMTG, but an incomplete or reduced metabolism of these lipids that induces insulin resistance (38-40).

It has been proposed that the metabolic overflow of TAG results in reductions in fatty acid oxidation (FAO) and subsequently an uncoupling of the TCA cycle and the electron transport chain (ETC), which ultimately results in the incomplete oxidation of FAs (41, 42). Specifically, it has been identified that the lipid products ceramide and diacylglycerol (DAG) are not only elevated in individuals with insulin resistance, but also capable of interfering and blocking the insulin signaling pathway (43-46). Ceramides are thought to activate

protein phosphatase 2A (PP2A), which dephosphorylates and inactivates Akt, resulting in the inhibition of GLUT4 translocation (47-50). Additionally, several studies have reported that ceramides activate protein kinase C-zeta (PKCζ), resulting in the inactivation of Akt through the phosphorylation its PH-domain (51, 52). Finally, numerous studies support a role for DAG in inhibition of GLUT4 translocation through the inhibition of IRS-1 through protein kinase C-theta (PKCθ) (42, 53-58).

A second major hallmark of T2DM is mitochondrial dysfunction and reduced mitochondrial biogenesis. Mitochondrial proteins are encoded by both the nuclear and mitochondrial genome. Mitochondrial biogenesis occurs primarily through a peroxisome proliferator-activated receptor γ coactivator 1-α (PGC1-α)-dependent pathway. In a healthy state, external stimuli (*i.e.,* exercise) can induce and activate the transcription factor PGC-1α, which in turn increases the expression of its target genes, including NRF-1 (nuclear respiratory factor 1). NRF-1 regulates the expression of numerous genes encoding mitochondrial proteins, including succinate dehydrogenase (SDH), cytochrome c (CytC), and ATP synthase. Finally, activation of mitochondrial transcription factor A (mTFA), results in the increased transcription and replication of mitochondrial DNA (reviewed in (59)). With sufficient stimuli, this cascade ultimately results in mitochondrial biogenesis.

Decreased mitochondrial content was initially identified in individuals with T2DM and in young insulin-resistant offspring of individuals with T2DM (55, 60-62). Although further work is needed, these studies suggest that insulin-resistant offspring of subjects with T2DM may have an inherited condition predisposing them to a reduced mitochondrial biogenesis,

which in turn may result in the accumulation of IMTG (reviewed in (63)). The molecular mechanisms underlying this defect in mitochondrial biogenesis are poorly understood. While it has been reported that elderly obese individuals with T2DM exhibit decreased expression of genes encoded by PGC-1α (64, 65), no decreases in PGC-1α, mTFA, or NRF-1 expression have been observed in the lean, insulin-resistant offspring of individuals with T2DM (55).

Treatment of Type 2 Diabetes Mellitus

Diabetes is a chronic condition that requires careful management in order to avoid both short- and long- term complications. Current treatments for T2DM usually consist of a combination of medical and nutritional management, physical activity, pharmacotherapy, and treatment of hypertension and dyslipidemia. The American Diabetes Association (ADA) currently recommends that individuals diagnosed or at high risk for the development of T2DM undertake structured programs that emphasize lifestyle modification with targeted goals of moderate weight loss (5-10%) and regular physical activity (30 min/day). Numerous oral pharmacotherapies are available for the treatment of T2DM, some of which include metformin, sulfonylureas, DPP-4 inhibitors, PPARγ agonists, α-glucosidase inhibitors, insulin, and GLP-1 analogs(66). Metformin, rosiglitazone, and pioglitazone are all thought to be indirect activators of AMP-activated protein kinase (AMPK; (67-70)). While activation of AMPK in the liver and skeletal muscle is thought to suppress hepatic glucose production and promote skeletal muscle glucose uptake, respectively there are negative consequences

of chronically activating AMPK in other organs (such as the heart and the brain), suggesting the need for tissue-specific activators of AMPK.

AMP- Activated Protein Kinase

AMPK was first identified in 1973 as an activator of two important enzymes involved in liver fat metabolism: 3-hydroxy-3-methylglutaryl coenzyme A (CoA) reductase (71) and acetyl-CoA carboxylase (ACC) (72). It was later named AMPK for its observed responsiveness to AMP levels following alterations in the cellular energy state (73-75). Over the last two decades, AMPK has been the subject of extensive investigation for its role in glucose and lipid metabolism (76-78), mitochondrial biogenesis (79, 80), and regulation of protein and gene expression (81). In recent years, AMPK has emerged as an important regulator of energy metabolism at both the cellular and whole body levels (Figure 0-2)

AMPK action in hypothalamic neurons is capable of bridging the gap between metabolic status and the neuro-peptide/transmitter systems that regulate feeding (reviewed in (82)). Fasting has been shown to increase AMPK activity, where as re-feeding has been shown to inhibit AMPK activity. Similarly, activation of AMPK in the hypothalamus increases food intake resulting in weight gain, while inhibition of AMPK promotes hypophagia resulting in weight loss (83, 84). AMPK is thought to coordinate this response through the modulation of carnitinepalmitoyl-transferase-1 (CPT-1) activation within the cell. Active AMPK is capable of phosphorylating and inactivating ACC, the rate limiting enzyme in the synthesis of malonyl-CoA (85). The subsequent reduction in malonyl CoA levels stimulates CPT-1 activity, which has previously been shown to increase food intake (84, 86).

Figure 0-2: AMPK function in different tissues of the body. Green – activated pathways Red – inactivated pathways.

Figure 0-2: AMPK function in different tissues of the body

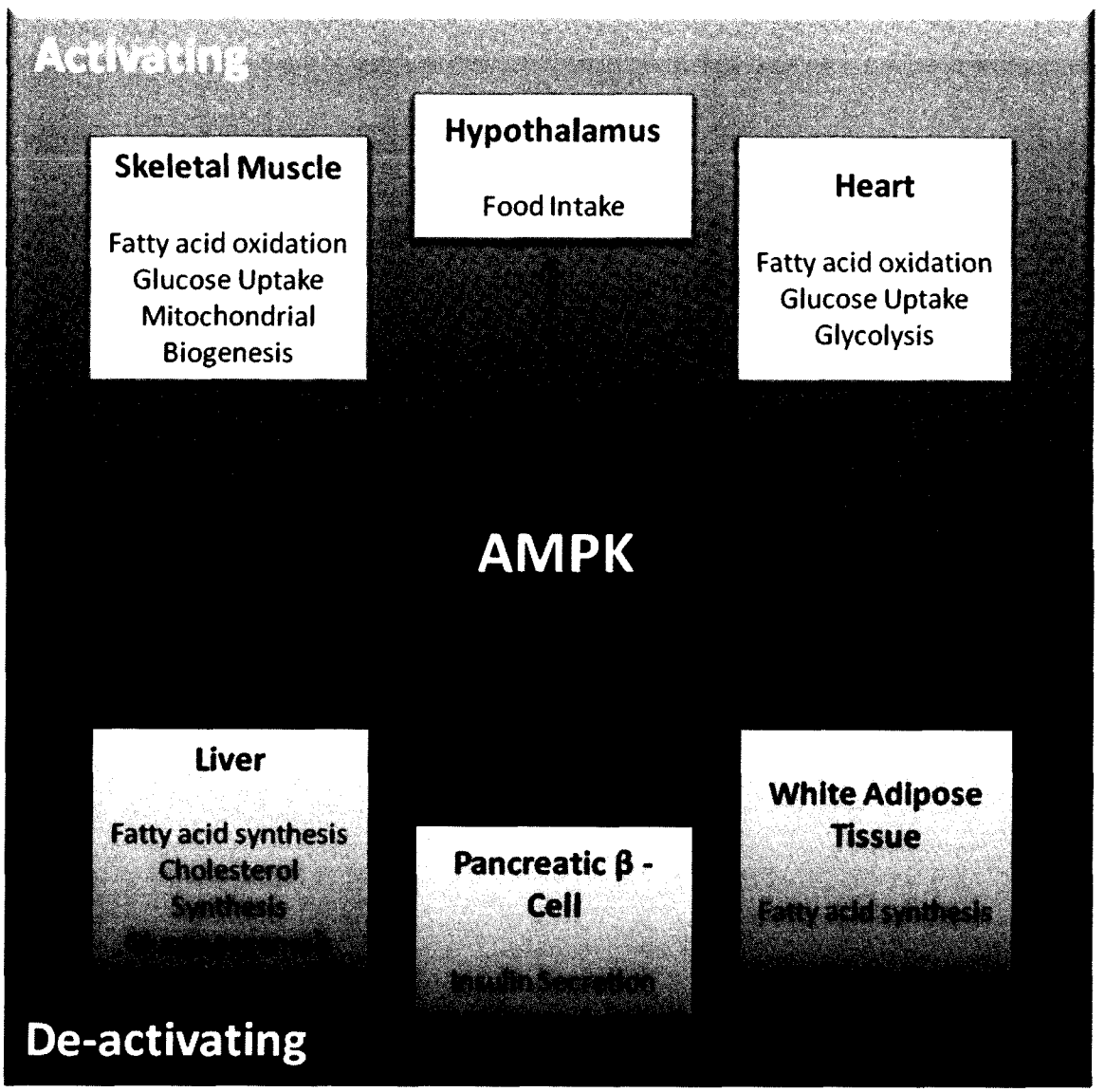

In the heart, AMPK activation primarily results in increased fatty acid oxidation and glucose uptake; however chronic induction of AMPK can have negative consequences which are thought to play a role in the development of Wolff-Parkinson-White (WPW) syndrome (87). WPW is characterized by a cardiac conduction system defect, the exact genetic basis for the majority of patients with WPW are not understood; however, a mutation (R302Q) in the

AMPKγ2 subunit is associated with a small percentage of patients affected by the syndrome (87). Similar to the effects of the R225W AMPKγ3 mutation in skeletal muscle (88), the R302Q mutation results in elevated glucose uptake and glycogen storage in the heart, leading to cardiac hypertrophy and conduction defects (89-91). It has been hypothesized that the increased risk of myocardial infarction associated with rosiglitazone treatment is associated with elevated AMPK activity in the heart (92, 93).

The effects of AMPK on the pancreatic islets and adipose tissue are not well understood. Evidence suggests that AMPK activation in both human islets and MIN6 β-cells results in an inhibition of insulin secretion (94), whereas other research has shown that the expression of a constitutively active form of AMPK in MIN6 β-cells and CD1 pancreatic islet cells induced apoptosis (95). Classically, it was believed that activation of AMPK in adipose tissue resulted in the inhibition of lipolysis through the phosphorylation of hormone-sensitive lipase (HSL) (96-98); however, more recent evidence has demonstrated that AMPK is in fact required for the activation of lipolysis in 3T3-L1 cells (99). Interestingly, another recent study has reported that AMPK phosphorylation of HSL actually stimulates lipolysis in isolated adipocytes (100).

Of most interest, given the rising incidence of diabetes worldwide, is the role for AMPK activation in countering liver and skeletal muscle insulin resistance through the control of glucose and lipid homeostasis. AMPK-mediated glucose homeostasis in the liver occurs through the suppressed expression of gluconeogenic genes, such as PEPCK (phosphoenolpyruvate carboxykinase) and G6Pase (glucose-6-phosphatase), which are regulated by a cAMP-responsive element (CRE). This is accomplished through the suppression of transcription factors that bind the CRE, namely CRTC2 (CRE-binding protein transcription coactivator 2) and FOXO1 (fork-head box O1). In skeletal muscle, AMPK contributes to glucose homeostasis through the enhancement of glucose uptake via an as of yet unidentified insulin-independent pathway.

Activation of AMPK in both liver and skeletal muscle results in the enhancement of FAO and the suppression of lipogenesis. Similar to the hypothalamus, AMPK phosphorylates and inactivates ACC and ACC2, the rate-determining enzymes in the synthesis of malonyl-CoA, an inhibitor of fatty acid oxidation and an essential precursor for fatty acid synthesis. Additionally, AMPK can activate malonyl-CoA decarboxylase to further reduce malonyl-CoA levels.

SUMMARY

As the prevalence of obesity, T2DM, and other non-communicable diseases continues to rise world-wide, there is a pressing need to understand the molecular basis and pathology of these diseases in order to develop novel therapies and treatment strategies. The next two chapters of this thesis will 1) characterize the skeletal muscle metabolism of subjects

with a history of obesity-associated T2DM and the effect of chronic high glucose and insulin in primary myotubes from these subjects, and 2) characterize the skeletal muscle metabolism of subjects carrying the AMPKγ3 R225W mutation.

While there is a significant amount of literature detailing the defects in skeletal muscle observed in individuals with type 2 diabetes, it is not known whether or not these defects persist following weight loss and whether or not there are fundamental defects in the skeletal muscle satellite cells. Chapter 1 begins to answer these questions by determining if impaired metabolism could be detected in primary muscle cells of subjects with a history of obesity-associated T2DM. Although no differences in oxidative capacity or oxidative damage were detected under standard low glucose and insulin conditions, cells were unable to undergo mitochondrial biogenesis and had an increased susceptibility to oxidative damage when exposed to chronic high glucose and insulin conditions. These novel findings define a muscle phenotype at risk for obesity-associated T2DM, and set the stage for future explorations.

The AMPKγ3 R225W mutation is the first gain-of-function mutation that has been identified in the gamma-3 subunit in humans. The findings reported in Chapter 2 begin to characterize the metabolic phenotype associated with the chronic activation of AMPK in skeletal muscle. Primary myotubes from subjects carrying the AMPKγ_3 R225W mutation had elevated mitochondrial content and oxidative capacity relative to matched controls. In addition, R225W carriers also showed evidence of increased muscle glucose uptake *in vivo*

and *in vitro*, leading to the conclusion that AMPKγ_3 may represent an novel pharmaceutical target for the control of hyperglycemia and the treatment of T2DM.

REFERENCES

1. Organization, W.H. 2006. Fact sheet N311 - Obesity and overweight. In.
2. Haslam, D.W., and W.P. James. 2005. Obesity. *Lancet* 366:1197-1209.
3. Ezzati, M., A.D. Lopez, A. Rodgers, S. Vander Hoorn, and C.J. Murray. 2002. Selected major risk factors and global and regional burden of disease. *Lancet* 360:1347-1360.
4. Organization, W.H. 1997. The World Health Report 1997 -- conquering suffering, enriching humanity. *World Health Forum*
5. Canada, S. 2004. Canadian Community Health Survey. In.
6. Katzmarzyk, P.T. 2002. The Canadian obesity epidemic, 1985-1998. *CMAJ* 166:1039-1040.
7. James, P.T., N. Rigby, and R. Leach. 2004. The obesity epidemic, metabolic syndrome and future prevention strategies. *Eur J Cardiovasc Prev Rehabil* 11:3-8.
8. Kopelman, P.G. 2000. Obesity as a medical problem. *Nature* 404:635-643.
9. Katzmarzyk, P.T., and I. Janssen. 2004. The economic costs associated with physical inactivity and obesity in Canada: an update. *Can J Appl Physiol* 29:90-115.
10. Birmingham, C.L., J.L. Muller, A. Palepu, J.J. Spinelli, and A.H. Anis. 1999. The cost of obesity in Canada. *CMAJ* 160:483-488.
11. Wild, S., G. Roglic, A. Green, R. Sicree, and H. King. 2004. Global prevalence of diabetes: estimates for the year 2000 and projections for 2030. *Diabetes Care* 27:1047-1053.
12. Ohinmaa, A., Jacobs P., Simpson, S, Johnson J. 2004. The Projection of Prevalence and Cost of Diabetes in Canada: 2000 to 2016. *Canadian Journal of Diabetes* 28:
13. Lillioja, S., D.M. Mott, B.V. Howard, P.H. Bennett, H. Yki-Jarvinen, D. Freymond, B.L. Nyomba, F. Zurlo, B. Swinburn, and C. Bogardus. 1988. Impaired glucose tolerance as a disorder of insulin action. Longitudinal and cross-sectional studies in Pima Indians. *N Engl J Med* 318:1217-1225.
14. DeFronzo, R.A., R.C. Bonadonna, and E. Ferrannini. 1992. Pathogenesis of NIDDM. A balanced overview. *Diabetes Care* 15:318-368.
15. Warram, J.H., B.C. Martin, A.S. Krolewski, J.S. Soeldner, and C.R. Kahn. 1990. Slow glucose removal rate and hyperinsulinemia precede the development of type II diabetes in the offspring of diabetic parents. *Ann Intern Med* 113:909-915.
16. Lillioja, S., D.M. Mott, M. Spraul, R. Ferraro, J.E. Foley, E. Ravussin, W.C. Knowler, P.H. Bennett, and C. Bogardus. 1993. Insulin resistance and insulin secretory dysfunction as precursors of non-insulin-dependent diabetes mellitus. Prospective studies of Pima Indians. *N Engl J Med* 329:1988-1992.
17. Rolfe, D.F., and G.C. Brown. 1997. Cellular energy utilization and molecular origin of standard metabolic rate in mammals. *Physiol Rev* 77:731-758.
18. Ferrannini, E., J.D. Smith, C. Cobelli, G. Toffolo, A. Pilo, and R.A. DeFronzo. 1985. Effect of insulin on the distribution and disposition of glucose in man. *J Clin Invest* 76:357-364.

19. Ottensmeyer, F.P., D.R. Beniac, R.Z. Luo, and C.C. Yip. 2000. Mechanism of transmembrane signaling: insulin binding and the insulin receptor. *Biochemistry* 39:12103-12112.
20. Voliovitch, H., D.G. Schindler, Y.R. Hadari, S.I. Taylor, D. Accili, and Y. Zick. 1995. Tyrosine phosphorylation of insulin receptor substrate-1 in vivo depends upon the presence of its pleckstrin homology region. *J Biol Chem* 270:18083-18087.
21. Downes, C.P., A. Gray, and J.M. Lucocq. 2005. Probing phosphoinositide functions in signaling and membrane trafficking. *Trends Cell Biol* 15:259-268.
22. Myers, M.G., Jr., J.M. Backer, X.J. Sun, S. Shoelson, P. Hu, J. Schlessinger, M. Yoakim, B. Schaffhausen, and M.F. White. 1992. IRS-1 activates phosphatidylinositol 3'-kinase by associating with src homology 2 domains of p85. *Proc Natl Acad Sci U S A* 89:10350-10354.
23. Filippa, N., C.L. Sable, B.A. Hemmings, and E. Van Obberghen. 2000. Effect of phosphoinositide-dependent kinase 1 on protein kinase B translocation and its subsequent activation. *Mol Cell Biol* 20:5712-5721.
24. Bandyopadhyay, G., M.L. Standaert, M.P. Sajan, L.M. Karnitz, L. Cong, M.J. Quon, and R.V. Farese. 1999. Dependence of insulin-stimulated glucose transporter 4 translocation on 3-phosphoinositide-dependent protein kinase-1 and its target threonine-410 in the activation loop of protein kinase C-zeta. *Mol Endocrinol* 13:1766-1772.
25. Berwick, D.C., G.C. Dell, G.I. Welsh, K.J. Heesom, I. Hers, L.M. Fletcher, F.T. Cooke, and J.M. Tavare. 2004. Protein kinase B phosphorylation of PIKfyve regulates the trafficking of GLUT4 vesicles. *J Cell Sci* 117:5985-5993.
26. Braiman, L., A. Alt, T. Kuroki, M. Ohba, A. Bak, T. Tennenbaum, and S.R. Sampson. 2001. Activation of protein kinase C zeta induces serine phosphorylation of VAMP2 in the GLUT4 compartment and increases glucose transport in skeletal muscle. *Mol Cell Biol* 21:7852-7861.
27. Goossens, G.H. 2008. The role of adipose tissue dysfunction in the pathogenesis of obesity-related insulin resistance. *Physiol Behav* 94:206-218.
28. Frayn, K.N. 2001. Adipose tissue and the insulin resistance syndrome. *Proc Nutr Soc* 60:375-380.
29. Forouhi, N.G., G. Jenkinson, E.L. Thomas, S. Mullick, S. Mierisova, U. Bhonsle, P.M. McKeigue, and J.D. Bell. 1999. Relation of triglyceride stores in skeletal muscle cells to central obesity and insulin sensitivity in European and South Asian men. *Diabetologia* 42:932-935.
30. Jacob, S., J. Machann, K. Rett, K. Brechtel, A. Volk, W. Renn, E. Maerker, S. Matthaei, F. Schick, C.D. Claussen, and H.U. Haring. 1999. Association of increased intramyocellular lipid content with insulin resistance in lean nondiabetic offspring of type 2 diabetic subjects. *Diabetes* 48:1113-1119.
31. Pan, D.A., S. Lillioja, A.D. Kriketos, M.R. Milner, L.A. Baur, C. Bogardus, A.B. Jenkins, and L.H. Storlien. 1997. Skeletal muscle triglyceride levels are inversely related to insulin action. *Diabetes* 46:983-988.

32. Koyama, K., G. Chen, Y. Lee, and R.H. Unger. 1997. Tissue triglycerides, insulin resistance, and insulin production: implications for hyperinsulinemia of obesity. *Am J Physiol* 273:E708-713.
33. Banerji, M.A., M.C. Buckley, R.L. Chaiken, D. Gordon, H.E. Lebovitz, and J.G. Kral. 1995. Liver fat, serum triglycerides and visceral adipose tissue in insulin-sensitive and insulin-resistant black men with NIDDM. *Int J Obes Relat Metab Disord* 19:846-850.
34. Phillips, D.I., S. Caddy, V. Ilic, B.A. Fielding, K.N. Frayn, A.C. Borthwick, and R. Taylor. 1996. Intramuscular triglyceride and muscle insulin sensitivity: evidence for a relationship in nondiabetic subjects. *Metabolism* 45:947-950.
35. Perseghin, G., P. Scifo, F. De Cobelli, E. Pagliato, A. Battezzati, C. Arcelloni, A. Vanzulli, G. Testolin, G. Pozza, A. Del Maschio, and L. Luzi. 1999. Intramyocellular triglyceride content is a determinant of in vivo insulin resistance in humans: a 1H-13C nuclear magnetic resonance spectroscopy assessment in offspring of type 2 diabetic parents. *Diabetes* 48:1600-1606.
36. Krssak, M., K. Falk Petersen, A. Dresner, L. DiPietro, S.M. Vogel, D.L. Rothman, M. Roden, and G.I. Shulman. 1999. Intramyocellular lipid concentrations are correlated with insulin sensitivity in humans: a 1H NMR spectroscopy study. *Diabetologia* 42:113-116.
37. Kelley, D.E., B. Goodpaster, R.R. Wing, and J.A. Simoneau. 1999. Skeletal muscle fatty acid metabolism in association with insulin resistance, obesity, and weight loss. *Am J Physiol* 277:E1130-1141.
38. Goodpaster, B.H., J. He, S. Watkins, and D.E. Kelley. 2001. Skeletal muscle lipid content and insulin resistance: evidence for a paradox in endurance-trained athletes. *J Clin Endocrinol Metab* 86:5755-5761.
39. Tarnopolsky, M.A., C.D. Rennie, H.A. Robertshaw, S.N. Fedak-Tarnopolsky, M.C. Devries, and M.J. Hamadeh. 2007. Influence of endurance exercise training and sex on intramyocellular lipid and mitochondrial ultrastructure, substrate use, and mitochondrial enzyme activity. *Am J Physiol Regul Integr Comp Physiol* 292:R1271-1278.
40. van Loon, L.J., R. Koopman, R. Manders, W. van der Weegen, G.P. van Kranenburg, and H.A. Keizer. 2004. Intramyocellular lipid content in type 2 diabetes patients compared with overweight sedentary men and highly trained endurance athletes. *Am J Physiol Endocrinol Metab* 287:E558-565.
41. Hulver, M.W., J.R. Berggren, R.N. Cortright, R.W. Dudek, R.P. Thompson, W.J. Pories, K.G. MacDonald, G.W. Cline, G.I. Shulman, G.L. Dohm, and J.A. Houmard. 2003. Skeletal muscle lipid metabolism with obesity. *Am J Physiol Endocrinol Metab* 284:E741-747.
42. Yu, C., Y. Chen, G.W. Cline, D. Zhang, H. Zong, Y. Wang, R. Bergeron, J.K. Kim, S.W. Cushman, G.J. Cooney, B. Atcheson, M.F. White, E.W. Kraegen, and G.I. Shulman. 2002. Mechanism by which fatty acids inhibit insulin activation of insulin receptor substrate-1 (IRS-1)-associated phosphatidylinositol 3-kinase activity in muscle. *J Biol Chem* 277:50230-50236.

43. Straczkowski, M., I. Kowalska, A. Nikolajuk, S. Dzienis-Straczkowska, I. Kinalska, M. Baranowski, M. Zendzian-Piotrowska, Z. Brzezinska, and J. Gorski. 2004. Relationship between insulin sensitivity and sphingomyelin signaling pathway in human skeletal muscle. *Diabetes* 53:1215-1221.
44. Gorska, M., A. Dobrzyn, and M. Baranowski. 2005. Concentrations of sphingosine and sphinganine in plasma of patients with type 2 diabetes. *Med Sci Monit* 11:CR35-38.
45. Adams, J.M., 2nd, T. Pratipanawatr, R. Berria, E. Wang, R.A. DeFronzo, M.C. Sullards, and L.J. Mandarino. 2004. Ceramide content is increased in skeletal muscle from obese insulin-resistant humans. *Diabetes* 53:25-31.
46. Itani, S.I., N.B. Ruderman, F. Schmieder, and G. Boden. 2002. Lipid-induced insulin resistance in human muscle is associated with changes in diacylglycerol, protein kinase C, and IkappaB-alpha. *Diabetes* 51:2005-2011.
47. Chavez, J.A., T.A. Knotts, L.P. Wang, G. Li, R.T. Dobrowsky, G.L. Florant, and S.A. Summers. 2003. A role for ceramide, but not diacylglycerol, in the antagonism of insulin signal transduction by saturated fatty acids. *J Biol Chem* 278:10297-10303.
48. Salinas, M., R. Lopez-Valdaliso, D. Martin, A. Alvarez, and A. Cuadrado. 2000. Inhibition of PKB/Akt1 by C2-ceramide involves activation of ceramide-activated protein phosphatase in PC12 cells. *Mol Cell Neurosci* 15:156-169.
49. Teruel, T., R. Hernandez, and M. Lorenzo. 2001. Ceramide mediates insulin resistance by tumor necrosis factor-alpha in brown adipocytes by maintaining Akt in an inactive dephosphorylated state. *Diabetes* 50:2563-2571.
50. Zinda, M.J., C.J. Vlahos, and M.T. Lai. 2001. Ceramide induces the dephosphorylation and inhibition of constitutively activated Akt in PTEN negative U87mg cells. *Biochem Biophys Res Commun* 280:1107-1115.
51. Powell, D.J., E. Hajduch, G. Kular, and H.S. Hundal. 2003. Ceramide disables 3-phosphoinositide binding to the pleckstrin homology domain of protein kinase B (PKB)/Akt by a PKCzeta-dependent mechanism. *Mol Cell Biol* 23:7794-7808.
52. Powell, D.J., S. Turban, A. Gray, E. Hajduch, and H.S. Hundal. 2004. Intracellular ceramide synthesis and protein kinase Czeta activation play an essential role in palmitate-induced insulin resistance in rat L6 skeletal muscle cells. *Biochem J* 382:619-629.
53. Kim, J.K., J.J. Fillmore, M.J. Sunshine, B. Albrecht, T. Higashimori, D.W. Kim, Z.X. Liu, T.J. Soos, G.W. Cline, W.R. O'Brien, D.R. Littman, and G.I. Shulman. 2004. PKC-theta knockout mice are protected from fat-induced insulin resistance. *J Clin Invest* 114:823-827.
54. Mothe, I., and E. Van Obberghen. 1996. Phosphorylation of insulin receptor substrate-1 on multiple serine residues, 612, 632, 662, and 731, modulates insulin action. *J Biol Chem* 271:11222-11227.
55. Morino, K., K.F. Petersen, S. Dufour, D. Befroy, J. Frattini, N. Shatzkes, S. Neschen, M.F. White, S. Bilz, S. Sono, M. Pypaert, and G.I. Shulman. 2005. Reduced mitochondrial density and increased IRS-1 serine phosphorylation in muscle of insulin-resistant offspring of type 2 diabetic parents. *J Clin Invest* 115:3587-3593.

56. Aguirre, V., E.D. Werner, J. Giraud, Y.H. Lee, S.E. Shoelson, and M.F. White. 2002. Phosphorylation of Ser307 in insulin receptor substrate-1 blocks interactions with the insulin receptor and inhibits insulin action. *J Biol Chem* 277:1531-1537.
57. Moeschel, K., A. Beck, C. Weigert, R. Lammers, H. Kalbacher, W. Voelter, E.D. Schleicher, H.U. Haring, and R. Lehmann. 2004. Protein kinase C-zeta-induced phosphorylation of Ser318 in insulin receptor substrate-1 (IRS-1) attenuates the interaction with the insulin receptor and the tyrosine phosphorylation of IRS-1. *J Biol Chem* 279:25157-25163.
58. Li, J., K. DeFea, and R.A. Roth. 1999. Modulation of insulin receptor substrate-1 tyrosine phosphorylation by an Akt/phosphatidylinositol 3-kinase pathway. *J Biol Chem* 274:9351-9356.
59. Ryan, M.T., and N.J. Hoogenraad. 2007. Mitochondrial-nuclear communications. *Annu Rev Biochem* 76:701-722.
60. Petersen, K.F., S. Dufour, D. Befroy, R. Garcia, and G.I. Shulman. 2004. Impaired mitochondrial activity in the insulin-resistant offspring of patients with type 2 diabetes. *N Engl J Med* 350:664-671.
61. Kelley, D.E., J. He, E.V. Menshikova, and V.B. Ritov. 2002. Dysfunction of mitochondria in human skeletal muscle in type 2 diabetes. *Diabetes* 51:2944-2950.
62. Ritov, V.B., E.V. Menshikova, J. He, R.E. Ferrell, B.H. Goodpaster, and D.E. Kelley. 2005. Deficiency of subsarcolemmal mitochondria in obesity and type 2 diabetes. *Diabetes* 54:8-14.
63. Morino, K., K.F. Petersen, and G.I. Shulman. 2006. Molecular mechanisms of insulin resistance in humans and their potential links with mitochondrial dysfunction. *Diabetes* 55 Suppl 2:S9-S15.
64. Mootha, V.K., C.M. Lindgren, K.F. Eriksson, A. Subramanian, S. Sihag, J. Lehar, P. Puigserver, E. Carlsson, M. Ridderstrale, E. Laurila, N. Houstis, M.J. Daly, N. Patterson, J.P. Mesirov, T.R. Golub, P. Tamayo, B. Spiegelman, E.S. Lander, J.N. Hirschhorn, D. Altshuler, and L.C. Groop. 2003. PGC-1alpha-responsive genes involved in oxidative phosphorylation are coordinately downregulated in human diabetes. *Nat Genet* 34:267-273.
65. Patti, M.E., A.J. Butte, S. Crunkhorn, K. Cusi, R. Berria, S. Kashyap, Y. Miyazaki, I. Kohane, M. Costello, R. Saccone, E.J. Landaker, A.B. Goldfine, E. Mun, R. DeFronzo, J. Finlayson, C.R. Kahn, and L.J. Mandarino. 2003. Coordinated reduction of genes of oxidative metabolism in humans with insulin resistance and diabetes: Potential role of PGC1 and NRF1. *Proc Natl Acad Sci U S A* 100:8466-8471.
66. Zhang, B.B., G. Zhou, and C. Li. 2009. AMPK: an emerging drug target for diabetes and the metabolic syndrome. *Cell Metab* 9:407-416.
67. Fryer, L.G., A. Parbu-Patel, and D. Carling. 2002. The Anti-diabetic drugs rosiglitazone and metformin stimulate AMP-activated protein kinase through distinct signaling pathways. *J Biol Chem* 277:25226-25232.
68. Kubota, N., Y. Terauchi, T. Kubota, H. Kumagai, S. Itoh, H. Satoh, W. Yano, H. Ogata, K. Tokuyama, I. Takamoto, T. Mineyama, M. Ishikawa, M. Moroi, K. Sugi, T. Yamauchi, K. Ueki, K. Tobe, T. Noda, R. Nagai, and T. Kadowaki. 2006. Pioglitazone

ameliorates insulin resistance and diabetes by both adiponectin-dependent and -independent pathways. *J Biol Chem* 281:8748-8755.

69. Zhou, G., R. Myers, Y. Li, Y. Chen, X. Shen, J. Fenyk-Melody, M. Wu, J. Ventre, T. Doebber, N. Fujii, N. Musi, M.F. Hirshman, L.J. Goodyear, and D.E. Moller. 2001. Role of AMP-activated protein kinase in mechanism of metformin action. *J Clin Invest* 108:1167-1174.
70. Shaw, R.J., K.A. Lamia, D. Vasquez, S.H. Koo, N. Bardeesy, R.A. Depinho, M. Montminy, and L.C. Cantley. 2005. The kinase LKB1 mediates glucose homeostasis in liver and therapeutic effects of metformin. *Science* 310:1642-1646.
71. Beg, Z.H., D.W. Allmann, and D.M. Gibson. 1973. Modulation of 3-hydroxy-3-methylglutaryl coenzyme A reductase activity with cAMP and wth protein fractions of rat liver cytosol. *Biochem Biophys Res Commun* 54:1362-1369.
72. Carlson, C.A., and K.H. Kim. 1973. Regulation of hepatic acetyl coenzyme A carboxylase by phosphorylation and dephosphorylation. *J Biol Chem* 248:378-380.
73. Ferrer, A., C. Caelles, N. Massot, and F.G. Hegardt. 1985. Activation of rat liver cytosolic 3-hydroxy-3-methylglutaryl coenzyme A reductase kinase by adenosine 5'-monophosphate. *Biochem Biophys Res Commun* 132:497-504.
74. Yeh, L.A., K.H. Lee, and K.H. Kim. 1980. Regulation of rat liver acetyl-CoA carboxylase. Regulation of phosphorylation and inactivation of acetyl-CoA carboxylase by the adenylate energy charge. *J Biol Chem* 255:2308-2314.
75. Sim, A.T., and D.G. Hardie. 1988. The low activity of acetyl-CoA carboxylase in basal and glucagon-stimulated hepatocytes is due to phosphorylation by the AMP-activated protein kinase and not cyclic AMP-dependent protein kinase. *FEBS Lett* 233:294-298.
76. Randle, P.J., P.B. Garland, C.N. Hales, and E.A. Newsholme. 1963. The glucose fatty-acid cycle. Its role in insulin sensitivity and the metabolic disturbances of diabetes mellitus. *Lancet* 1:785-789.
77. Ruderman, N.B., and A.K. Saha. 2006. Metabolic syndrome: adenosine monophosphate-activated protein kinase and malonyl coenzyme A. *Obesity (Silver Spring)* 14 Suppl 1:25S-33S.
78. Winder, W.W., and D.G. Hardie. 1999. AMP-activated protein kinase, a metabolic master switch: possible roles in type 2 diabetes. *Am J Physiol* 277:E1-10.
79. Winder, W.W., B.F. Holmes, D.S. Rubink, E.B. Jensen, M. Chen, and J.O. Holloszy. 2000. Activation of AMP-activated protein kinase increases mitochondrial enzymes in skeletal muscle. *J Appl Physiol* 88:2219-2226.
80. Zong, H., J.M. Ren, L.H. Young, M. Pypaert, J. Mu, M.J. Birnbaum, and G.I. Shulman. 2002. AMP kinase is required for mitochondrial biogenesis in skeletal muscle in response to chronic energy deprivation. *Proc Natl Acad Sci U S A* 99:15983-15987.
81. Hardie, D.G., J.W. Scott, D.A. Pan, and E.R. Hudson. 2003. Management of cellular energy by the AMP-activated protein kinase system. *FEBS Lett* 546:113-120.
82. Lage, R., C. Dieguez, A. Vidal-Puig, and M. Lopez. 2008. AMPK: a metabolic gauge regulating whole-body energy homeostasis. *Trends Mol Med* 14:539-549.
83. Minokoshi, Y., T. Alquier, N. Furukawa, Y.B. Kim, A. Lee, B. Xue, J. Mu, F. Foufelle, P. Ferre, M.J. Birnbaum, B.J. Stuck, and B.B. Kahn. 2004. AMP-kinase regulates food

intake by responding to hormonal and nutrient signals in the hypothalamus. *Nature* 428:569-574.

84. Andersson, U., K. Filipsson, C.R. Abbott, A. Woods, K. Smith, S.R. Bloom, D. Carling, and C.J. Small. 2004. AMP-activated protein kinase plays a role in the control of food intake. *J Biol Chem* 279:12005-12008.
85. Lopez, M., R. Lage, A.K. Saha, D. Perez-Tilve, M.J. Vazquez, L. Varela, S. Sangiao-Alvarellos, S. Tovar, K. Raghay, S. Rodriguez-Cuenca, R.M. Deoliveira, T. Castaneda, R. Datta, J.Z. Dong, M. Culler, M.W. Sleeman, C.V. Alvarez, R. Gallego, C.J. Lelliott, D. Carling, M.H. Tschop, C. Dieguez, and A. Vidal-Puig. 2008. Hypothalamic fatty acid metabolism mediates the orexigenic action of ghrelin. *Cell Metab* 7:389-399.
86. Hu, Z., Y. Dai, M. Prentki, S. Chohnan, and M.D. Lane. 2005. A role for hypothalamic malonyl-CoA in the control of food intake. *J Biol Chem* 280:39681-39683.
87. Arad, M., C.E. Seidman, and J.G. Seidman. 2007. AMP-activated protein kinase in the heart: role during health and disease. *Circ Res* 100:474-488.
88. Costford, S.R., N. Kavaslar, N. Ahituv, S.N. Chaudhry, W.S. Schackwitz, R. Dent, L.A. Pennacchio, R. McPherson, and M.E. Harper. 2007. Gain-of-function R225W mutation in human AMPKgamma3 causing increased glycogen and decreased triglyceride in skeletal muscle. *PLoS ONE* 2:e903.
89. Arad, M., D.W. Benson, A.R. Perez-Atayde, W.J. McKenna, E.A. Sparks, R.J. Kanter, K. McGarry, J.G. Seidman, and C.E. Seidman. 2002. Constitutively active AMP kinase mutations cause glycogen storage disease mimicking hypertrophic cardiomyopathy. *J Clin Invest* 109:357-362.
90. Gollob, M.H., M.S. Green, A.S. Tang, T. Gollob, A. Karibe, A.S. Ali Hassan, F. Ahmad, R. Lozado, G. Shah, L. Fananapazir, L.L. Bachinski, and R. Roberts. 2001. Identification of a gene responsible for familial Wolff-Parkinson-White syndrome. *N Engl J Med* 344:1823-1831.
91. Gollob, M.H., J.J. Seger, T.N. Gollob, T. Tapscott, O. Gonzales, L. Bachinski, and R. Roberts. 2001. Novel PRKAG2 mutation responsible for the genetic syndrome of ventricular preexcitation and conduction system disease with childhood onset and absence of cardiac hypertrophy. *Circulation* 104:3030-3033.
92. Nissen, S.E., S.J. Nicholls, K. Wolski, D.C. Howey, E. McErlean, M.D. Wang, E.V. Gomez, and J.M. Russo. 2007. Effects of a potent and selective PPAR-alpha agonist in patients with atherogenic dyslipidemia or hypercholesterolemia: two randomized controlled trials. *JAMA* 297:1362-1373.
93. Hardie, D.G. 2008. Role of AMP-activated protein kinase in the metabolic syndrome and in heart disease. *FEBS Lett* 582:81-89.
94. Leclerc, I., W.W. Woltersdorf, G. da Silva Xavier, R.L. Rowe, S.E. Cross, G.S. Korbutt, R.V. Rajotte, R. Smith, and G.A. Rutter. 2004. Metformin, but not leptin, regulates AMP-activated protein kinase in pancreatic islets: impact on glucose-stimulated insulin secretion. *Am J Physiol Endocrinol Metab* 286:E1023-1031.
95. Riboulet-Chavey, A., F. Diraison, L.K. Siew, F.S. Wong, and G.A. Rutter. 2008. Inhibition of AMP-activated protein kinase protects pancreatic beta-cells from cytokine-mediated apoptosis and CD8+ T-cell-induced cytotoxicity. *Diabetes* 57:415-423.

96. Sullivan, J.E., K.J. Brocklehurst, A.E. Marley, F. Carey, D. Carling, and R.K. Beri. 1994. Inhibition of lipolysis and lipogenesis in isolated rat adipocytes with AICAR, a cell-permeable activator of AMP-activated protein kinase. *FEBS Lett* 353:33-36.
97. Corton, J.M., J.G. Gillespie, S.A. Hawley, and D.G. Hardie. 1995. 5-aminoimidazole-4-carboxamide ribonucleoside. A specific method for activating AMP-activated protein kinase in intact cells? *Eur J Biochem* 229:558-565.
98. Dagon, Y., Y. Avraham, and E.M. Berry. 2006. AMPK activation regulates apoptosis, adipogenesis, and lipolysis by eIF2alpha in adipocytes. *Biochem Biophys Res Commun* 340:43-47.
99. Yin, W., J. Mu, and M.J. Birnbaum. 2003. Role of AMP-activated protein kinase in cyclic AMP-dependent lipolysis In 3T3-L1 adipocytes. *J Biol Chem* 278:43074-43080.
100. Smith, A.J., B.R. Thompson, M.A. Sanders, and D.A. Bernlohr. 2007. Interaction of the adipocyte fatty acid-binding protein with the hormone-sensitive lipase: regulation by fatty acids and phosphorylation. *J Biol Chem* 282:32424-32432.

Chapter 1 - Obesity-Associated Diabetes

Contribution of Collaborators

Sean A. Crawford

Collected *vastus lateralis* samples at muscle biopsies, processed muscle biopsies for histology and myoblast isolation, isolated myoblasts, maintained cell cultures, took micrographs of OsO_4 staining for IMTG and fiber typing and performed image analysis/quantification, performed glucose uptake, glycogen synthesis, membrane potential, oxidative damage, and Western blotting assays. Analyzed data for the above described experiments. Table/Figure contributions: Figures 1-8 (Sheila R. Costford contributed equally to the generation of Figures 2-8). Assisted in the writing, editing and submission of the manuscript.

Sheila R. Costford

Collected *vastus lateralis* samples at muscle biopsies, processed muscle biopsies for histology and myoblast isolation, isolated myoblasts, maintained cell cultures, performed glucose uptake, glycogen synthesis, membrane potential, oxidative damage, qRT-PCR, and Western blotting assays. Analyzed data for the above described experiments. Table/Figure contributions: Figures 2-8 (Sean A. Crawford contributed equally to the generation of Figures 2-8). Wrote first draft of manuscript and assisted in writing, editing and submission of the manuscript.

ROBERT DENT

Contacted and recruited proband. Conducted some muscle biopsies. Supervised hyperinsulinemic-euglycemic clamps. Table/Figure contributions: Tables 1-2. Assisted in interpretation of findings and in the writing of the manuscript.

RUTH MCPHERSON

Assisted in the design of the study. Conducted some muscle biopsies and supervised hyperinsulinemic-euglycemic clamps. Table/Figure contributions: Tables 1-2. Assisted in data analysis and interpretation of findings. Assisted in writing the manuscript. Was awarded as PI the peer-reviewed funding for this research (Heart and Stroke Foundation of Ontario).

MARY-ELLEN HARPER

Assisted in study design, and the overall organization amongst collaborators. Assisted in data analysis and interpretation. Assisted in writing the manuscript and submitting it for publication. Was awarded as co-applicant the peer-reviewed funding for this research (Heart and Stroke Foundation of Ontario).

INTRODUCTION

Obesity is a major risk factor for several chronic diseases including cardiovascular disease, certain cancers and type 2 diabetes mellitus (T2DM) (reviewed in (1)). Among adults diagnosed with diabetes, 57% are obese and 28% are overweight (2). Conversely, only 14% of obese adults have diabetes (3). Thus while obesity is a well-recognized risk factor for T2DM, the relatively small percentage of obese individuals who also develop T2DM is consistent with the knowledge that T2DM has a strong genetic component. However, despite recent advances, genetic and other determinants of risk for obesity-associated T2DM have not been fully elucidated (4).

One of the hallmarks of T2DM is insulin resistance. Normally, skeletal muscle accounts for ~80% of postprandial glucose disposal, but in T2DM it becomes the primary site of insulin resistance (5, 6). The molecular mechanisms responsible for the progression of insulin resistance are still poorly understood. Ectopic accumulation of lipid in skeletal muscle (intramuscular triglyceride, IMTG) is associated with obesity and highly correlated with the development of insulin resistance (7-9). However, the observation of high levels of IMTG in lean, insulin-sensitive endurance-trained athletes has led to the hypothesis that altered or incomplete lipid metabolism may be an important factor in the progression of insulin resistance (reviewed in (10)). Along these lines, it has been proposed that the overflow of triacylglycerol metabolites in skeletal muscle mitochondria lead to an uncoupling of the tricarboxylic acid (TCA) cycle and the electron transport chain (ETC), resulting in an accumulation of incompletely oxidized long chain fatty acids (11). Incompletely oxidized

long chain fatty acids thus may be diverted from the TCA cycle into other lipid metabolites such as ceramides, diacylglycerol and/or acylcarnitines, which in turn can interfere with the insulin signaling pathway ((11, 12); reviewed in (13-15)). Indeed, decreased mitochondrial content and impaired oxidative capacity are correlated with insulin resistance and associated with obesity (16-19), but effects can be mitigated by weight loss and physical activity (20, 21).

The delivery of a surfeit of metabolic substrates to mitochondria can lead to augmented reactive oxygen species (ROS) production and impaired mitochondrial function. ROS can cause lipid peroxidation, generating products such as methylcholanthrene and 4-hydroxynonenal (HNE), which can subsequently bind proteins, forming adducts and impairing protein function (reviewed in (22-24)). Oxidative stress has been implicated in the development of insulin resistance (25-29), however the role of ROS in diabetic skeletal muscle is an emerging field. Recently, Chung *et al* demonstrated that treatment of human skeletal muscle cells with high levels of hydrogen peroxide led to the destruction of the insulin signaling pathway, but that pre-treatment with troglitazone could prevent this ROS-induced insulin resistance (30). The production of ROS by skeletal muscle and the mechanisms by which this tissue mitigates oxidative damage in the context of T2DM are areas of great interest.

The overall aim of the current preliminary study was to determine if impaired metabolism could be detected in primary muscle cells of subjects with a history of obesity-associated T2DM. Although no differences in oxidative capacity or oxidative damage were detected

under standard low glucose and insulin conditions, cells were unable to undergo mitochondrial biogenesis and had an increased susceptibility to oxidative damage when exposed to chronic high glucose and insulin conditions. These novel findings define a muscle phenotype at risk for obesity-associated T2DM, and set the stage for future explorations.

Hypothesis

Chronic exposure to high glucose and insulin will re-elicit impaired skeletal muscle metabolism in primary myotubes from subjects with a history of T2DM.

Objectives

The specific objects of this study were:

- To examine muscle fiber type distribution and intramuscular triglyceride (IMTG) content in *vastus lateralis* skeletal muscle
- To evaluate glycogen content, IMTG content, insulin sensitivity, citrate synthase activity, cytochrome c oxidase activity, HNE-adduct content and UCP-3 content in primary human myotubes under two conditions: 1) standard low glucose and insulin conditions and 2) 'diabetic-like' high glucose and insulin conditions

Research Design and Methods

Subjects

Test subjects, referred to as the 'post-diabetes mellitus' (Post-DM) group, were obese and had documented obesity-associated T2DM. Inclusion criteria for this population consisted

of a BMI of ≥30 kg/m^2, a fasting blood glucose of >7.0 mM and an HbA1C level of >7% or treatment with hypoglycemic agent(s) prior to weight loss. Age-, sex- and BMI-matched subjects who had been similarly obese but normoglycemic (Non-DM) acted as controls. Non-DM subjects had no history of T2DM. Family history of T2DM was defined as having at least one parent or sibling with T2DM. None of the Non-DM subjects had a family history of T2DM, however 2 of the 7 Post-DM subjects had a family history of T2DM. Physical activity was measured by a questionnaire adapted from (31). Both populations underwent a 26-week standard clinical weight loss program at the Ottawa Hospital Weight Management Clinic (described in (32, 33)). Subjects participated in weekly 3-hour meetings consisting of a 90-minute workshop (Novartis Nutrition Optifast program), weight, waist circumference and blood pressure determinations, as well as a physician visit. Subjects received the Optifast(R) 900 meal replacement (formerly Novartis Nutrition, currently Nestle Canada Inc., North York, ON) for the first 12 weeks of the program. The Optifast(R) program was modified by the use of closed educational groups, software that gave patient feedback reports on multiple outcomes every 4 months (32), and long-term follow-up every 1-3 months. Following weight loss, Post-DM subjects exhibited consistently normal blood glucose and HbA1C levels (≤6.1 mM and ≤5.7%, respectively). After the completion of the program, some subjects experienced a modest weight gain, however, all subjects were weight stable for a minimum of 14 weeks prior to study (weight stability ranged from 14 to 102 weeks). Weight stability was defined as weight maintenance within 5% of body weight. Following the period of weight stability, a hyperinsulinemic-euglycemic clamp, dual energy X-ray absorptiometry (DEXA) scan and muscle biopsy were performed. Subject

characteristics pre- and post-weight loss as well as at the time of study are described in Table 1-1.

Hyperinsulinemic-Euglycemic Clamp

The insulin infusate was prepared in isotonic saline to which 2 ml of the subject's blood had been added per 50 ml infusate to prevent absorption of insulin to glass and plastic. Regular insulin was diluted to 300 mU/ml in 0.9% saline. Insulin was infused as a 10 min. priming infusion followed by a fixed infusion of 40 mU/m^2. Glucose was infused as 20% dextrose. The glucose infusion was started 4 min. after initiation of insulin infusion at a rate of 2.0 mg/kg/min for 4–10 min. and at 2.5 mg/kg/min for 10–15 min. Blood samples were taken every 5 min. and the glucose infusion adjusted to maintain plasma glucose at 5.0 mM (34).

Body Composition. Whole body fat mass, fat free mass and regional fat distribution were assessed by DEXA using a GE-LUNAR Prodigy module (GE Medical Systems, Madison, WI, USA). Precision of the repeated measurements expressed as the percent coefficient of variation was 2.2% for fat mass percentage.

Muscle Biopsies

After local anaesthesia, biopsies of the *vastus lateralis* were obtained from 7 Post-DM and 7 Non-DM subjects using a 5 mm Bergstrom needle (Opitek). Subjects refrained from physical activity for three days and were fasting for 12 hours prior to the biopsy. Visible adipose tissue was removed from the biopsy and a ~10 mg sample of muscle was frozen in OCT (Optimal Cutting Temperature) compound for fiber type ratio and IMTG

determinations. The remainder of the muscle biopsy was processed for satellite cell isolation and culture.

Cell Culture

Fresh biopsied *vastus lateralis* was minced, subjected to a trypsin digestion for 30 min. and plated in Ham's F-10 media (supplemented with 15% FBS, 0.5 mg/mL BSA, 1 uM dexamethazone, 10 ng/ml EGF, 0.5 mg/ml fetuin and 0.25 pM insulin). Muscle satellite cells were isolated at ~80% confluency using an immuno-based magnetic sorting technique as previously described (35). Isolated myoblasts were grown to ~80% confluency prior to differentiation in either low glucose and insulin (LGI) DMEM (5.5 mM glucose, supplemented with 0.25 pM insulin, 2% horse serum, 1% antibiotic-antimycotic and 2.5 mg/mL gentamycin) or high glucose and insulin (HGI) DMEM (25 mM glucose, supplemented with 10 pM insulin, 2% horse serum, 1% antibiotic-antimycotic and 2.5 mg/mL gentamycin) for 7 days prior to experimentation.

Fiber Type Ratio Determination

O.C.T.-encased frozen tissues were sectioned (10um) and mounted on Superfrost slides and then immunostained sequentially for type 1 fibers (A4.840, Developmental Studies Hybridoma Bank) and type 2 fibers (N2.261, Developmental Studies Hybridoma Bank). Biotinylated goat anti-mouse (BA-9200, Vector Laboratories) was used as the secondary antibody. Type 1 fibers were stained red (SK5100, Vector Laboratories) and type 2 fibers were stained blue (SK5300, Vector Laboratories). The number of type 1 and type 2 fibers

were counted in 3 fields of view in each of 3 sections per subject, from which the fiber type ratio was determined.

Intramuscular Triglyceride Content

IMTG content was evaluated both *ex vivo* and *in vitro*. *Ex vivo* determinations were conducted as described previously (35). Frozen tissues were sectioned (10um), mounted on Superfrost slides and fixed in 10% neutral buffered formalin. Sections were stained with 1% osmium tetroxide and counter-stained with hematoxylin and eosin. Three fields of view in each of 3 sections per subject were quantified using Northern Eclipse imaging software to determine the amount of IMTG relative to the cross-sectional fiber area.

In vitro determinations of IMTG content were determined in differentiated myotubes: ~$2.4x10^6$ cells were re-suspended in IMTG buffer (25 mM Tris-HCl pH 7.5, 1 mM EDTA) and total triglycerides were extracted using chloroform-methanol (2:1). The organic phase was evaporated under N_2 gas and lipids were re-suspended in 2-propanol. Triglyceride concentration was determined spectrophotometrically using the L-Type TG H assay (WAKO) and normalized to protein content as determined by bicinchoninic acid (BCA) assay.

Glycogen Content

~$2.4x10^6$ differentiated myotubes were re-suspended in PBM buffer (20 mM KH_2PO_4, 10 uM $CaCl_2$, 1 mM $MgCl_2$, pH 6.1) and lysed using the freeze-thaw method. Samples were boiled for 20 min. in 30% KOH saturated with anhydrous Na_2SO_4. Glycogen was precipitated with 95% ethanol, dissolved in ddH_2O and incubated with 0.2% anthrone in H_2SO_4 at 100°C for 20 min. Glycogen concentration was determined spectrophotometrically by measuring

the absorbance at 620nm relative to an oyster glycogen standard curve and normalized to protein content as determined by BCA assay.

Mitochondrial Yield and Enzyme Activities

Intact mitochondria were isolated from differentiated myotubes using a mitochondrial isolation kit (MITOISO2; Sigma). Mitochondrial yield was determined by dividing mitochondrial protein content by cellular protein content, as determined by BCA assay. Cytochrome c oxidase activity was assayed in intact mitochondria using the CYTOCOX1 kit (Sigma) in which the oxidation of dithiothreitol-reduced cytochrome c was monitored spectrophotometrically at 550 nm. Citrate synthase activity was determined in lysed mitochondria using the CS0720 kit (Sigma) in which the conversion of oxaloacetate to citrate was monitored spectrophotometrically at 412 nm. Enzyme activities were normalized to both mitochondrial and cellular protein contents.

Mitochondrial Membrane Potential Determination

20,000 myoblasts per well were seeded onto a 96-well tissue culture plate and differentiated in LGI or HGI media for 7 days. Cells were incubated with 800 nM tetramethylrhodamine, ethyl ester, perchlorate (TMRE) in either LGI-PBS (5.5 mM glucose, 0.25 pM insulin) or HGI-PBS (25 mM glucose, 10 pM insulin) for 15 min. at 37°C in the dark. TMRE solutions were removed, cells were washed in PBS and solutions were replaced with LGI/HGI-PBS or LGI/HGI-PBS. Control wells contained no cells. Fluorescence was measured 15 min. post-incubation (excitation: 544nm, emission: 590nm). TMRE is a lypophilic cationic dye that accumulates in the mitochondria proportional to membrane potential, and

mitochondrial accumulation quenches TMRE fluorescence (36). Membrane potential was expressed as the absolute value of the decrease in TMRE fluorescence and normalized to mitochondrial protein content as determined by BCA assay (see Enzyme Activities above).

Western Blotting

Differentiated myotubes were lysed in RIPA buffer (150mM NaCl, 50mM Tris (pH 7.4), 1mM EDTA, 1% (v/v) NP-40, 0.25% (w/v) sodium deoxycholate) and protein content was determined via BCA assay. Lysates were separated on a 10% bis-tris polyacrylamide gel and proteins transferred to a nitrocellulose membrane. UCP3 and β-actin (loading control) were detected using rabbit anti-UCP3 (ab-3477; Abcam) and rabbit anti-β-actin (4967; Cell Signaling), following by goat anti-rabbit HRP (sc-2030; Santa Cruz Biotechnology). Visualization was achieved using an Enhanced Chemi-Luminescence kit (Amersham Pharmacia). Spot densitometry was performed using an Alpha multi-image light camera and Alpha imaging software. Values represent the integrated density value (IDV) of UCP3 divided by the IDV of β-actin. Manganese superoxide dismutase (mnSOD) and succinate dehydrogenase (SDH; loading control) were detected in isolated mitochondria using rabbit anti-mnSOD (sc-30080; Santa Cruz Biotechnology) and mouse anti-SDH (sc-59687; Santa Cruz Biotechnology), followed by goat anti-rabbit HRP and goat anti-mouse HRP (sc-2031; Santa Cruz Biotechnology), respectively.

4-Hydroxynonenal-Histidine Adduct Content

HNE-His adduct content was determined by ELISA (STA-334, Cell Biolabs, Inc.). Protein samples (as described in Western Blotting above) were absorbed onto a 96-well ELISA plate

in triplicate for 2 hrs at 37°C. Wells were probed with an anti-HNE-His antibody and HRP-conjugated secondary antibody. Absolute HNE-His adduct content was determined spectrophotometrically by comparing samples to a standard curve of HNE-BSA standards at 600nm.

Glucose Uptake

Glucose uptake assays were performed as described previously (37). Myoblasts were seeded in 24-well plates at 37,000 cells/cm^2, incubated for 24 hours and then differentiated for 7 days. Differentiated myotubes were washed twice with uptake buffer (136 mM NaCl, 4.7 mM KCl, 1.25 mM MgSO4·7H2O, 1.2 mM $CaCl{\cdot}2H_2O$, 20 mM HEPES; pH 7.4) and then incubated for 20 minutes in the presence or absence of 100 nM insulin. Cells were incubated at 37°C for 10 min with 0.5 uCi/ml [H^3]-2-deoxy-glucose and 100 mM cold 2-deoxy-glucose. Cells were then washed 3X with ice-cold PBS and lysed with ice-cold RIPA lysis buffer (Sigma, St. Louis, MO) supplemented with ROCHE mini protease inhibitor cocktail. Total radioactivity was then determined in cell lysate by liquid scintillation counting. Protein content was determined via BCA assay.

Glycogen Synthesis

Glycogen synthesis assays were performed as described previously (38). Myoblasts were seeded and differentiated as described above. Differentiated myotubes were glucose and serum starved for 1.5 hours in glucose-free DMEM media and then incubated with DMEM containing 5.5 mM glucose and 0.5 uCi/ml [H^3]-2-deoxy-glucose with or without 100 nM insulin for 3 h. Cells were then washed 3X with ice-cold PBS and harvested in 30% KOH

saturated with anhydrous Na_2SO_4. Cell lysates were incubated at 100°C for 20 mins. in the presence of 6.3 ug/ul oyster glycogen. Glycogen was precipitated in ethanol, washed and then dissolved in ddH_2O. Radioactive glycogen was determined by liquid scintillation counting. Protein content was determined in cell lysates via BCA assay.

Statistical Methods

A Student's *t* test was employed to assess statistical differences between clinical parameters (Tables 1 and 2) as well as differences in fiber type percentage, mnSOD expression and UCP3 expression (Figures 1, 5 and 7). A one-way ANOVA with Tukey post-test was used to assess statistical differences in IMTG content, glycogen content, mitochondrial yield, citrate synthase activity, cytochrome c oxidase activity, HNE-His adducts and mitochondrial membrane potential (Figures 2, 3, 4 and 6). Confidence intervals were set at 95%.

RESULTS

STUDY SUBJECTS

Subjects in the Non-DM and Post-DM groups were individually matched for age and sex as well as pre- and post-weight loss BMI. There were no differences in physical activity between Non-DM and Post-DM groups (3.3 ± 3.8 h/wk and 4.6 ± 3.2 h/wk, respectively). Prior to weight loss, all Post-DM subjects met the American Diabetes Association criteria for diabetes or were taking oral anti-diabetic agents. Following weight loss, Post-DM subjects became normoglycemic and remained so at the time of study. Non-DM subjects did not meet the criteria for diabetes before or after weight loss (mean fasting glucose 5.7 ± 0.76 mM). At the time of study, the two groups showed no differences in fasting blood glucose, HbA1c or fat free mass; however, the Non-DM group had a slightly higher percentage body fat (Table 1-1). As assessed by a hyperinsulinemic-euglycemic clamp, the Post-DM and Non-DM subjects demonstrated similar insulin-stimulated glucose disposal rates and insulin sensitivity indices (Table 1-2). No differences were detected in the insulin sensitivity of primary myotubes from Non-DM compared to Post-DM subjects, as assessed by insulin-stimulated glucose uptake and insulin-stimulated glycogen synthesis (Figure 1-1).

FIBER TYPE RATIO

Quantitative histological analysis of *vastus lateralis* skeletal muscle biopsies was performed to assess the muscle fibre type ratio and IMTG content. No differences were observed in the fiber type distribution between the Non-DM and the Post-DM populations (Figure 1-2).

Table 1-1: Pre- and post-weight loss characteristics of Post-DM and Non-DM subjects.

Means ± SD, n=7, Student's *t* test for each parameter (NS, except where noted)

	Non-DM Subjects	Post-DM Subjects
Age (years)	52.1 ± 11.0	51.8 ± 11.0
Male/Female	6/1	6/1
Family History of T2DM/No Family History of T2DM	0/7	2/5
Pre-Weight Loss		
Body Weight (kg)	144.7 ± 30.3	137.6 ± 35.4
Body Mass Index (kg/m^2)	47.6 ± 9.7	45.6 ± 9.5
Fasting Blood Glucose (mM)	5.7 ± 0.76	6.4 ± 1.28[a]
Fasting Blood Glucose Range (mM)	4.3 – 6.8	4.4 – 7.8[a]
HbA1C (%)	n/a[b]	7.0 ± 1.6
Diabetes Medication	0	5
Post-Weight Loss at Week 26		
Weight (kg)[d]	104.9 ± 21.9	108.5 ± 25.6
Body Mass Index (kg/m^2)	34.5 ± 6.8	36.06 ± 6.9
Fasting Blood Glucose (mM)	5.03 ± 0.72	4.96 ± 0.35
HbA1C (%)	n/a[b]	5.2 ± 0.4
Diabetes Medication	0	0
At Time of Study		
Time Between Week 26 & Study (weeks)	52.0 ± 10.5	50.8 ± 10.4
Duration of Weight Stability (weeks)	31.7 ± 31.8	32.4 ± 13.1
Body Weight (kg)[d]	117.5 ± 20.0	113.4 ± 23.5
Body Mass Index (kg/m^2)	38.7 ± 6.4	37.9 ± 5.9
Basal Metabolic Rate (kcal/d)	2175.7 ± 335.8	2004.3 ± 397.9
Percent Fat Free Mass (DEXA)	61.8 ± 6.0	59.8 ± 3.4
Percent Fat Mass (DEXA)	39.6 ± 3.41	34.7 ± 2.85[c]
Percent Total Body Fat as Truncal Fat (DEXA)	64.4 ± 2.8	58.5 ± 4.7
Fasting Blood Glucose (mM)	5.0 ± 0.8	4.9 ± 0.5
HbA1C (%)	5.3 ± 0.1	5.4 ± 0.2
Diabetes Medication	0	0

[a]Blood glucose for Post-DM was measured while on diet and pharmacological treatment for diabetes

[b]HbA1C not evaluated in non-diabetic subjects prior to or during weight loss program

[c]Non-DM vs. Post-DM, $p<0.05$

[d]The moderate weight gain in both Non-DM and Post-DM groups occurred in the period between the end of the weight loss program (at week 26) and the beginning of the weight stability period (all subjects were weight stable for a minimum of 14 weeks prior to study)

Table 1-2: Post-weight loss measurements - hyperinsulinemic-euglycemic clamp.

Means ± SD, n=7, Student's *t* test for each parameter (NS).

	Non-DM Subjects	**Post-DM Subjects**
Baseline Blood Glucose (mM)	5.67 ± 0.63	5.40 ± 0.71
Baseline Blood Insulin (pM)	47.6 ± 33.6	70.0 ± 21.4
HOMA Index	1.66 ± 2.86	2.32 ± 4.24
60-120 min Insulin (pM)	1071 ± 413	1002 ± 222
Insulin-Stimulated Glucose Disposal (mmol/kg/min)	0.272 ± 0.103	0.262 ± 0.132
Insulin Sensitivity (M/I_{clamp}) (nmol kg^{-1} min^{-1} $pmol^{-1}$)	319.8 ± 232.0	282.5 ± 180.7

Figure 1-1*: Glucose Uptake and Glycogen Synthesis* A) Fold-change in glucose uptake in response to insulin stimulation in cells from Non-DM subjects (white bars) and Post-DM subjects (black bars) differentiated under low glucose and insulin (LGI) or high glucose and insulin (HGI) conditions (B) Fold-change in glycogen synthesis in response to stimulation with 100 mM Insulin in cells from Non-DM subjects (white bars) and Post-DM subjects (black bars) differentiated under low glucose and insulin (LGI) or high glucose and insulin (HGI) conditions: means ± SD, n=3, two-way ANOVA, Bonferroni correction, NS.

Figure 1-1: Glucose uptake and glycogen synthesis

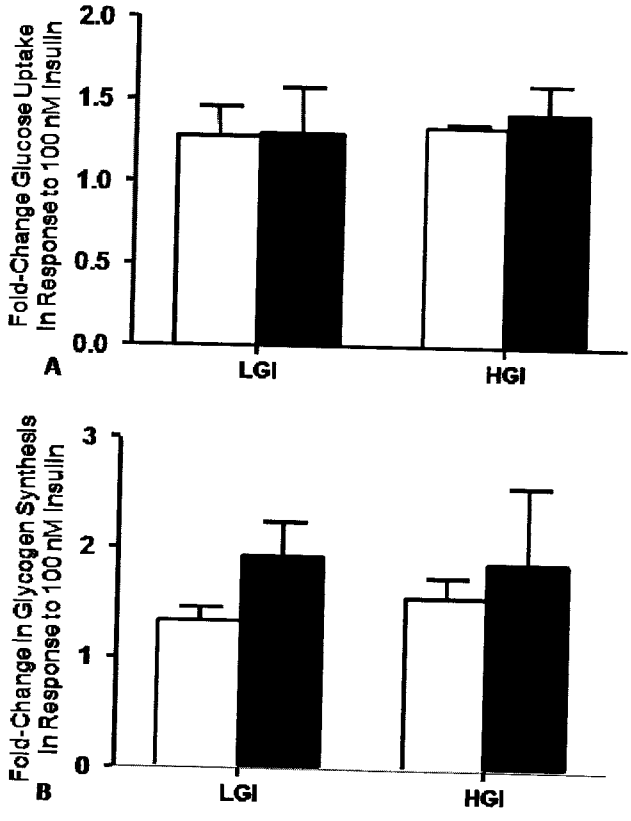

Figure 1-2: Fiber Type Ratio. Type 1 fibers stained red and type 2 fibers stained blue in representative muscle sections of (A) a Non-DM subject and (B) a Post-DM subject. (C) Fiber type ratio expressed as a percentage: means ± SD, n=6, Student's *t* test for each fiber type, NS.

Figure 1-2: Fiber type ratio

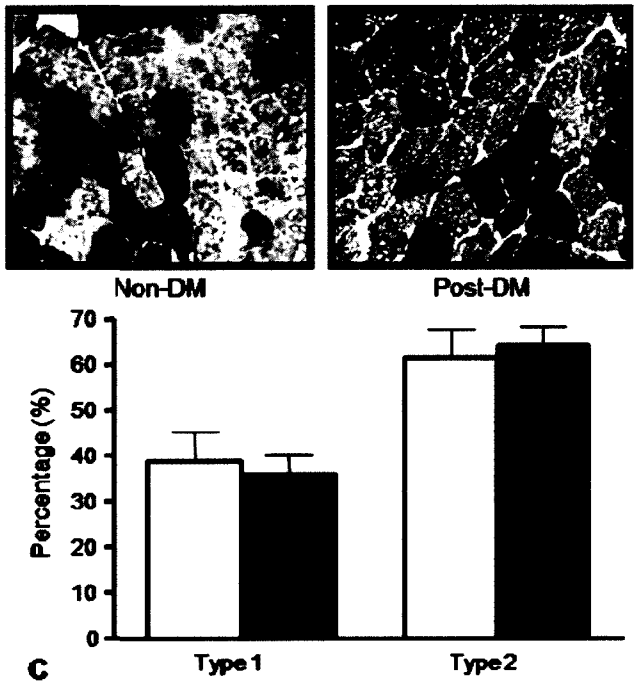

The fiber type distribution for both populations was approximately 40% Type 1 and 60% Type 2.

Fuel Storage

Quantitative histology also revealed no differences in IMTG content between Non-DM and Post-DM subjects (63.78 ± 6.58 AU vs. 71.79 ± 12.18 AU, respectively). IMTG content was also assessed *in vitro* in myotubes differentiated in standard LGI conditions or in 'diabetic-like' HGI conditions. Surprisingly, no differences were detected in IMTG content between in HGI conditions compared to LGI conditions in either Post-DM or Non-DM subjects. Additionally, there were no differences in IMTG content between Post-DM and Non-DM subjects in either LGI conditions or when challenged with HGI (Figure 1-3A). Post-DM subjects exhibited ~50% lower intracellular glycogen levels compared to Non-DM subjects when myotubes were differentiated in LGI ($p<0.01$) and ~30% lower levels of glycogen when myotubes were differentiated in HGI (Figure 1-3B).

Mitochondrial Content and Oxidative Capacity

There were no differences in mitochondrial content, as measured by mitochondrial yield, when myotubes from Non-DM and Post-DM subjects were exposed to LGI conditions. However, mitochondrial content was nearly doubled in Non-DM subjects when exposed to HGI conditions ($p<0.01$), but no increase in mitochondrial content was observed in Post-DM subjects under the same conditions (Figure 1-4A).

Cellular citrate synthase activity was assessed as a marker of mitochondrial content. Myotubes from Non-DM subjects showed an overall increase of ~65% in citrate synthase

Figure 1-3: Fuel Storage. (A) Intramuscular triglyceride (IMTG) normalized to cellular protein in myotubes from Non-DM subjects (white bars) and Post-DM subjects (black bars) differentiated under low glucose and insulin (LGI) or high glucose and insulin (HGI) conditions: means ± SD, n=3, one-way ANOVA, Tukey post-test, NS. (B) Glycogen normalized to cellular protein in myotubes from Non-DM subjects (white bars) and Post-DM subjects (black bars) differentiated under LGI or HGI conditions: means ± SD, n=5, one-way ANOVA, Tukey post-test, **p<0.01, ***p<0.001.

Figure 1-3: Fuel storage

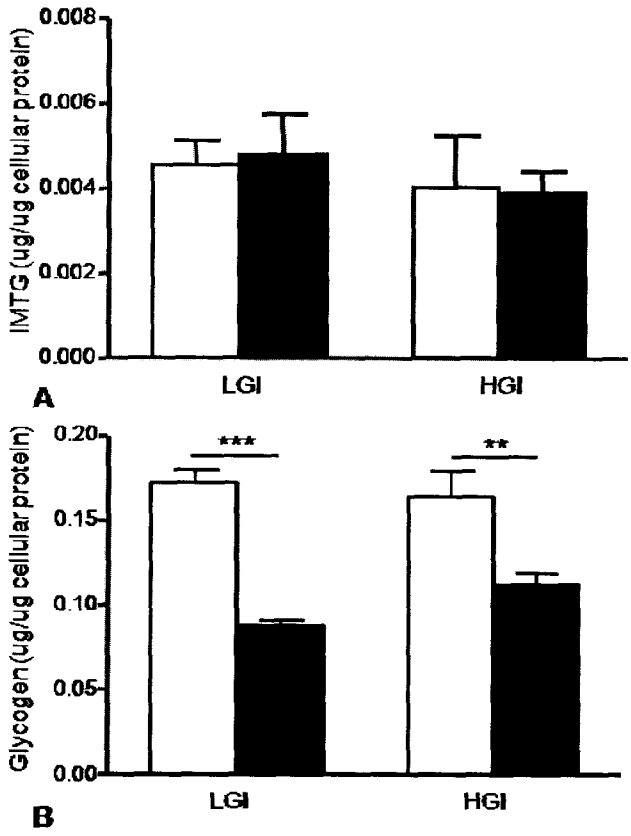

Figure 1-4: Oxidative Capacity. Myotubes from Non-DM subjects (white bars) and Post-DM subjects (black bars) differentiated under low glucose and insulin (LGI) or high glucose and insulin (HGI) conditions. Means ± SD, n=3, one-way ANOVA, Tukey post-test, *$p<0.05$, **$p<0.01$, ***$p<0.001$. (A) Mitochondrial yield (mitochondrial protein content per cellular protein content). (B) Citrate synthase activity normalized to cellular protein. (C) Citrate synthase activity normalized to mitochondrial protein. (D) Cytochrome c oxidase activity normalized to cellular protein. (E) Cytochrome c oxidase activity normalized to mitochondrial protein.

Figure 1-4: Oxidative capacity

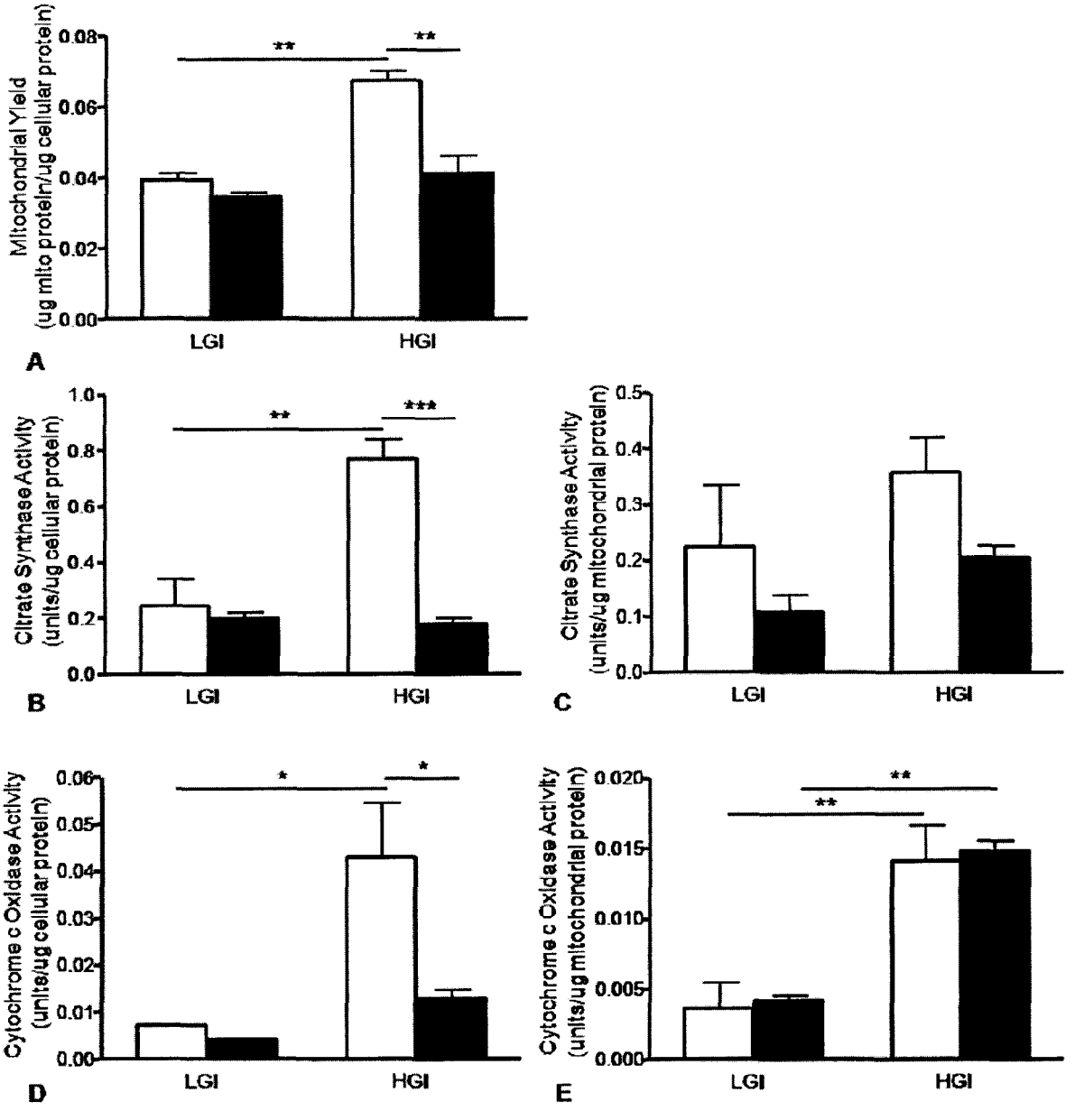

activity when exposed to HGI conditions ($p<0.01$), however cells from Post-DM subjects showed no differences in citrate synthase activity when exposed to HGI conditions (Figure 1-4B). When normalized to mitochondrial content, there was a trend for myotubes from Post-DM subjects to have lower citrate synthase activity compared to Non-DM subjects in both LGI and HGI conditions, although this did not reach statistical significance (Figure 1-4C). These data suggest that the lack of an HGI-induced increase in citrate synthase activity in Post-DM subjects is due mainly to the lack of mitochondrial biogenesis under these conditions.

Cellular cytochrome c oxidase activity was used as a second marker of mitochondrial content. When normalized to cellular protein, Non-DM subjects showed an overall increase of ~80% in cytochrome c oxidase activity when exposed to HGI conditions ($p<0.05$), whereas cells from Post-DM subjects did not show a significant increase in overall cytochrome c oxidase activity (Figure 1-4D). When normalized to mitochondrial content, both Non-DM and Post-DM subjects showed an increase in cytochrome c oxidase activity in HGI conditions compared to LGI conditions ($p<0.01$), indicating an upregulation of ETC chain capacity per mitochondrion (Figure 1-4E). There were no differences in ETC capacity between Non-DM and Post-DM subjects in either LGI or HGI conditions at the level of the mitochondrion. Altogether, these data are indicative of higher overall oxidative capacity in the Non-DM myotubes compared to the Post-DM myotubes when exposed to HGI conditions due to higher mitochondrial content.

Oxidative Damage and Mitochondrial Membrane Potential

Oxidative damage was assessed by measuring HNE-protein adducts. ROS produced in the mitochondria as a result of electrons escaping from the ETC during oxidative phosphorylation can react with lipid species to form lipid peroxides. The latter decompose to form more complex and reactive compounds such as HNE, which can then form stable adducts with cellular proteins, potentially altering their function. Myotubes differentiated in LGI conditions showed no difference in HNE-protein adducts between the Non-DM and Post-DM subjects as measured by ELISA. However, when myotubes were differentiated in HGI conditions, a significant increase was observed in HNE-adduct content in the Post-DM group ($p<0.01$), but not in the Non-DM group. Overall levels of HNE-adducts were higher in Post-DM subjects under HGI conditions relative to the Non-DM controls ($p<0.05$; Figure 1-5).

In response to higher ROS production, genes involved in antioxidant pathways are typically upregulated. mnSOD, the mitochondrial form of superoxide dismutase, is responsible for catalyzing the dismutation of superoxide to protect the cell from ROS damage. Levels of mnSOD protein were found to be higher in Post-DM cells when differentiated under both LGI ($p<0.05$) and HGI ($p<0.01$) conditions (Figure 1-6), indicating that although higher oxidative damage was not observed in Post-DM cells under LGI conditions, it is likely that higher amounts of ROS were being produced. The upregulation of mnSOD seemed to be enough to prevent increased oxidative damage under LGI conditions, but was not sufficient to prevent oxidative damage under HGI conditions, where higher amounts of ROS were presumably being produced.

Figure 1-5: Oxidative Damage. 4-hydroxynonenal-histidine (HNE-His) adducts normalized to cellular protein content. Myotubes from Non-DM subjects (white bars) and Post-DM subjects (black bars) differentiated under low glucose and insulin (LGI) or high glucose and insulin (HGI) conditions. Means ± SD, n=4, one-way ANOVA, Tukey post-test, *$p<0.05$, **$p<0.01$.

Figure 1-5: Oxidative damage

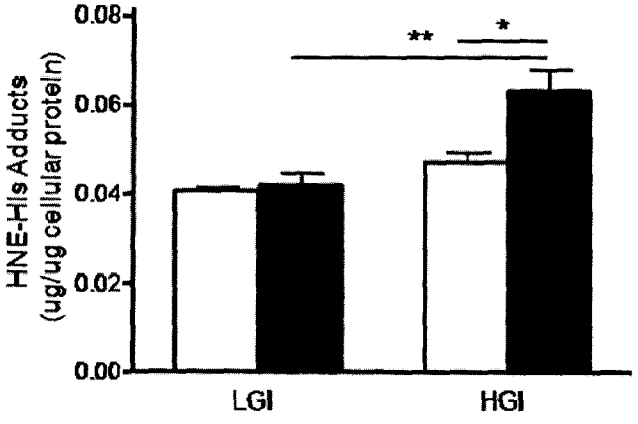

Figure 1-6: Manganese Superoxide Dismutase (mnSOD) Content. Representative Western blots of mnSOD and succinate dehydrogenase (SDH) loading controls. Mitochondria derived from Non-DM/Post-DM myotubes differentiated under (A) low glucose and insulin (LGI) and (B) high glucose and insulin (HGI) conditions. Quantitation of mnSOD content: integrated densitometry value (IDV) of mnSOD normalized to SDH IDV for (C) LGI and (D) HGI conditions. Means ± SD, n=4, Student's *t* test, *$p<0.05$, **$p<0.01$.

Figure 1-6: Manganese superoxide dismutase (mnSOD) content

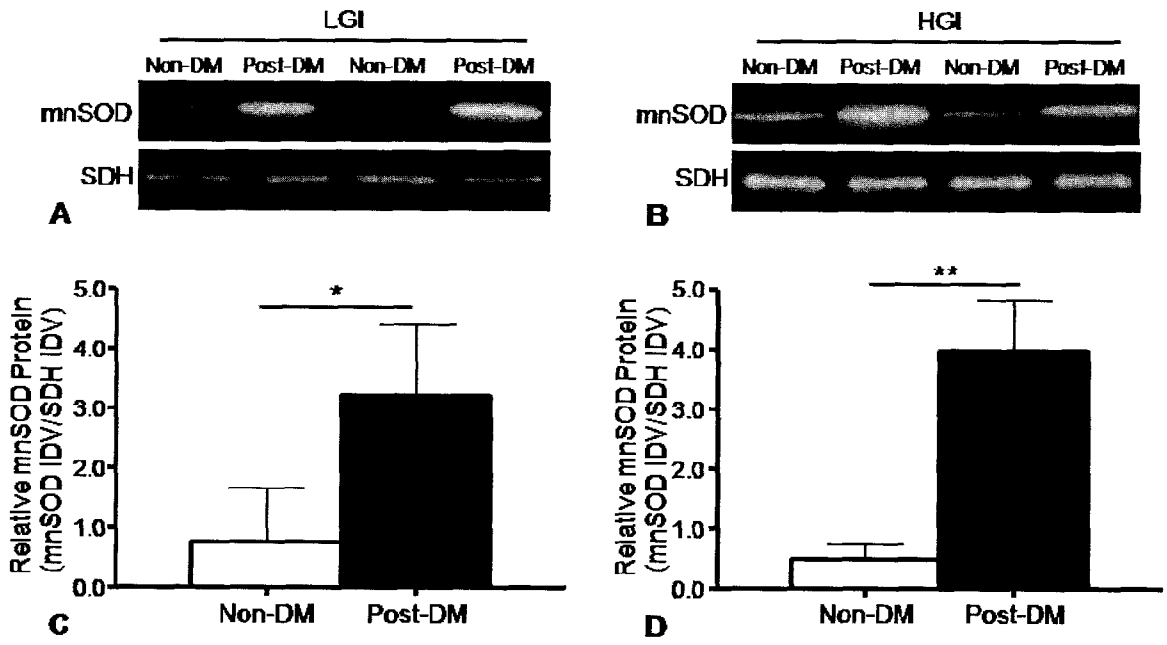

Lower rates of ROS production have been associated with lower mitochondrial membrane potential. Compared to LGI conditions, mitochondrial membrane potential was decreased in the Non-DM cells when subjected to HGI conditions ($p<0.01$), but this was not observed in cells from Post-DM subjects (Figure 1-7). It has been hypothesized that uncoupling protein-3 (UCP3) may mitigate ROS production by uncoupling oxidative phosphorylation in situations of high membrane potential (39-41). ROS production is thought to be mitigated via a UCP3-mediated mechanism in which protons leak back into the mitochondrial matrix thereby reducing membrane potential. No overall differences in UCP3 protein content were observed between Post-DM and Non-DM cells under LGI conditions (Figure 1-8A,C). Upon exposure to HGI conditions, however, Post-DM cells exhibited a marked 3-fold lower expression of UCP3 ($p<0.05$; Figure 1-8B,D). When UCP3 was normalized to mitochondrial content, Post-DM subjects had ~35% less UCP3 compared to Non-DM subjects ($p<0.05$), indicating a decreased level of UCP3 expression per mitochondrion (Figure 1-8F).

Figure 1-7: Mitochondrial Membrane Potential. Relative mitochondrial membrane potential expressed in fluorescence units (FU) normalized to mitochondrial yield. Myotubes from Non-DM subjects (white bars) and Post-DM subjects (black bars) differentiated under low glucose and insulin (LGI) or high glucose and insulin (HGI) conditions. Means ± SD, n=4, one-way ANOVA, Tukey post-test, **$p<0.01$.

Figure 1-7: Mitochondrial membrane potential

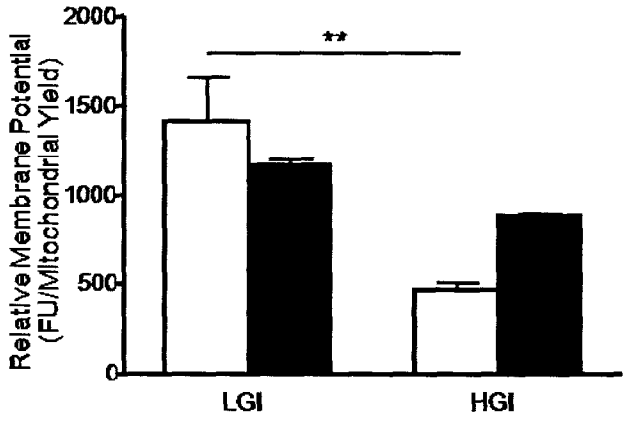

Figure 1-8: Uncoupling Protein-3 (UCP3) Content. Representative Western blots of UCP3 and β-actin loading controls. Lysates from Non-DM/Post-DM myotubes differentiated under (A) low glucose and insulin (LGI) and (B) high glucose and insulin (HGI) conditions. Quantitation of UCP3 content: integrated densitometry value (IDV) of UCP3 normalized to β-actin IDV for (C) LGI and (D) HGI conditions. UCP3 content normalized to mitochondrial yield for (E) LGI and (F) HGI conditions. Means ± SD, n=4, Student's *t* test, *$p<0.05$, ***$p<0.001$.

Figure 1-8: Uncoupling protein 3 (UCP3) content

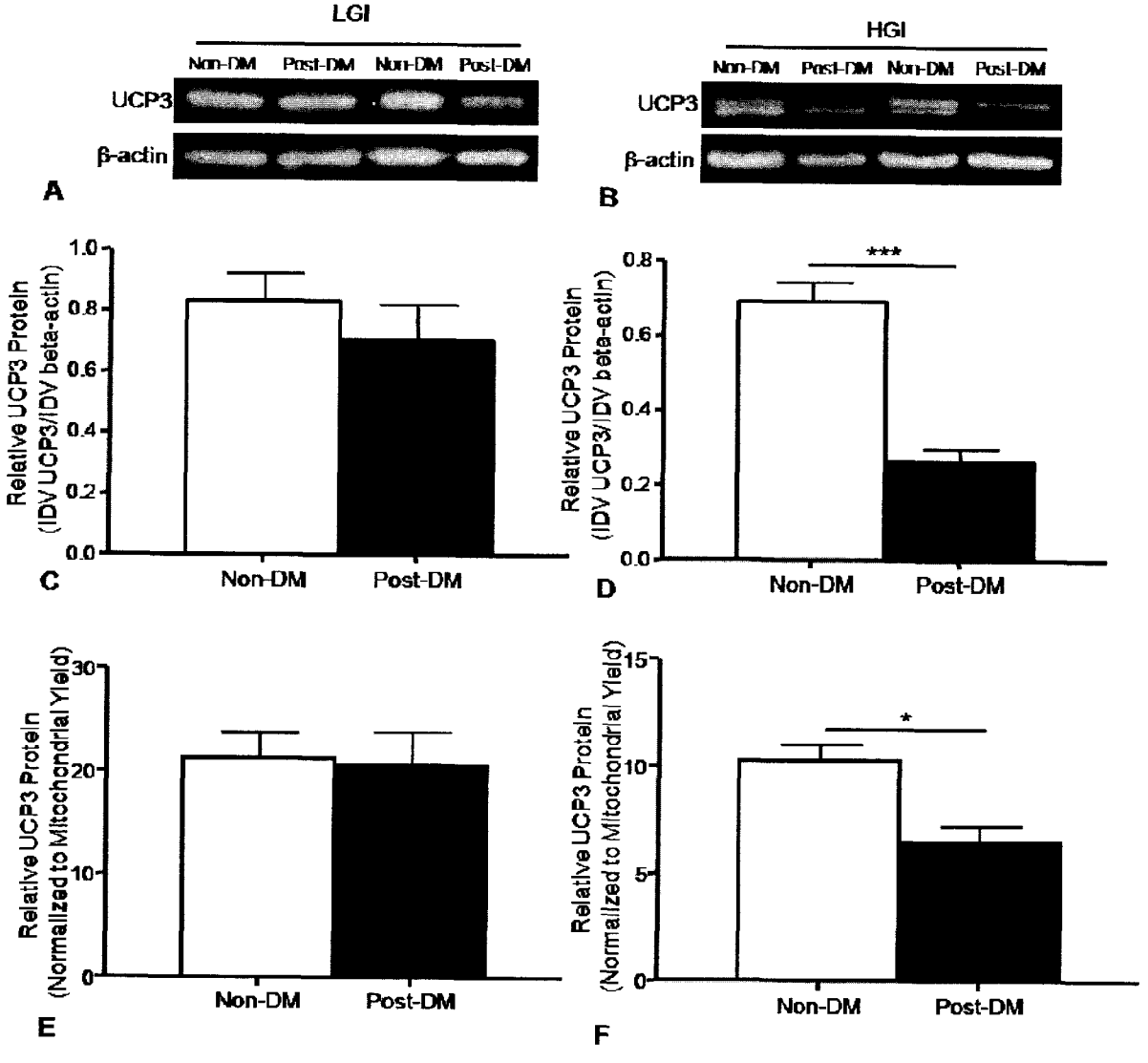

DISCUSSION

Weight loss through calorie restriction improves glycemic control in subjects with T2DM (42, 43). In order to better understand the mechanistic associations between obesity and T2DM, and to avoid the confounding effects of concurrent hyperglycemia or diabetes medications, we compared the skeletal muscle characteristics of subjects with or without a history of obesity-associated diabetes, all of whom were similarly euglycemic following weight loss.

Increased IMTG has been observed in subjects who are obese but do not have T2DM (44), but IMTG is best correlated with the degree of insulin resistance of the subject, regardless of BMI (7-9, 45, 46). No differences in IMTG were observed in either LGI or HGI conditions, indicating that hyperglycemia-hyperinsulinemia is not sufficient to elicit higher levels of IMTG in myotubes of Post-DM subjects. Conversely, glycogen levels in Post-DM myotubes were lower in both LGI and HGI conditions. These results are consistent with reports that insulin-stimulated glycogen synthesis in skeletal muscle is impaired in subjects with T2DM (47, 48) and overall muscle glycogen content is lower in both individuals at risk for T2DM as well as those who have the disease (49, 50). It is interesting, however, that glycogen levels were lower in Post-DM cells despite no differences in insulin sensitivity between Non-DM and Post-DM cells. Glycogen deficit may therefore be an early marker of dysfunctional metabolism in muscle of individuals prone to the development of obesity-associated diabetes, or perhaps an imprint left in the satellite cells of individuals who have had T2DM, despite the reversal of clinical symptoms of the disease via weight loss.

It has been previously shown that genes involved in oxidative metabolism and mitochondrial biogenesis are downregulated in skeletal muscle of individuals with T2DM, individuals who are insulin resistant and healthy offspring of individuals with T2DM (17, 51). Functional impairment of skeletal muscle mitochondria has also been shown in these populations (19, 52). Our data suggest that in individuals prone to the development of obesity-associated diabetes, the defect in oxidative metabolism lies in the inability of myotubes to undergo mitochondrial biogenesis in response to situations of high glucose and insulin. Although there was overall impaired induction of citrate synthase and cytochrome c oxidase activities in Post-DM cells, these deficiencies can be accounted for by the lack of mitochondrial biogenesis. Cytochrome c oxidase activity was upregulated per mitochondrion in both Non-DM and Post-DM subjects when exposed to HGI conditions, indicating no impairment in ETC function at the level of the mitochondrion. These results indicate that the re-elicitation of impaired oxidative metabolism in Post-DM subjects when exposed to HGI conditions is due to impaired stimulus of mitochondrial biogenesis.

Increased oxidative stress has been closely associated with insulin resistance and diabetes in a number of tissues, including skeletal muscle and adipose (reviewed in (53)). We found no differences in oxidative damage between Non-DM and Post-DM cells under LGI conditions, but increased oxidative damage in Post-DM cells under HGI conditions. Taken alone, this result suggests that there was an increase in ROS produced under HGI conditions, but Post-DM cells were unable to mitigate the ROS. However, the fact that mnSOD protein expression was increased in Post-DM cells under both LGI and HGI conditions suggests increased ROS production under both conditions, and that this

antioxidant system was sufficient to prevent ROS damage in these cells under LGI conditions, but not under HGI conditions. In order to explore a possible mechanism to explain the differences in oxidative damage between Post-DM and Non-DM cells, we measured mitochondrial membrane potential. The decrease in membrane potential that was observed in Non-DM cells exposed to HGI conditions may explain their resistance to oxidative damage. Post-DM cells were not able to lower their membrane potential in the face of increased reducing equivalents entering the ETC (*i.e.,* under HGI conditions), and therefore ROS production was augmented.

There are at least two possible explanations for the underlying mechanism of decreased mitochondrial membrane potential in Non-DM cells but not Post-DM cells exposed to chronic HGI. The decrease in membrane potential in Non-DM cells can at least be partially explained by the HGI-induced increase in mitochondrial content. With an ~85% increase in mitochondrial content, the Non-DM cells would be well equipped to metabolize the reducing equivalents provided by increased glycolytic flux, unlike the Post-DM cells which had no increase in mitochondrial content. The robust increase in oxidative capacity seen in Non-DM cells may explain the resultant drop in mitochondrial membrane potential: substrates would be distributed amongst almost double the amount of mitochondria. Fewer reducing equivalents being delivered to the ETC per mitochondrion would result in a lower membrane potential.

The mechanisms underlying the absence of a drop in membrane potential in Post-DM cells are likely multi-factorial. A second possible explanation relates to ROS signalling within the

mitochondrion. High glucose exposure (*i.e.*, more substrates being delivered to cells) would initially result in more reducing equivalents being delivered to the ETC per mitochondrion, driving up mitochondrial membrane potential and increasing ROS production. HNE can then be produced by ROS-lipid interaction. UCP3 is a mitochondrial inner membrane protein with unresolved physiological function(s). However, it has been hypothesized to mediate a proton leak when activated by HNE, reducing mitochondrial membrane potential and mitigating production of ROS in a negative feedback loop (41). Interestingly, there were no differences in UCP3 expression between Non-DM and Post-DM subjects under LGI conditions, but Post-DM cells had lower expression of UCP3 at both the cellular and mitochondrial levels when exposed to HGI conditions. These results corroborate previous reports of decreased UCP3 expression documented in *vastus lateralis* of individuals with T2DM (54), but now link decreased UCP3 expression with failed membrane potential response and increased oxidative damage under conditions of high glucose and insulin. Thus, although the HNE signal is being generated in Post-DM cells, it appears as though the signal is not able to activate UCP3 to affect a lower membrane potential and ultimately decrease ROS production.

Overall, this preliminary study has shown that impaired metabolism can be elicited in muscle cells from euglycemic subjects with a past history of obesity-associated diabetes, despite resolution of the clinical diabetic state through weight loss. We have documented defects in mitochondrial biogenesis as well as the inability of muscle cells to mitigate ROS production and oxidative damage in response to situations of chronic high glucose and insulin. These results provide new insight into the metabolic differences between

individuals who are prone to the development of obesity-associated diabetes and those who are not; however, it should be noted that these results do not necessarily apply to lean individuals at risk for T2DM. Although this study has provided clues as to the mechanisms of the disordered metabolism, it remains to be determined whether these phenotypic characteristics are genetically programmed or acquired epigenetically.

REFERENCES

1. Kopelman, P.G. 2000. Obesity as a medical problem. *Nature* 404:635-643.

2. Gregg, E.W., Y.J. Cheng, K.M. Narayan, T.J. Thompson, and D.F. Williamson. 2007. The relative contributions of different levels of overweight and obesity to the increased prevalence of diabetes in the United States: 1976-2004. *Prev Med* 45:348-352.

3. Gregg, E.W., Y.J. Cheng, B.L. Cadwell, G. Imperatore, D.E. Williams, K.M. Flegal, K.M. Narayan, and D.F. Williamson. 2005. Secular trends in cardiovascular disease risk factors according to body mass index in US adults. *JAMA* 293:1868-1874.

4. Frayling, T.M. 2007. Genome-wide association studies provide new insights into type 2 diabetes aetiology. *Nat Rev Genet* 8:657-662.

5. Ferrannini, E., J.D. Smith, C. Cobelli, G. Toffolo, A. Pilo, and R.A. DeFronzo. 1985. Effect of insulin on the distribution and disposition of glucose in man. *J Clin Invest* 76:357-364.

6. DeFronzo, R.A., R. Gunnarsson, O. Bjorkman, M. Olsson, and J. Wahren. 1985. Effects of insulin on peripheral and splanchnic glucose metabolism in noninsulin-dependent (type II) diabetes mellitus. *J Clin Invest* 76:149-155.

7. Phillips, D.I., S. Caddy, V. Ilic, B.A. Fielding, K.N. Frayn, A.C. Borthwick, and R. Taylor. 1996. Intramuscular triglyceride and muscle insulin sensitivity: evidence for a relationship in nondiabetic subjects. *Metabolism* 45:947-950.

8. Perseghin, G., P. Scifo, F. De Cobelli, E. Pagliato, A. Battezzati, C. Arcelloni, A. Vanzulli, G. Testolin, G. Pozza, A. Del Maschio, and L. Luzi. 1999. Intramyocellular triglyceride content is a determinant of in vivo insulin resistance in humans: a 1H-13C nuclear magnetic resonance spectroscopy assessment in offspring of type 2 diabetic parents. *Diabetes* 48:1600-1606.

9. Krssak, M., K. Falk Petersen, A. Dresner, L. DiPietro, S.M. Vogel, D.L. Rothman, M. Roden, and G.I. Shulman. 1999. Intramyocellular lipid concentrations are correlated with insulin sensitivity in humans: a 1H NMR spectroscopy study. *Diabetologia* 42:113-116.

10. van Loon, L.J., and B.H. Goodpaster. 2006. Increased intramuscular lipid storage in the insulin-resistant and endurance-trained state. *Pflugers Arch* 451:606-616.

11. Koves, T.R., J.R. Ussher, R.C. Noland, D. Slentz, M. Mosedale, O. Ilkayeva, J. Bain, R. Stevens, J.R. Dyck, C.B. Newgard, G.D. Lopaschuk, and D.M. Muoio. 2008.

Mitochondrial overload and incomplete fatty acid oxidation contribute to skeletal muscle insulin resistance. *Cell Metab* 7:45-56.

12. Hegarty, B.D., G.J. Cooney, E.W. Kraegen, and S.M. Furler. 2002. Increased efficiency of fatty acid uptake contributes to lipid accumulation in skeletal muscle of high fat-fed insulin-resistant rats. *Diabetes* 51:1477-1484.

13. Muoio, D.M., and C.B. Newgard. 2008. Mechanisms of disease: molecular and metabolic mechanisms of insulin resistance and beta-cell failure in type 2 diabetes. *Nat Rev Mol Cell Biol* 9:193-205.

14. Kelley, D.E., B.H. Goodpaster, and L. Storlien. 2002. Muscle triglyceride and insulin resistance. *Annu Rev Nutr* 22:325-346.

15. Ravussin, E., and S.R. Smith. 2002. Increased fat intake, impaired fat oxidation, and failure of fat cell proliferation result in ectopic fat storage, insulin resistance, and type 2 diabetes mellitus. *Ann N Y Acad Sci* 967:363-378.

16. Lowell, B.B., and G.I. Shulman. 2005. Mitochondrial dysfunction and type 2 diabetes. *Science* 307:384-387.

17. Patti, M.E., A.J. Butte, S. Crunkhorn, K. Cusi, R. Berria, S. Kashyap, Y. Miyazaki, I. Kohane, M. Costello, R. Saccone, E.J. Landaker, A.B. Goldfine, E. Mun, R. DeFronzo, J. Finlayson, C.R. Kahn, and L.J. Mandarino. 2003. Coordinated reduction of genes of oxidative metabolism in humans with insulin resistance and diabetes: Potential role of PGC1 and NRF1. *Proc Natl Acad Sci U S A* 100:8466-8471.

18. Morino, K., K.F. Petersen, S. Dufour, D. Befroy, J. Frattini, N. Shatzkes, S. Neschen, M.F. White, S. Bilz, S. Sono, M. Pypaert, and G.I. Shulman. 2005. Reduced mitochondrial density and increased IRS-1 serine phosphorylation in muscle of insulin-resistant offspring of type 2 diabetic parents. *J Clin Invest* 115:3587-3593.

19. Kelley, D.E., J. He, E.V. Menshikova, and V.B. Ritov. 2002. Dysfunction of mitochondria in human skeletal muscle in type 2 diabetes. *Diabetes* 51:2944-2950.

20. Toledo, F.G., E.V. Menshikova, V.B. Ritov, K. Azuma, Z. Radikova, J. DeLany, and D.E. Kelley. 2007. Effects of physical activity and weight loss on skeletal muscle mitochondria and relationship with glucose control in type 2 diabetes. *Diabetes* 56:2142-2147.

21. Menshikova, E.V., V.B. Ritov, F.G. Toledo, R.E. Ferrell, B.H. Goodpaster, and D.E. Kelley. 2005. Effects of weight loss and physical activity on skeletal muscle mitochondrial function in obesity. *Am J Physiol Endocrinol Metab* 288:E818-825.

22. Eriksson, J.W. 2007. Metabolic stress in insulin's target cells leads to ROS accumulation - a hypothetical common pathway causing insulin resistance. *FEBS Lett* 581:3734-3742.

23. Pieczenik, S.R., and J. Neustadt. 2007. Mitochondrial dysfunction and molecular pathways of disease. *Exp Mol Pathol* 83:84-92.

24. Civitarese, A.E., and E. Ravussin. 2008. Mitochondrial energetics and insulin resistance. *Endocrinology* 149:950-954.

25. Evans, J.L., I.D. Goldfine, B.A. Maddux, and G.M. Grodsky. 2002. Oxidative stress and stress-activated signaling pathways: a unifying hypothesis of type 2 diabetes. *Endocr Rev* 23:599-622.

26. Evans, J.L., B.A. Maddux, and I.D. Goldfine. 2005. The molecular basis for oxidative stress-induced insulin resistance. *Antioxid Redox Signal* 7:1040-1052.

27. Houstis, N., E.D. Rosen, and E.S. Lander. 2006. Reactive oxygen species have a causal role in multiple forms of insulin resistance. *Nature* 440:944-948.

28. Evans, J.L., I.D. Goldfine, B.A. Maddux, and G.M. Grodsky. 2003. Are oxidative stress-activated signaling pathways mediators of insulin resistance and beta-cell dysfunction? *Diabetes* 52:1-8.

29. Anderson, E.J., M.E. Lustig, K.E. Boyle, T.L. Woodlief, D.A. Kane, C.T. Lin, J.W. Price, 3rd, L. Kang, P.S. Rabinovitch, H.H. Szeto, J.A. Houmard, R.N. Cortright, D.H. Wasserman, and P.D. Neufer. 2009. Mitochondrial H2O2 emission and cellular redox state link excess fat intake to insulin resistance in both rodents and humans. *J Clin Invest*

30. Chung, S.S., M. Kim, B.S. Youn, N.S. Lee, J.W. Park, I.K. Lee, Y.S. Lee, J.B. Kim, Y.M. Cho, H.K. Lee, and K.S. Park. 2009. Glutathione peroxidase 3 mediates the antioxidant effect of peroxisome proliferator-activated receptor gamma in human skeletal muscle cells. *Mol Cell Biol* 29:20-30.

31. Wilson, P.W., R.S. Paffenbarger, Jr., J.N. Morris, and R.J. Havlik. 1986. Assessment methods for physical activity and physical fitness in population studies: report of a NHLBI workshop. *Am Heart J* 111:1177-1192.

32. Dent, R.M., R.M. Penwarden, N. Harris, and S.B. Hotz. 2002. Development and evaluation of patient-centered software for a weight-management clinic. *Obes Res* 10:651-656.

33. Ahituv, N., N. Kavaslar, W. Schackwitz, A. Ustaszewska, J. Martin, S. Hebert, H. Doelle, B. Ersoy, G. Kryukov, S. Schmidt, N. Yosef, E. Ruppin, R. Sharan, C. Vaisse, S.

Sunyaev, R. Dent, J. Cohen, R. McPherson, and L.A. Pennacchio. 2007. Medical sequencing at the extremes of human body mass. *Am J Hum Genet* 80:779-791.

34. DeFronzo, R.A., J.D. Tobin, and R. Andres. 1979. Glucose clamp technique: a method for quantifying insulin secretion and resistance. *Am J Physiol* 237:E214-223.

35. Costford, S.R., N. Kavaslar, N. Ahituv, S.N. Chaudhry, W.S. Schackwitz, R. Dent, L.A. Pennacchio, R. McPherson, and M.E. Harper. 2007. Gain-of-function R225W mutation in human AMPKgamma3 causing increased glycogen and decreased triglyceride in skeletal muscle. *PLoS ONE* 2:e903.

36. Scaduto, R.C., Jr., and L.W. Grotyohann. 1999. Measurement of mitochondrial membrane potential using fluorescent rhodamine derivatives. *Biophys J* 76:469-477.

37. McIntyre, E.A., R. Halse, S.J. Yeaman, and M. Walker. 2004. Cultured muscle cells from insulin-resistant type 2 diabetes patients have impaired insulin, but normal 5-amino-4-imidazolecarboxamide riboside-stimulated, glucose uptake. *J Clin Endocrinol Metab* 89:3440-3448.

38. Wensaas, A.J., A.C. Rustan, K. Lovstedt, B. Kull, S. Wikstrom, C.A. Drevon, and S. Hallen. 2007. Cell-based multiwell assays for the detection of substrate accumulation and oxidation. *J Lipid Res* 48:961-967.

39. Echtay, K.S., D. Roussel, J. St-Pierre, M.B. Jekabsons, S. Cadenas, J.A. Stuart, J.A. Harper, S.J. Roebuck, A. Morrison, S. Pickering, J.C. Clapham, and M.D. Brand. 2002. Superoxide activates mitochondrial uncoupling proteins. *Nature* 415:96-99.

40. Echtay, K.S., M.P. Murphy, R.A. Smith, D.A. Talbot, and M.D. Brand. 2002. Superoxide activates mitochondrial uncoupling protein 2 from the matrix side. Studies using targeted antioxidants. *J Biol Chem* 277:47129-47135.

41. Echtay, K.S., T.C. Esteves, J.L. Pakay, M.B. Jekabsons, A.J. Lambert, M. Portero-Otin, R. Pamplona, A.J. Vidal-Puig, S. Wang, S.J. Roebuck, and M.D. Brand. 2003. A signalling role for 4-hydroxy-2-nonenal in regulation of mitochondrial uncoupling. *Embo J* 22:4103-4110.

42. Kelley, D.E., R. Wing, C. Buonocore, J. Sturis, K. Polonsky, and M. Fitzsimmons. 1993. Relative effects of calorie restriction and weight loss in noninsulin-dependent diabetes mellitus. *J Clin Endocrinol Metab* 77:1287-1293.

43. Goodpaster, B.H., D.E. Kelley, R.R. Wing, A. Meier, and F.L. Thaete. 1999. Effects of weight loss on regional fat distribution and insulin sensitivity in obesity. *Diabetes* 48:839-847.

44. Goodpaster, B.H., R. Theriault, S.C. Watkins, and D.E. Kelley. 2000. Intramuscular lipid content is increased in obesity and decreased by weight loss. *Metabolism* 49:467-472.

45. Szczepaniak, L.S., E.E. Babcock, F. Schick, R.L. Dobbins, A. Garg, D.K. Burns, J.D. McGarry, and D.T. Stein. 1999. Measurement of intracellular triglyceride stores by H spectroscopy: validation in vivo. *Am J Physiol* 276:E977-989.

46. Weiss, R., S. Dufour, S.E. Taksali, W.V. Tamborlane, K.F. Petersen, R.C. Bonadonna, L. Boselli, G. Barbetta, K. Allen, F. Rife, M. Savoye, J. Dziura, R. Sherwin, G.I. Shulman, and S. Caprio. 2003. Prediabetes in obese youth: a syndrome of impaired glucose tolerance, severe insulin resistance, and altered myocellular and abdominal fat partitioning. *Lancet* 362:951-957.

47. Kelley, D.E., M. Mokan, and L.J. Mandarino. 1992. Intracellular defects in glucose metabolism in obese patients with NIDDM. *Diabetes* 41:698-706.

48. Shulman, G.I., D.L. Rothman, T. Jue, P. Stein, R.A. DeFronzo, and R.G. Shulman. 1990. Quantitation of muscle glycogen synthesis in normal subjects and subjects with non-insulin-dependent diabetes by 13C nuclear magnetic resonance spectroscopy. *N Engl J Med* 322:223-228.

49. He, J., and D.E. Kelley. 2004. Muscle glycogen content in type 2 diabetes mellitus. *Am J Physiol Endocrinol Metab* 287:E1002-1007.

50. Eriksson, J., A. Franssila-Kallunki, A. Ekstrand, C. Saloranta, E. Widen, C. Schalin, and L. Groop. 1989. Early metabolic defects in persons at increased risk for non-insulin-dependent diabetes mellitus. *N Engl J Med* 321:337-343.

51. Mootha, V.K., C.M. Lindgren, K.F. Eriksson, A. Subramanian, S. Sihag, J. Lehar, P. Puigserver, E. Carlsson, M. Ridderstrale, E. Laurila, N. Houstis, M.J. Daly, N. Patterson, J.P. Mesirov, T.R. Golub, P. Tamayo, B. Spiegelman, E.S. Lander, J.N. Hirschhorn, D. Altshuler, and L.C. Groop. 2003. PGC-1alpha-responsive genes involved in oxidative phosphorylation are coordinately downregulated in human diabetes. *Nat Genet* 34:267-273.

52. Petersen, K.F., D. Befroy, S. Dufour, J. Dziura, C. Ariyan, D.L. Rothman, L. DiPietro, G.W. Cline, and G.I. Shulman. 2003. Mitochondrial dysfunction in the elderly: possible role in insulin resistance. *Science* 300:1140-1142.

53. Unoki, H., and S. Yamagishi. 2008. Advanced glycation end products and insulin resistance. *Curr Pharm Des* 14:987-989.

54. Schrauwen, P., M.K. Hesselink, E.E. Blaak, L.B. Borghouts, G. Schaart, W.H. Saris, and H.A. Keizer. 2001. Uncoupling protein 3 content is decreased in skeletal muscle of patients with type 2 diabetes. *Diabetes* 50:2870-2873.

Chapter 2 - Metabolic Characterization of the Human AMPKγ3 R225W Mutation

Contribution of Collaborators

Sean A. Crawford

Collected *vastus lateralis* samples at muscle biopsies, processed muscle biopsies for histology and myoblast isolation, isolated myoblasts, maintained cell cultures, performed assays for glucose uptake, glycogen synthesis, mitochondrial content, oxidative capacity, glycogen content, IMTG content, TCA cycle metabolites, and western blotting. Assisted with muscular fatigue, strength testing and positron emission tomography (PET) scanning, and performed blood metabolite data analysis. Analyzed data for the above described experiments. Table/Figure contributions: Figures 1-12, and 14-17.

Sheila R. Costford

Collected *vastus lateralis* samples at muscle biopsies, processed muscle biopsies for histology and myoblast isolation, isolated myoblasts, performed qRT-PCR. Analyzed data for the above described experiments. Assisted with muscular fatigue, strength testing and PET scanning. Table/Figure contributions: Table 1 and Figure 13. Contributed to project design and data analysis.

Robert Dent

Clinician for one of the probands. Contacted and recruited this subject and members of her family. Conducted some muscle biopsies. Assisted in interpretation of findings.

RUTH MCPHERSON

As Principal Investigator of the Thin Gene Study, Dr McPherson contacted and recruited the other proband and members of their family. Assisted in the design of the study. Conducted some muscle biopsies and. Assisted in data analysis and interpretation of findings.

ROBERT BEANLANDS

Assisted in study design, interpretation of findings, and coordinated PET scanning.

MARY-ELLEN HARPER

Assisted in study design, and the overall organization amongst collaborators. Assisted in data analysis and interpretation. Was awarded as PI the peer-reviewed funding for this research (Heart and Stroke Foundation of Ontario).

INTRODUCTION

AMP-ACTIVATED PROTEIN KINASE (AMPK) STRUCTURE

AMPK is a heterotrimeric enzyme that can form 12 distinct complexes, each comprising an α catalytic subunit (α1 or α2), as well as β and γ regulatory subunits (β1 or β2 and γ1, γ2 or γ3) (reviewed in (1)). The α catalytic subunit is responsible for the kinase activity of AMPK. It also possesses an important phosphorylation site at Thr172, that when phosphorylated, significantly enhances enzyme activity (2). The β regulatory subunit contains a glycogen binding domain (CBM; (3, 4)). The binding of mature glycogen granules to the β-subunit results in the allosteric inhibition of AMPK activity (5). Finally, the γ regulatory subunit contains two Bateman domains which can each bind a single AMP or ATP molecule, as determined by crystallographic studies of fission yeast (6). The binding of AMP induces a conformational change which results in the allosteric activation of AMPK and renders it an inferior substrate for phosphatases (7-9).

The expression of all AMPK subunits can be detected to some extent in skeletal muscle; however, it is thought that only three of the possible 12 heterotrimeric complexes are formed:α1/β2/γ1, α2/β2/γ1 and α2/β2/γ3 (10). Of these three complexes, α2/β2/γ3 is thought to be the predominant active complex in skeletal muscle as it is the only complex that is responsive to high-intensity exercise (11). Expression of the γ3 subunit is specific to skeletal muscle (12).

AMPK Activation

The activation of AMPK is controlled through two known pathways: **1)** a Ca^{2+}-dependent pathway mediated by the calmodulin-dependent protein kinase, CaMKKβ (13-15), and **2)** an AMP-dependent pathway mediated by the tumor suppressor, LKB1 (7, 16, 17). The latter of these two pathways is best characterized in skeletal muscle and enables AMPK to act as a central energy sensor within the cell by monitoring intracellular levels of ATP, AMP and glycogen through the specific binding sites on the β and γ regulatory subunits.

The binding of AMP to the γ subunit of AMPK results in a 5 to 10-fold increase in enzymatic activity (18, 19). In addition to this allosteric activation, the binding of AMP also induces a conformational change that makes the α-subunit a better substrate for upstream kinases while at the same time protecting it from dephosphorylation, resulting in up to a 50-fold increase in activity (2, 16, 20). In contrast, high ATP levels are capable of inhibiting AMPK activity through the displacement of AMP from the γ-subunit (8). The typical ATP:ADP ratio within a cell is 10:1. As this ratio declines, adenylate kinase converts two ADP molecules into one ATP and one AMP molecule, thus raising AMP levels within the cell and activating AMPK (Figure 2-1; (21)).

AMPK Function

When activated, AMPK acts to restore the cellular energy balance by stimulating ATP-producing pathways and inhibiting ATP-consuming pathways. AMPK activation 'turns on' processes and pathways associated with fuel catabolism such as glucose uptake, fatty

Figure 2-1: AMP/ATP regulation of AMPK (adapted From [21]). AMP (adenosine monophosphate); ADP (adenosine diphosphate); ATP (adenosine triphosphate); AMPK (AMP-activated protein kinase)

Figure 2-1: AMP/ADP/ATP regulation of AMPK

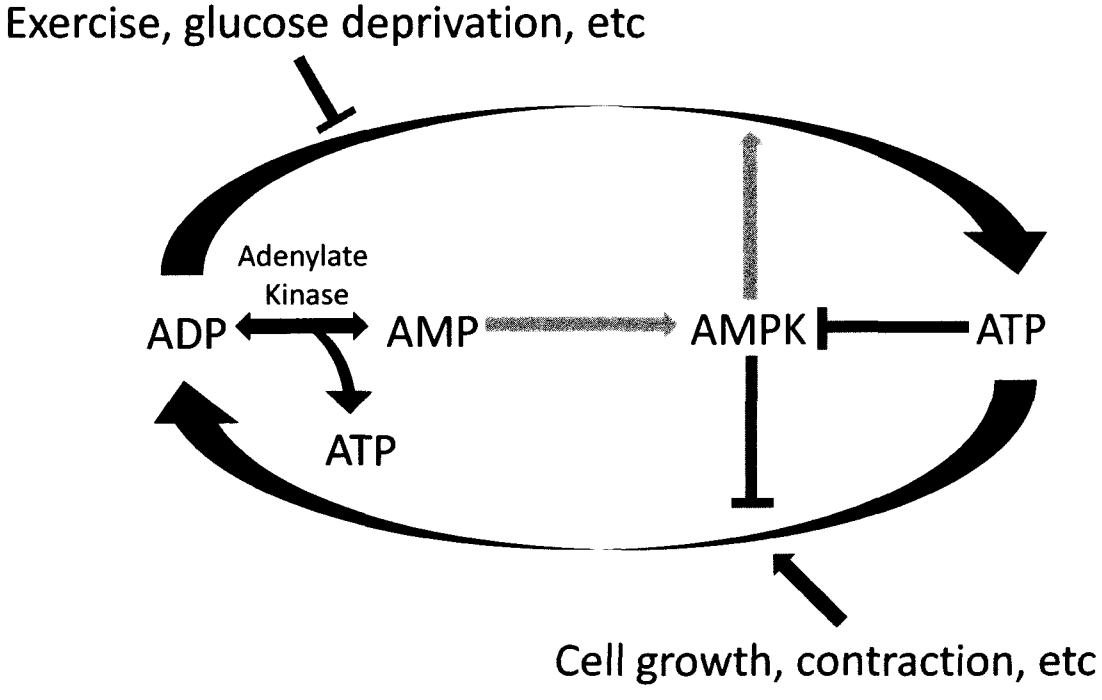

acid oxidation, and mitochondrial biogenesis (22-25) while 'turning off' those that are anabolic, such as fatty acid synthesis, glycogen synthesis, and protein synthesis (26-30) (Figure 2-2).

In a recent study, it was demonstrated that overexpression or ablation of the AMPKγ_3 subunit in mice did not alter mitochondrial biogenesis. However, overexpression of the gain-of-function AMPKγ_3 R225Q mutation (similar to the R225W mutation studied herein) resulted in enhanced mitochondrial biogenesis (31). This enhanced mitochondrial biogenesis was associated with increases in several transcription factors that regulate mitochondrial biogenesis, including peroxisome proliferator-activated receptor γ coactivator-1α (PGC-1α), mitochondrial transcription factor A (mTFA), and nuclear respiratory factor 1 (NRF-1) (31). Additionally, chronic AMPK activation through either AICAR treatment or endurance training has been shown to increase skeletal muscle expression of both glucose transporter 4 (GLUT4) and hexokinase in mice (32).

Human AMPKγ_3 R225W Mutation

The naturally occurring R225W mutation was identified in humans by our laboratory as a gain-of-function mutation that results in a doubling of both basal and AMP-stimulated AMPK activity ((33)). This mutation is analogous to both the γ_3 R225Q mutation identified in RN$^-$ Hampshire Pigs (34) as well as the γ_2 R302Q mutation in humans (35-37). All three of these mutations are paradoxically characterized by the storage of excess glycogen in skeletal muscle (γ_3 R225Q and R225W) or in the heart (γ_2 R302Q) (33-35). Despite the inhibitory effects of AMPK on glycogen synthase, it is hypothesized that increased glucose

Figure 2-2: Molecular regulation of AMPK and downstream targets of AMPK (Adapted from [21, 59]). IL-6 (interleukin-6); CNTF (ciliary neurotrophic factor); PFK2 (phosphofructokinase); ACC (acetyl-CoA carboxylase); PGC1α (PPARγ coactivator1α); GS (glycogen synthase); mTOR (mammalian target of rapamycin); EF2K (eukaryotic elongation factor-2 kinase

Figure 2-2: Whole body regulation of AMPK

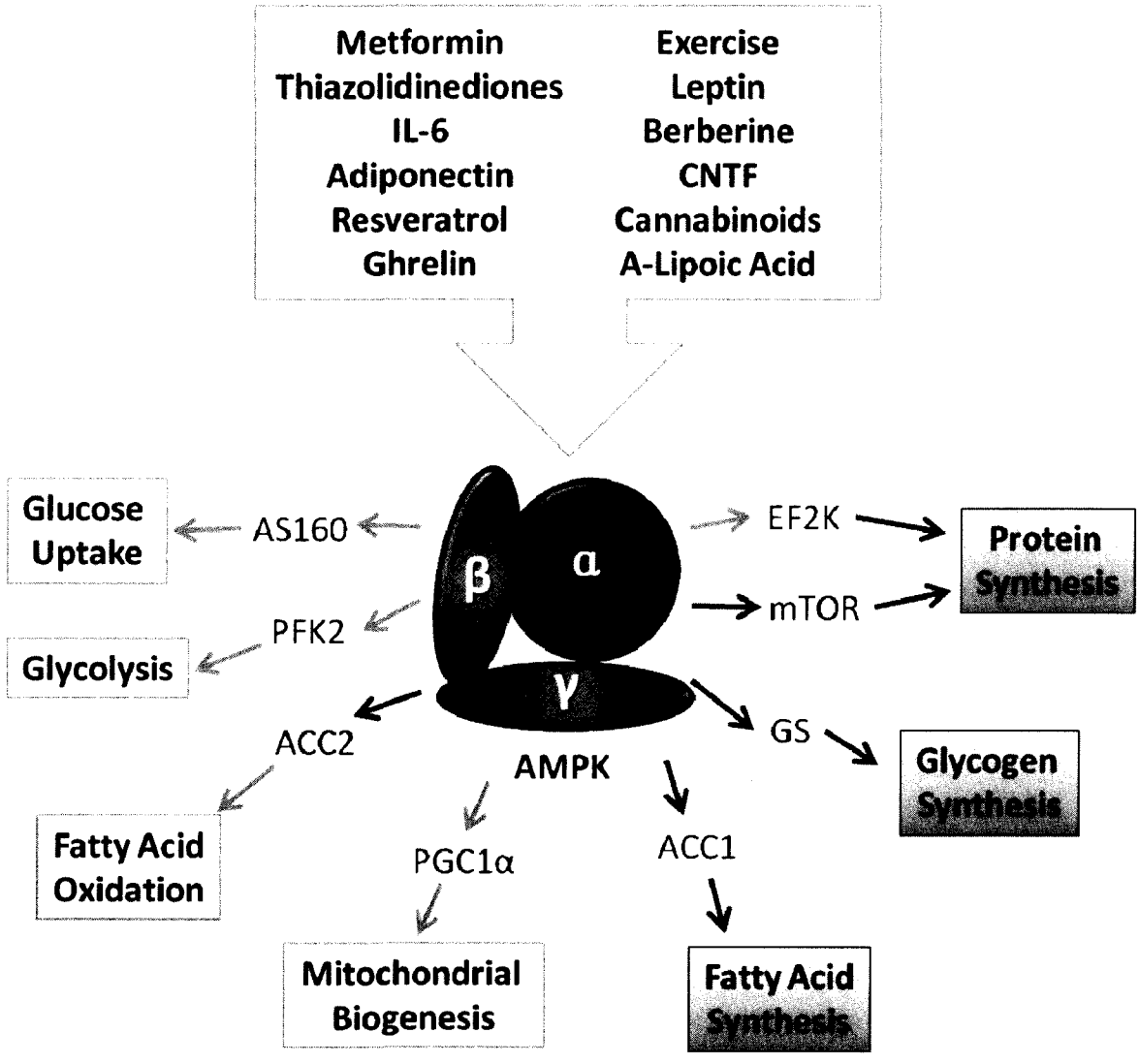

uptake may overwhelm and override the AMPK dependent inhibition of glycogen synthase (5, 32). Subjects with the γ_3 R225W mutation also exhibit a 30% decrease in the levels of intracellular triglycerides (33).

In subjects carrying the AMPKγ_3 R225W mutation, the characterization of skeletal muscle fuel metabolism, oxidative capacity, and insulin sensitivity will help further elucidate the role of AMPKγ_3 in human skeletal muscle metabolism. The AMPK-mediated induction of glucose uptake in many cell types (38) and the inhibition of hepatic glucose production (39) make AMPK an ideal pharmaceutical target for the treatment of type 2 diabetes mellitus (T2DM). The drugs metformin, rosiglitazone, and pioglitazone are often prescribed for the treatment of T2DM, and all in fact act partially through activation of AMPK (40, 41). While the advantages of AMPK activation in the liver and skeletal muscle are evident, there are also negative consequences of activating AMPK in other tissues of the body. Enhanced AMPK activation in the hypothalamus results in increased food intake, which would adversely affect individuals with T2DM (42). Enhanced activation of AMPK in the heart causes increased glycogen storage which can lead to Wolf-Parkinson White syndrome, conduction syndrome disease, and cardiac hypertrophy (35-37). Furthermore, it has been suggested that the increased risk of myocardial infarction associated with rosiglitazone treatment is associated with elevated AMPK activity in the heart (43, 44). These negative side-effects of systemic AMPK activation make the γ_3 subunit an ideal pharmacological target for the treatment of T2DM. Since the γ_3 subunit is expressed exclusively in skeletal muscle (12), its pharmalogical activation would result in AMPK activation in skeletal muscle alone. The gain-of-function nature of the AMPKγ_3 R225W

mutation (33) renders its carriers exciting subjects for studies of the potential of the γ subunit as a pharmacological target for the treatment of T2DM.

Overall Aim

The overall aim of this project was to characterize skeletal muscle metabolism of subjects carrying the R225W AMPKγ_3 mutation.

Hypothesis

The R225W gain-of-function mutation in the AMPKγ_3 subunit will result in 1) increased skeletal muscle glucose uptake *in vivo,* and 2) increased glucose uptake and oxidative capacity in primary human myotubes *in vitro.*

Specific Objectives

The specific objectives of this study were:

- To examine *in vivo* skeletal muscle glucose uptake in AMPKγ_3 R225W carriers and matched control subjects in the resting and exercised states via positron emission tomography (PET)

To examine basal and insulin-stimulated glucose uptake and glycogen synthesis, fuel storage (glycogen and intramuscular triglyceride content), oxidative capacity (citrate synthase and cytochrome c oxidase activity) and specific aspects of cell signaling (phospho-AMPK/AMPK, PGC1-α, mTFA, NRF-1) in differentiated primary myotubes from AMPKγ_3 R225W carriers and matched control subjects

RESEARCH DESIGN AND METHODS

SUBJECTS

Two probands carrying the R225W mutation in the γ_3 subunit of AMPK were initially identified through the Ottawa Hospital Weight Management Clinic (33). Three R225W carriers were recruited for this study and matched for age, sex, body mass index (BMI), and physical activity (International Physical Activity Questionnaire) to control subjects.

MUSCULAR STRENGTH AND ENDURANCE/FATIGUE DETERMINATIONS

Following a 12-hour overnight fast, R225W carriers and matched control subjects underwent testing to determine the quadriceps maximal force output in the dominant leg. These analyses were performed using a KinCom leg extension machine (Isokinetic International, Harrison, TN). Quadriceps maximal force output was assessed based on a series of 3-5 constant velocity (60 deg/sec) concentric and eccentric contractions performed by the subjects.

Muscular endurance/fatigue was evaluated using the KinCom machine and electromyography (EMG) following the assessment of maximal force output. EMG was used to monitor the mean frequency of contraction during a 1-min. isometric contraction of the quadriceps at 80% of the maximal eccentric force.

[^{18}F]-FLUORODEOXYGLUCOSE (FDG) POSITRON EMISSION TOMOGRAPHY (PET)

Subjects refrained from exercise during the 48-hour period between muscular strength testing and PET analysis. Following a 12-hour overnight fast, subjects were given an

intravenous (IV) line in one arm and a second arterialized IV line in the other arm. A baseline blood sample was taken immediately before the initiation of the exercise intervention for the determination of free fatty acid (FFA), cortisol, insulin, lactate, and glucose concentrations. Subjects then performed leg extensions with their dominant leg for 30 min., bearing a load equivalent to 11% of their maximal concentric force output as determined during strength testing. The leg extension consisted of a 1-second concentric phase and a 2-second eccentric phase. Subjects were prompted to perform the exercise at the correct speed using a metronome. FDG was injected 10 min. post exercise initiation (referred to as 'time 0'). Following 30 min. of exercise, subjects underwent a CT scan followed by a 20 min. PET scan. Blood samples were taken for metabolite analysis immediately prior to FDG injection, 20 min. post-injection, and 60 min. post-injection. Samples for [^{18}F] activity determination were taken immediately following injection, every 20 seconds for the first 3 min., then every 10 min. until 60 min. post-injection.

Skeletal Muscle Biopsies

Subjects refrained from physical activity for three days and were fasting for 12 hours prior to the biopsy. After local anaesthesia, biopsies of the *vastus lateralis* were obtained from the 3 R225W carriers and 3 control subjects using a 5 mm Bergstrom needle (Opitek) as described previously (33). Visible adipose tissue was removed from the biopsy and a ~25mg sample of muscle was processed for satellite cell isolation and culture.

Cell Culture

Freshly biopsied *vastus lateralis* was minced, subjected to a trypsin digestion for 30 min. and plated in Ham's F-10 medium supplemented with 15% FBS, 0.5 mg/mL BSA, 1 uM dexamethazone, 10 ng/ml EGF, 0.5 mg/ml fetuin and 25 pM insulin [growth medium]. Muscle satellite cells were isolated at ~80% confluency using an immuno-based magnetic sorting technique as previously described (33); the primary antibody used was anti-5.1H11 (Developmental Studies Hybridoma Bank) and the secondary antibody used was MACS goat anti-mouse IgG microbeads. Isolated myoblasts were grown to ~80% confluence prior to differentiation in DMEM (5.5 mM glucose, supplemented with 25 pM insulin, 2% horse serum, 1% antibiotic-antimycotic and 2.5 mg/mL gentamycin) for 7 days prior to experimentation.

Mitochondrial Yield and Enzyme Activities

Intact mitochondria were isolated from differentiated myotubes using a mitochondrial isolation kit (MITOISO2; Sigma). Mitochondrial yield was determined by dividing mitochondrial protein content by total cellular protein content, as determined by BCA assay. Cytochrome c oxidase activity was assayed in intact mitochondria using the CYTOCOX1 kit (Sigma) in which the oxidation of dithiothreitol-reduced cytochrome c was monitored spectrophotometrically at 550 nm. Citrate synthase activity was determined in lysed mitochondria using the CS0720 kit (Sigma) in which the conversion of oxaloacetate to citrate was monitored spectrophotometrically at 412 nm. Enzyme activities were normalized to both mitochondrial and total cellular protein contents.

Oxygen Consumption and H^+ Production

Oxygen consumption rate was measured in 7-day differentiated myotubes using a Seahorse Extracellular Flux Analyzer. 50,000 myoblasts were seeded per well in specialized 24-well plates (Seahorse Bioscience, North Billerica, MA) and incubated in growth medium (described above) at 37°C with 5% CO_2 for 5 h, washed once with differentiation medium and then allowed to differente for 7 days. Differentiated myotubes were then washed once in Seahorse medium (DMEM [5030; Sigma] supplemented with 5.5 mM D-glucose, 0.584 g/L L-glutamine) and incubated at 37°C for 1 h. Baseline rates were measured 4 times for 3 min. each and were separated by 7 min. intervals. Carbonyl cyanide-p-trifluoromethoxyphenylhydrazone (FCCP) or oligomycin was then injected into each well for a final concentration of 1 µM or 500 ng/mL, respectively. After a mixing period of 10 min. oxygen consumption rates were measured three additional times following these injections.

HPLC Organic Acid Analysis

2-3 x 10^6 7-day differentiated myotubes were lifted and resuspended in 300 µL of PBS. Cells were lysed by sonication and protein content determined by BCA assay. Samples were then diluted in 20 mM K_2PO_4 to a concentration of 2 mg/mL. Proteins were precipitated by the addition of 100 µL 1% perchlorate followed by centrifugation at 10,000 x g for 10 min.. Following 0.2 µM filtration of the supernatant, 20 µL of sample was injected into a 0.44 mm reverse-phase C-18 column (Agilent, Santa Clara, CA) using an isocratic solution of 20mM

K_2PO_4 as the mobile phase with detection at 210 nM. Metabolites were identified by co-elution with known standards.

Intramuscular Triglyceride Content

Intramuscular triglyceride (IMTG) content was determined in 7-day differentiated myotubes treated with or without 2 mM aminoimidazole carboxamide ribonucleotide (AICAR) for 2 h. 2-3 x 10^6 myotubes were lifted and resuspended in 1 mL of IMTG buffer (25mM Tris-HCl pH 7.5, 1mM EDTA). Total triglycerides were then extracted with chloroform-methanol (2:1)(45). The organic phase was dried under N_2 gas and the lipids were resuspended in 50 µL of 2-propanol. The concentration of triglycerides was determined using the L-Type TG H assay (WAKO).

Glycogen Content

2-3 x 10^6 7-day differentiated myotubes treated with or without 2 mM AICAR for 2 h were lifted and resuspended in 100 µL of PBM buffer (20 mM KH_2PO_4, 10 uM $CaCl_2$, 1 mM $MgCl_2$, pH 6.1) and lysed by 5 freeze–thaw cycles. Samples were boiled for 20 min. in 10 volumes of 30% KOH saturated with anhydrous Na_2SO_4 to extract the glycogen from the cells. Glycogen was precipitated with 12 volumes of 95% ethanol, dissolved in ddH_2O and incubated with 2 volumes of 0.2% anthrone in H_2SO_4 at 100°C for 20 min. The glycogen concentration was determined spectrophotometrically by measuring the absorbance at 620 nm relative to an oyster glycogen standard (Sigma).

Glucose Uptake

Glucose uptake assays were performed as described previously (46). Myoblasts were seeded in 24-well plates at 37,000 cells/cm^2, incubated for 24 h and then differentiated for 7 days. Differentiated myotubes were washed twice with uptake buffer (136 mM NaCl, 4.7 mM KCl, 1.25 mM MgSO4·7H2O, 1.2 mM CaCl·$2H_2O$, 20 mM HEPES; pH 7.4) and then incubated for 20 min. in the presence or absence of 100 nM insulin. Cells were incubated at 37°C for 10 min. with 0.5 uCi/ml [H^3]-2-deoxy-glucose and 100 µM cold 2-deoxy-glucose. Cells were then washed 3X with ice-cold PBS and lysed with ice-cold RIPA lysis buffer (Sigma) supplemented with a protease inhibitor cocktail (Roche). Total radioactivity was determined by liquid scintillation counting. Protein content was determined via BCA assay.

Glycogen Synthesis

Glycogen synthesis assays were performed as described previously (47). Myoblasts were seeded and differentiated as described above. Differentiated myotubes were glucose and serum starved for 1.5 h in glucose-free DMEM medium and then incubated with DMEM containing 5.5 mM glucose and 0.5uCi/ml [H^3]-2-deoxy-glucose with or without 100 nM insulin for 3 h. Cells were then washed 3X with ice-cold PBS and harvested in 30% KOH saturated with anhydrous Na_2SO_4. Cell lysates were incubated at 100°C for 20 min. in the presence of 6.3 ug/ul oyster glycogen. Glycogen was precipitated in ethanol, washed and then dissolved in ddH_2O. Radioactive glycogen was determined by liquid scintillation counting. Protein content was determined in cell lysates via BCA assay.

RNA Extraction and qRT-PCR

RNA was extracted with Trizol from 7-day differentiated myotubes, flash frozen and shipped to the Pennington Biomedical Research Center (Baton Rouge, LA) for analysis. RNA was column purified using the Qiagen RNeasy Fibrous Mini Kit (Qiagen). RNA purity was determined on an Agilent 2100 Bioanalyzer (Agilent Technologies, Palo Alto, CA) and RNA quantity was determined using an ND-1000 Nanodrop Spectrophotometer (Thermo Fisher Scientific, Wilmington, MA). Primers and probes were designed for PGC-1α, mTFA, and NRF-1 using Primer Express version 2.1 (Applied Biosystems, Foster City, CA) (Table 2-1). The concentration of target mRNAs was determined by quantitative reverse transcriptase PCR (qRT-PCR) using Taqman primers and fluorescent probes as the detection system. The qRT-PCR was performed on an ABI PRISM 7900 (Applied Biosystems, Foster City, CA) using the following parameters: one cycle of 48°C for 30 min., then 95°C for 10 min., followed by 40 cycles at 95°C for 15 s and 60°C for 1 min. All expression data was normalized to the ribosomal phosphoprotein large P0 housekeeping gene (RPLP0).

WESTERN BLOTTING

7-day differentiated myotubes were lysed in RIPA buffer (150 mM NaCl, 50 mM Tris (pH 7.4), 1 mM EDTA, 1% (v/v) NP-40, 0.25% (w/v) sodium deoxycholate) supplemented with 50 mM NaF, 5mM NaPP, 1 mM $NaVO_3$, and a protease inhibitor cocktail (Roche). Protein content was determined via BCA assay. Lysates were separated on a 10% bis-tris polyacrylamide gel and proteins transferred to a nitrocellulose membrane. Antibodies against phospho-AMPK (2535; Cell Signaling; dilution 1:1000), manganese superoxide dismutase (mnSOD) (sc-30080; Santa Cruz; dilution 1:1000), Peroxisome proliferator-activated receptor gamma, coactivator 1 alpha (PGC-1α) (sc-13067; Santa Cruz; dilution

1:100), succinate dehydrogenase (SDH, sc-59687, Santa Cruz, Dilution 1:2000), cytochrome c oxidase (MS404; MitoSciences; 1:500), and β-actin (4967L; Cell Signaling; dilution 1:1000) were incubated overnight at 4°C and detected using anti-rabbit HRP (sc-2030; Santa Cruz; 1:1000) or anti-mouse HRP (sc-2031; Santa Cruz; 1:2000). Visualization was achieved using an Enhanced Chemi-Luminescence kit (Amersham Pharmacia). Spot densitometry was performed using an Alpha multi-image light camera and Alpha imaging software.

Table 2-1: Oligonucleotide sequences for primer/probe sets used in Taqman analysis.

PGC-1α (peroxisome proliferator-activated receptor γ coactivator-1α); mTFA (mitochondrial transcription factor A); NRF-1 (nuclear respiratory factor 1); RPLP0 (ribosomal protein, large, P0).

Gene	Sense (5'-3')	Antisense (3'-5')	Probe (5' 6-FAM-BHQ-1 3')
PGC-1α	AGGTGAAAGTGTAATACTGTTGGT TGA	CATGTAGAATTGGCAGGTGGAA	TGCTGAAGAGGGAAAGTGAGCGA TTAGTTGA
mTFA	CCAGATGCAAAAACTACAGAACTA A	AGTTCTACGAATATCCCGCCT	TCCAACGCTGGGCAATTCTTCTA
NRF-1	CGTTGCCCAAGTGAATTATTCTG	TAACCCGGTGCAATGTCCC	TTGTTCCACCTCTCCATCAGCCA
RPLP0	CCATTCTATCATCAACGGGTACAA	AGCAAGTGGGAAGGTGTAATCC	TCTCCACAGACAAGGCCAGGACTC G

RESULTS

MUSCULAR FATIGUE DETERMINATIONS

All subjects underwent a 60-second isometric contraction of the quadriceps at 80% of their maximal force during which electromyography (EMG) traces were recorded for the *vastus lateralis*, *vastus medialis*, and *rectus femoris* muscles. The R225W carriers demonstrated a remarkable resistance to fatigue as compared to matched controls (Figure 2-3; $p<0.05$). In these determinations, the rate of fatigue was determined through a linear regression of the mean frequency over time (mV/s), and a negative slope (a decrease in contractile force) is indicative of fatigue. Interestingly, the R225W subjects had a positive slope, indicating an increase in the mean frequency over time, which may suggest the recruitment of a larger number of muscle fibers.

GLUCOSE UPTAKE IN VIVO

Glucose uptake was measured *in vivo* by positron emission tomography (PET) in resting and exercised quadriceps following a unilateral 30 min leg extension exercise against a constant resistance equivalent to 11% of the subject's maximal force output. While two of the three R225W subjects exhibited a strong trend for increased total and maximal glucose uptake in the exercised leg, one of R225W subjects exhibited very low levels of glucose uptake in the exercised leg. A trend toward a larger volume of muscle actively taking up glucose in the exercising leg was also apparent in R225W carriers, as defined by the volume of skeletal muscle meeting the threshold standard uptake value (SUV) of 1.0 in exercising leg (Figure 2-4). No differences were observed in the resting leg; however, due to the low number of

Figure 2-3: Rates of muscular fatigue. (A) Representative EMG traces of Vastus Lateralis (Blue), Vastus Medialis (Green), and Femoris (Pink) Quadriceps. Traces represent the mean frequency of contraction over a 60 second period. B) Quantification of EMG, values represent the slope of the mean frequency (mV/s) ± SEM, student's T-test ($P<0.05$)

Figure 2-3: Rates of muscular fatigue

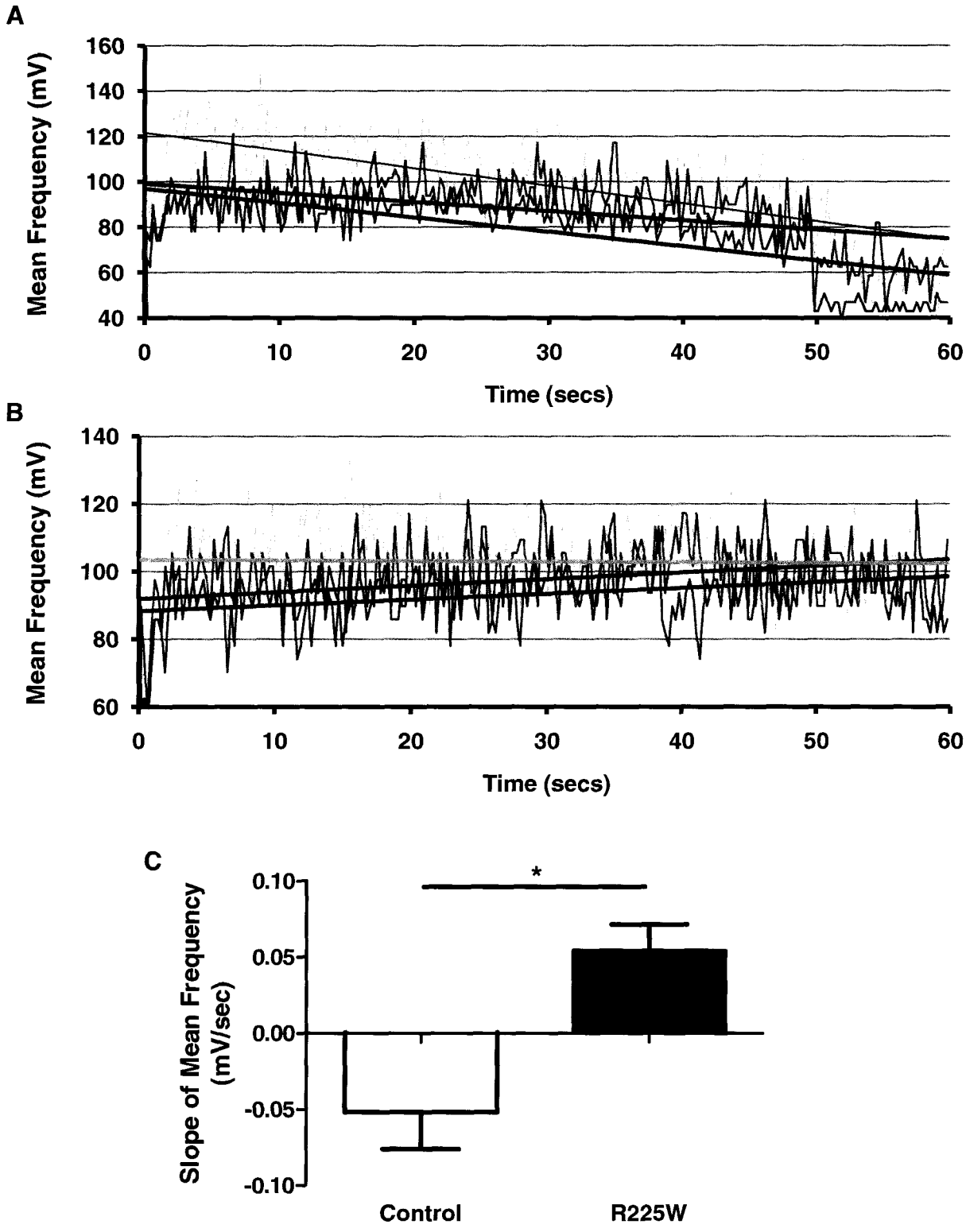

Figure 2-4: Glucose uptake *in vivo* via positron emission tomography (PET). Subjects performed a leg extension exercise on their dominant leg against a resistance equivalent to 11% of their maximal force output followed by a PET/CT scan. (A,C) Representative PET and (B,D) PET/CT overlay images (left leg– resting; right leg – exercised); (E) total volume of quadriceps muscle group with an standard uptake value SUV > 1.0; (F) total FDG uptake in the exercised leg; and (G) plasma cortisol levels. Red symbol denotes an outlier excluded from the analysis.

Figure 2-4: Glucose *vivo via* positron emission tomography (PET)

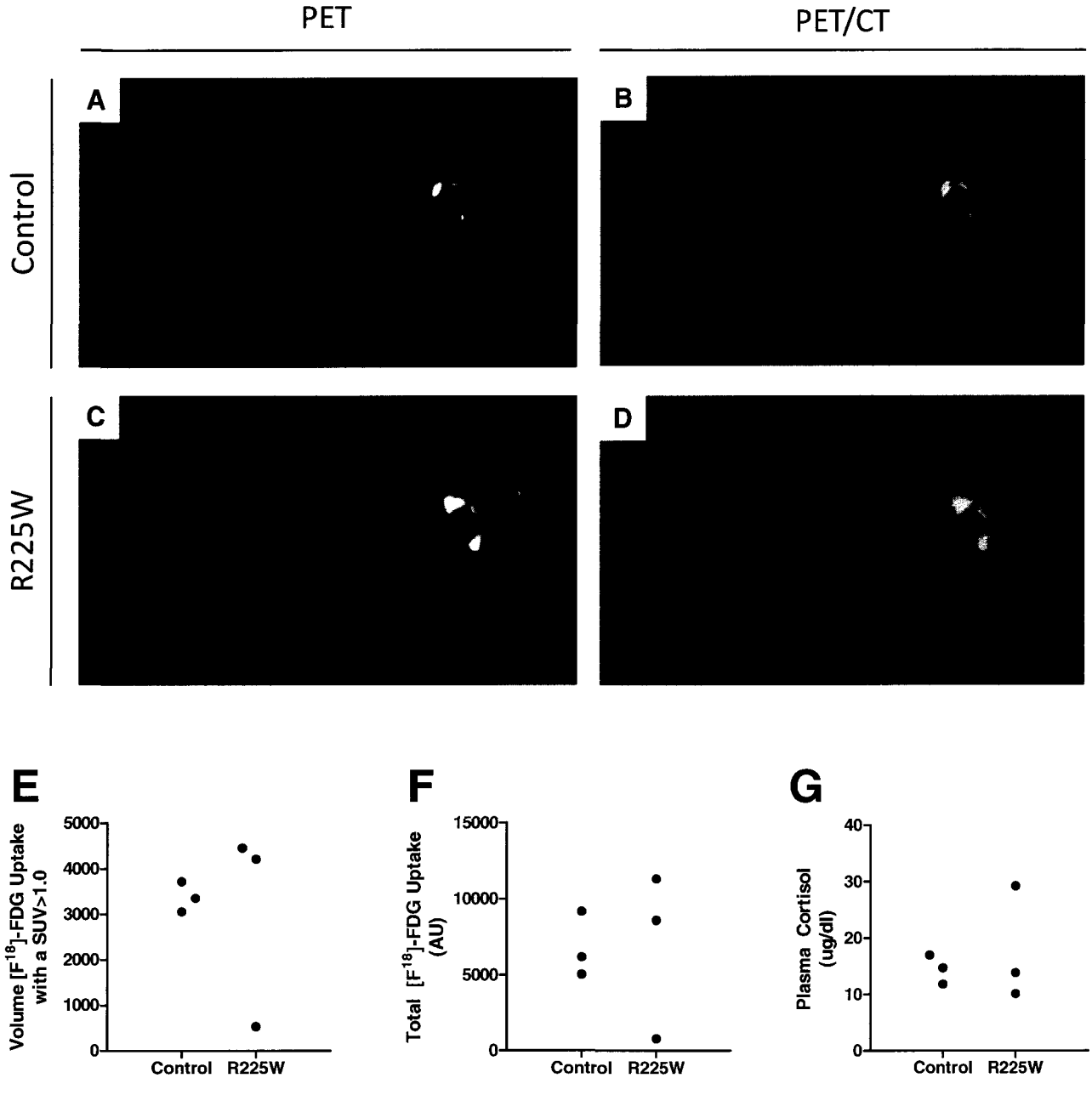

subjects in this study, the power of this technique to detect differences in glucose uptake in the non-exercised state is low. Serum glucose, lactate, and FFA were also measured at -10, 0, 20, 60 minutes. No differences were observed in either serum glucose or lactate; however, the relative increase in serum FFA was higher in the carriers of the R225W mutation relative to matched controls (Figure 2-5).

Glucose Uptake and Glycogen Synthesis in vitro

Differentiated myotubes from R225W carriers exhibited a 1.8-fold higher basal glucose uptake rates relative to those in cells from matched controls ($p<0.01$; Figure 2-6A). The myotubes from R225W carriers also demonstrated similar absolute changes in glucose uptake following insulin stimulation compared to changes in cells from control subjects (Figure 2-6B).

Basal glycogen-synthesis rates were measured for 3 hours in the presence or absence of insulin following a 1.5 hour 'fast' in glucose- and serum- free medium. Basal glycogen synthesis was significantly enhanced (2.3-fold, $p<0.05$) in R225W carriers relative to matched controls. Insulin stimulation resulted in a 1.8 fold of the rate of glycogen synthesis in control myotubes (Figure 2-7, effect of genotype, $p<0.05$); however, insulin stimulation did not result in any further increase in the R225W myotubes (Figure 2-7).

Fuel Storage

Previously our laboratory has shown *ex vivo* that muscle fibers from R225W carriers have ~30% lower IMTG content and ~90% higher glycogen content (33). AMPK has also been shown previously to enhance fatty acid oxidation (48). In the current study we examined

Figure 2-5: Relative change in serum free fatty acid levels (FFA). Percent increase in serum free fatty acid levels post-exercise in R225W carriers (black bars) and matched controls (white bars). N=3, means ± SEM, paired t-test, *$p<0.05$

Figure 2-5: Relative change in serum free fatty acid levels (FFA)

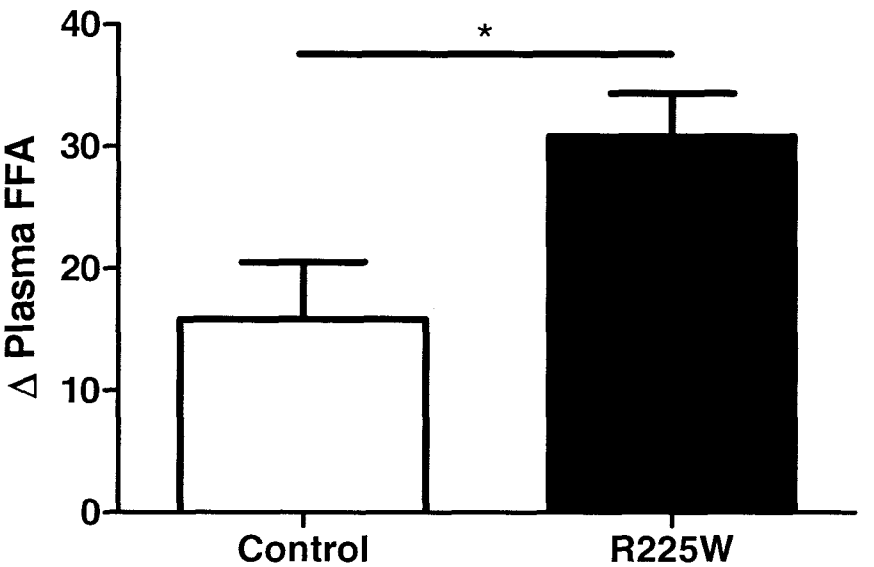

Figure 2-6: Glucose uptake *in vitro* (A) Basal and insulin-stimulated uptake of [H^3]-2-deoxy-glucose and (B) absolute change in [H^3]-2-deoxy-glucose uptake from basal following insulin-stimulation in differentiated control (white bars) and R225W (black bars) myotubes. N=3, means ± SEM, two-way ANOVA, Bonferroni correction, *$p<0.05$, **$p<0.01$

Figure 2-6: Glucose uptake *in vitro*

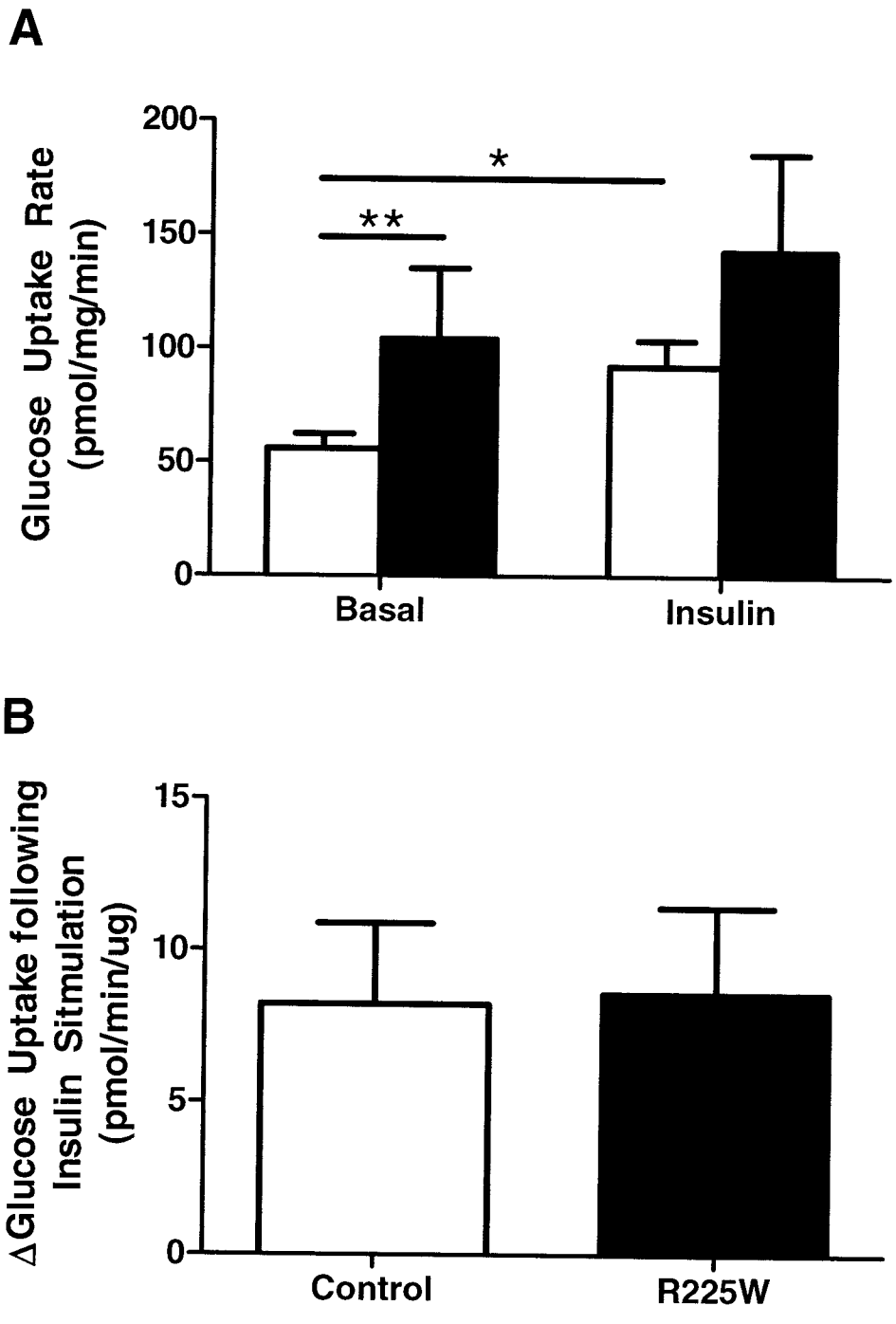

Figure 2-7: Rates of glycogen synthesis. Rate of glycogen synthesis as determined by [H^3]-2-deoxy-glucose incorporation into glycogen in the presence or absence of insulin in differentiated control (white bars) and R225W (black bars) myotubes. N=3, means ± SEM, two-way ANOVA, affect of genotype $p<0.05$

Figure 2-7: Rates of glycogen synthesis

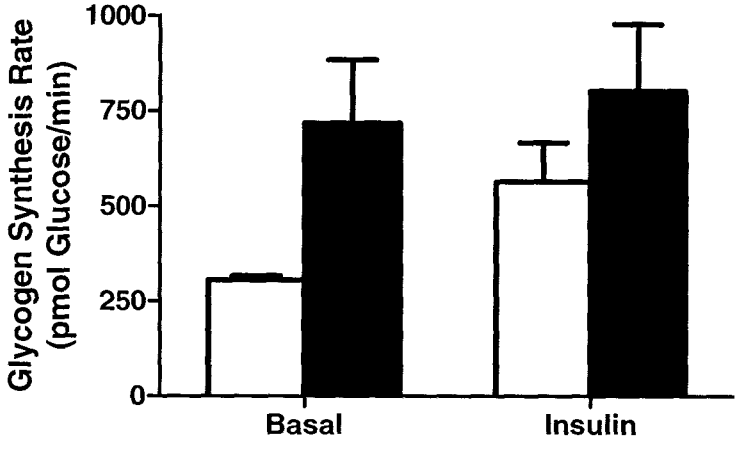

fuel storage in 7-day differentiated myotubes from R225W carriers and matched controls. Cells from R225W carriers exhibited a trend for decreased IMTG stores (Figure 2-8B). Similarly, the acute treatment of myotubes with the AMPK activator, aminoimidazole carboxamide ribonucleotide (AICAR), resulted in a trend for decreased IMTG stores in the control cells, but not in the R225W cells.

Differentiated myotubes from R225W carriers had a 1.3-fold increase in glycogen relative to matched controls ($p<0.01$). Paradoxically, the acute treatment of both control and R225W myotubes with the AMPK activator AICAR, resulted in a decrease in glycogen content (Figure 2-8A, $p<0.001$).

Oxidative Capacity

Myotubes from subjects carrying the R225W mutation were found to have a ~3-fold increase in total mitochondrial content ($p<0.01$), as assessed by the ratio of mitochondrial protein to cellular protein (Figure 2-9). Cytochrome c oxidase activity and citrate synthase activity were measured as markers for electron transport chain (ETC) and TCA cycle capacity, respectively. R225W cells exhibited a 2.5-fold higher cellular cytochrome c oxidase activity compared to control cells ($p<0.01$), but exhibited no difference in cytochrome c oxidase activity at the mitochondrial level (Figure 2-10A,B). Interestingly, citrate synthase activity was 9-fold higher in R225W myotubes at the cellular level ($p<0.05$) and 3-fold higher at the mitochondrial level ($p<0.05$) compared to control cells (Figure 2-10C,D). These results suggest that R225W carriers have enhanced TCA cycle capacity in addition to increased mitochondrial content.

Figure 2-8: Glycogen and IMTG content (A) Glycogen content of control and R225W differentitated myotubes in the presence (white bars) or absence (black bars) of AICAR, (B) Intramuscular triglyceride content of control and R225W differentiated myotubes in the presence (black bars) or absence (white bars) of AICAR. N=3, means ± SEM, two-way ANOVA, Bonferroni correction, **p<0.01, ***p<0.001

Figure 2-8: Glycogen and IMTG content

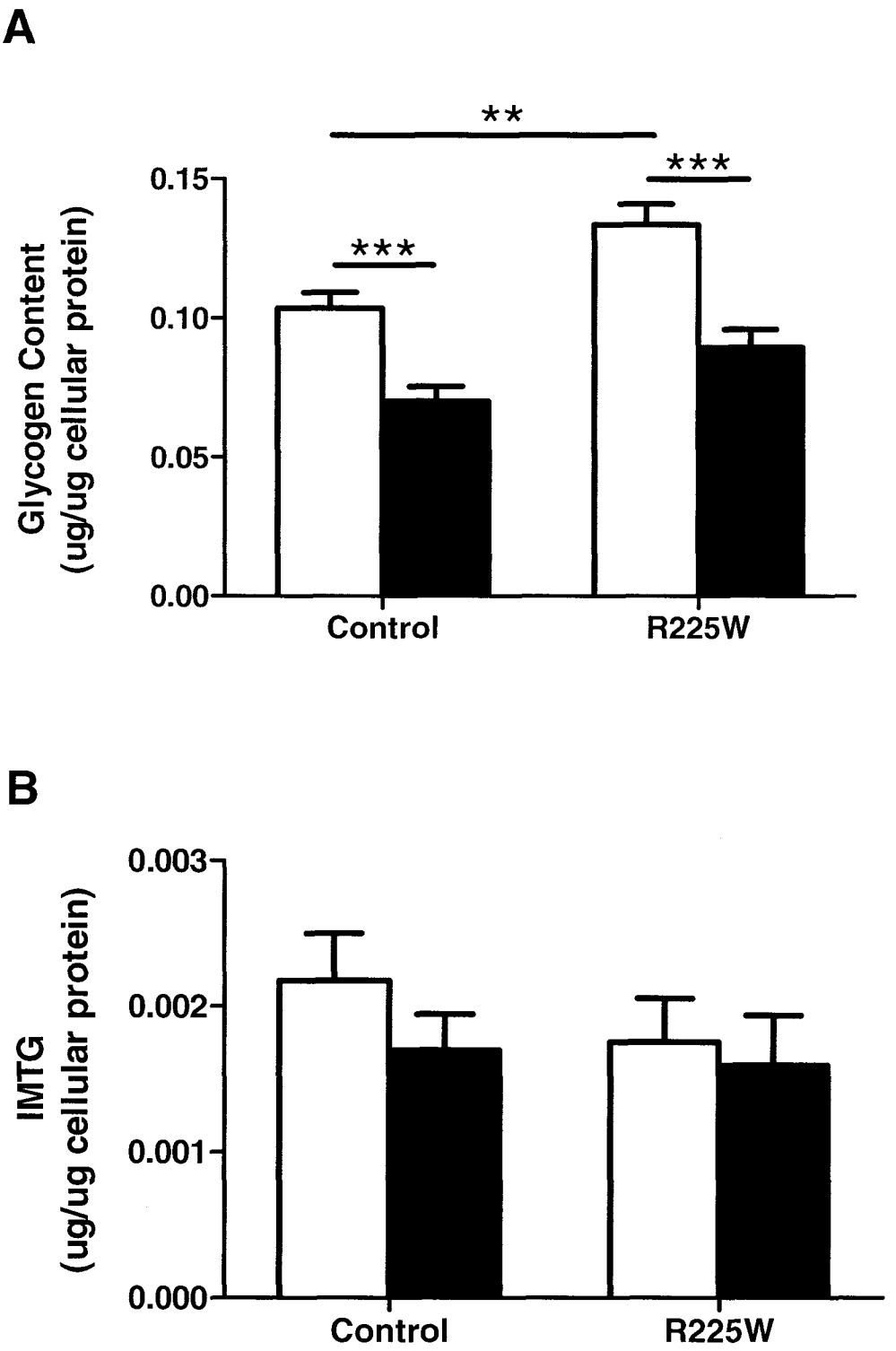

Figure 2-9: Mitochondrial content. Mitochondrial content of control and R225W differentiated myotubes as determined by the ratio between total mitochondrial protein and total cellular protein. N=3, paired Student's *t* test, **p<0.01

Figure 2-9: Mitochondrial content

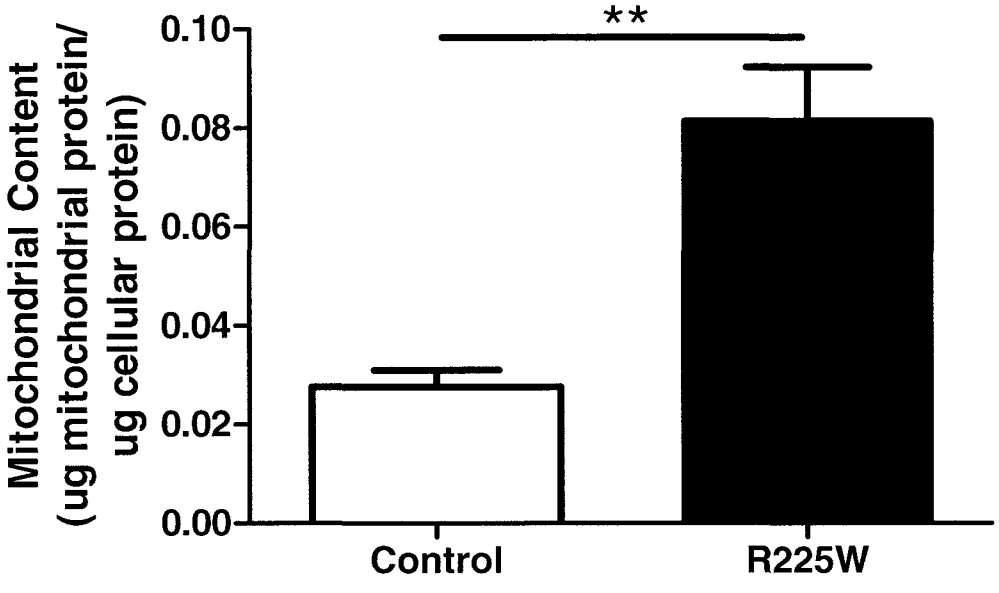

Figure 2-10: Oxidative capacity. (A,B) Cytochrome c oxidase activity in isolated mitochondria of control and R225W differentiated myotubes normalized to cellular and mitochondrial protein, respectively; (C,D) citrate synthase activity in isolated mitochondria of control and R225W differentiated myotubes normalized to cellular and mitochondrial protein, respectively. N=3, paired student's *t* test, *p<0.05 **p<0.01

Figure 2-10: Oxidative capacity

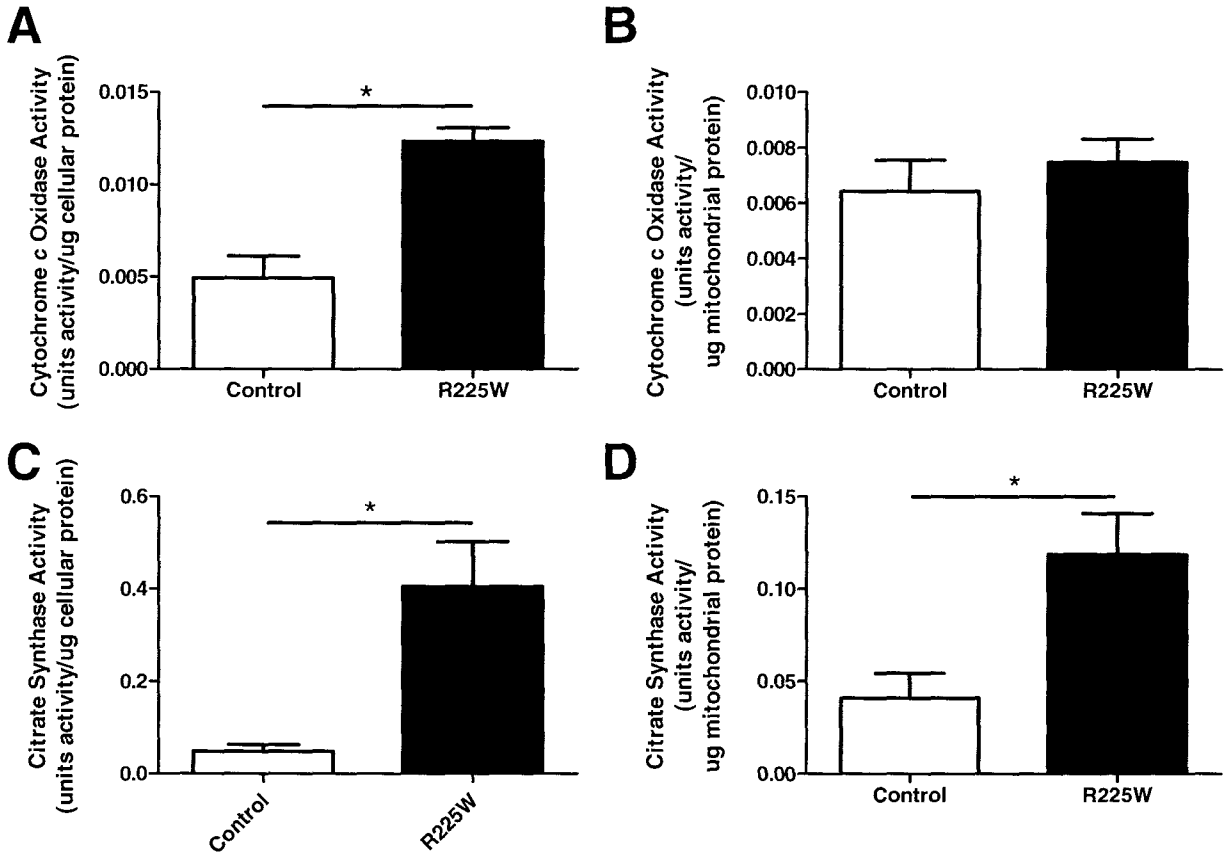

To further assess this discrepancy between the ETC and TCA cycle capacities , the relative amounts of several TCA cycle metabolites were evaluated. Succinate, α-ketoglutarate, citrate, fumarate, and malate were separated from whole cell lysates on a C-18 column by high performance liquid chromatography (HPLC) and quantified at 210 nm by co-elution with known standards. No significant differences were observed between the concentrations of these metabolites in R225W carriers and those of matched controls (Figure 2-11).

Oxygen Consumption and Extracellular Acidification Rates

Oxygen consumption and extracellular acidification rates were evaluated in differentiated myotubes using an extracellular flux analyzer (XF-24, Seahorse Bioscience). Maximal oxygen consumption and leak-dependent respiration were evaluated in the presence of the chemical uncoupler, FCCP or the inhibitor of ATP synthase, oligomycin, respectively. Myotubes from R225W carriers demonstrated a ~2.5-fold increase in maximal oxygen consumption (Figure 2-12A, $p<0.01$), consistent with the observed increases in mitochondrial content. R225W carriers also exhibited elevated leak-dependent respiration ($p<0.05$) and a trend toward increases in basal oxygen consumption. No significant changes were observed in the extracellular acidification rate (Figure 2-12B).

mRNA Analyses

To further assess the factors mediating the increased mitochondrial content seen in R225W carriers, mRNA expression of the mitochondrial transcription factors PGC-1α, mTFA, and NRF-1 was quantified in R225W carriers and matched controls by qRT-PCR (Figure 2-13). No

Figure 2-11: TCA cycle metabolites. Relative amounts of (A) malate; (B) α-ketoglutarate; (C) citrate; (D) fumarate and (E) succinate normalized to cellular protein. N=3, means ± SEM, paired student's *t* test, NS

Figure 2-11: TCA cycle metabolites

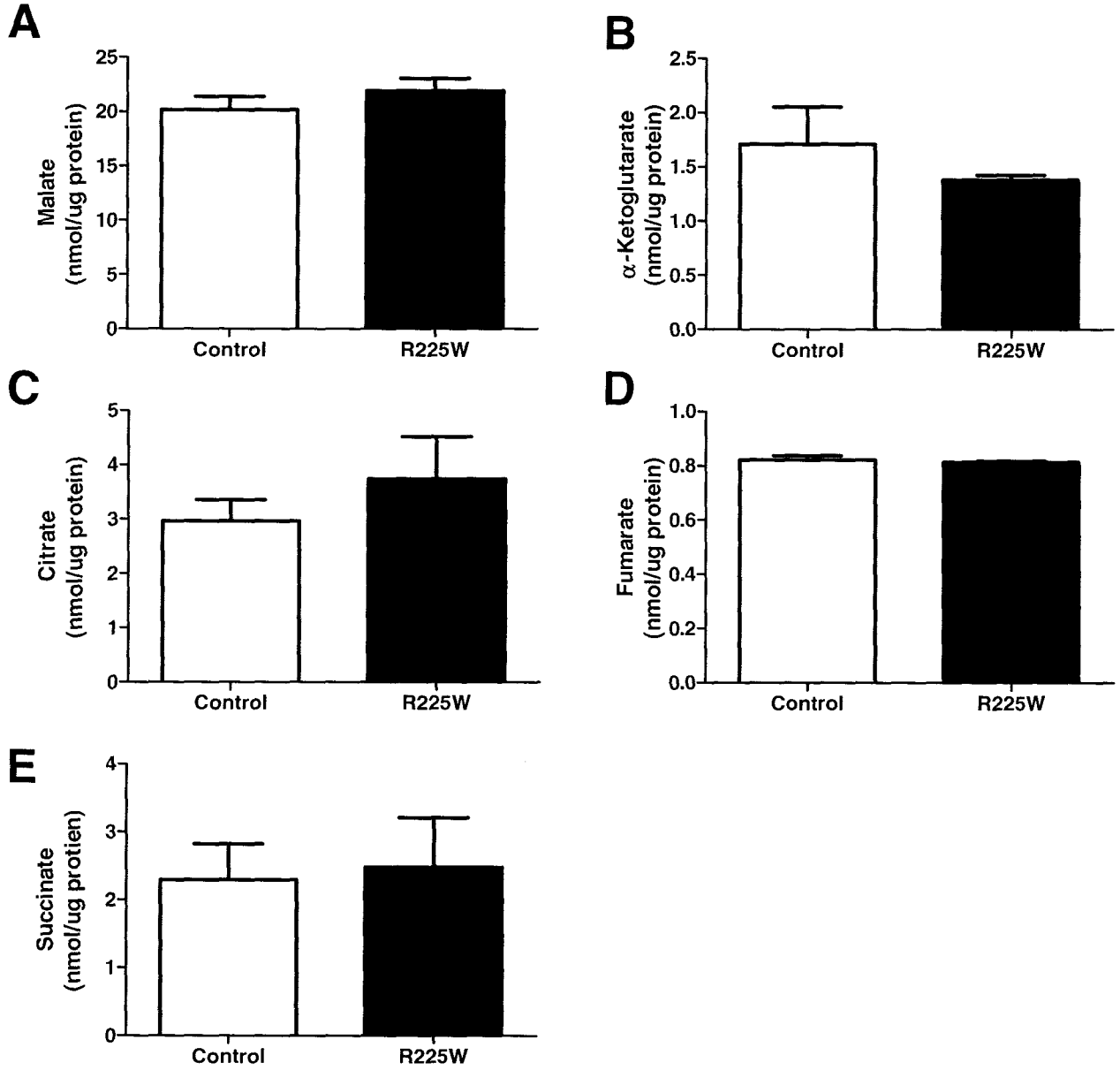

Figure 2-12: Oxygen consumption and extracellular acidification rate. (A) Cellular oxygen consumption and (B) extracellular acidification rate in R225W (black bars) or control (white bars) differentiated myotubes in the presence of oligomycin or FCCP. N=3, means ± SEM, paired student's *t* test, *p<0.05, **p<0.01

Figure 2-12: Oxygen consumption and extracellular acidification rate

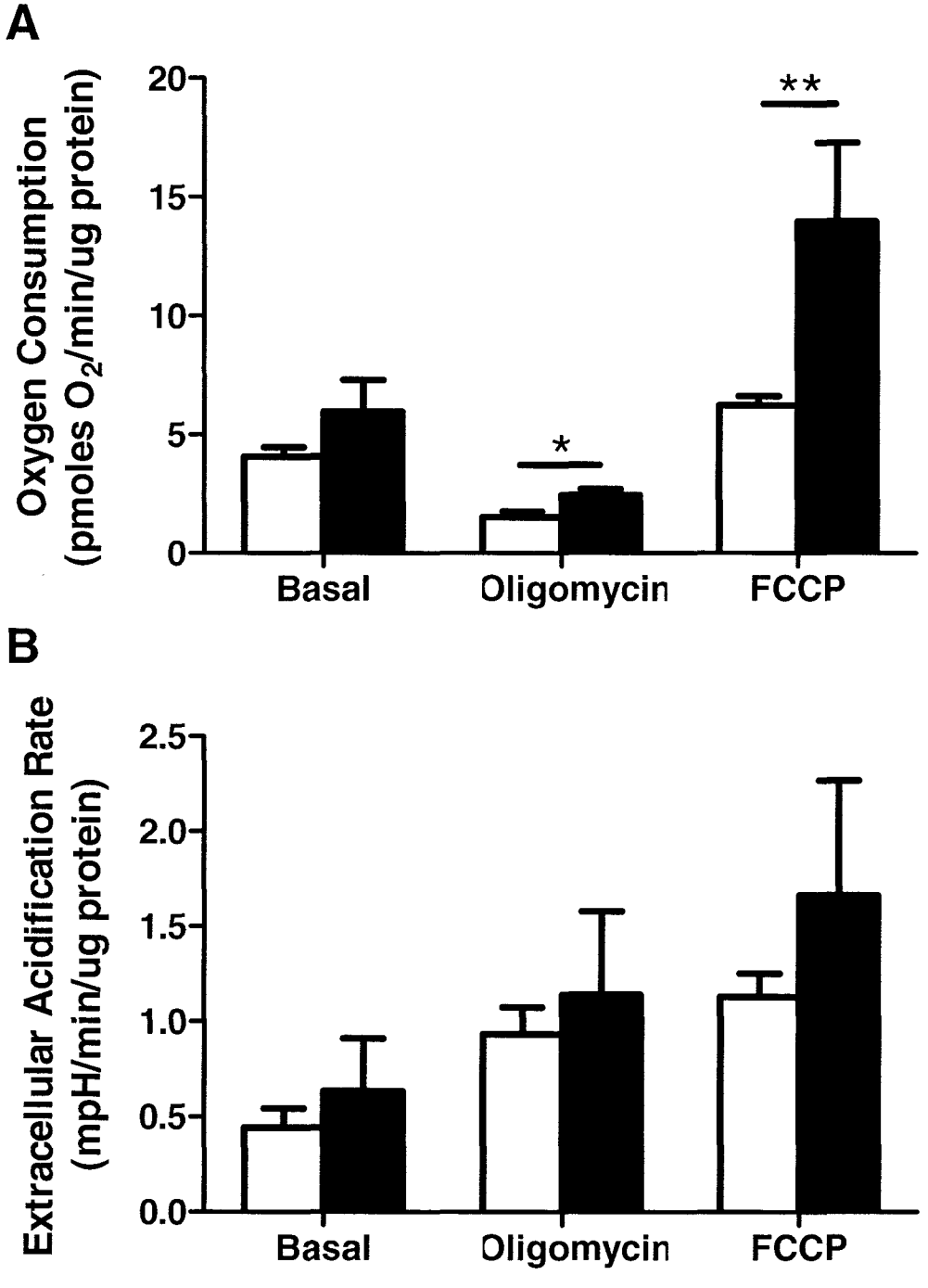

Figure 2-13: PGC-1α, mTFA, and NRF-1 mRNA. (A) PGC-1α, (B) mTFA, and (C) NRF-1 mRNA expression normalized to the ribosomal protein, large, P0 housekeeping gene (RPLP0). N=3, means ± SEM, two-way ANOVA, NS

Figure 2-13: PGC-1α, mTFA, and NRF-1 mRNA

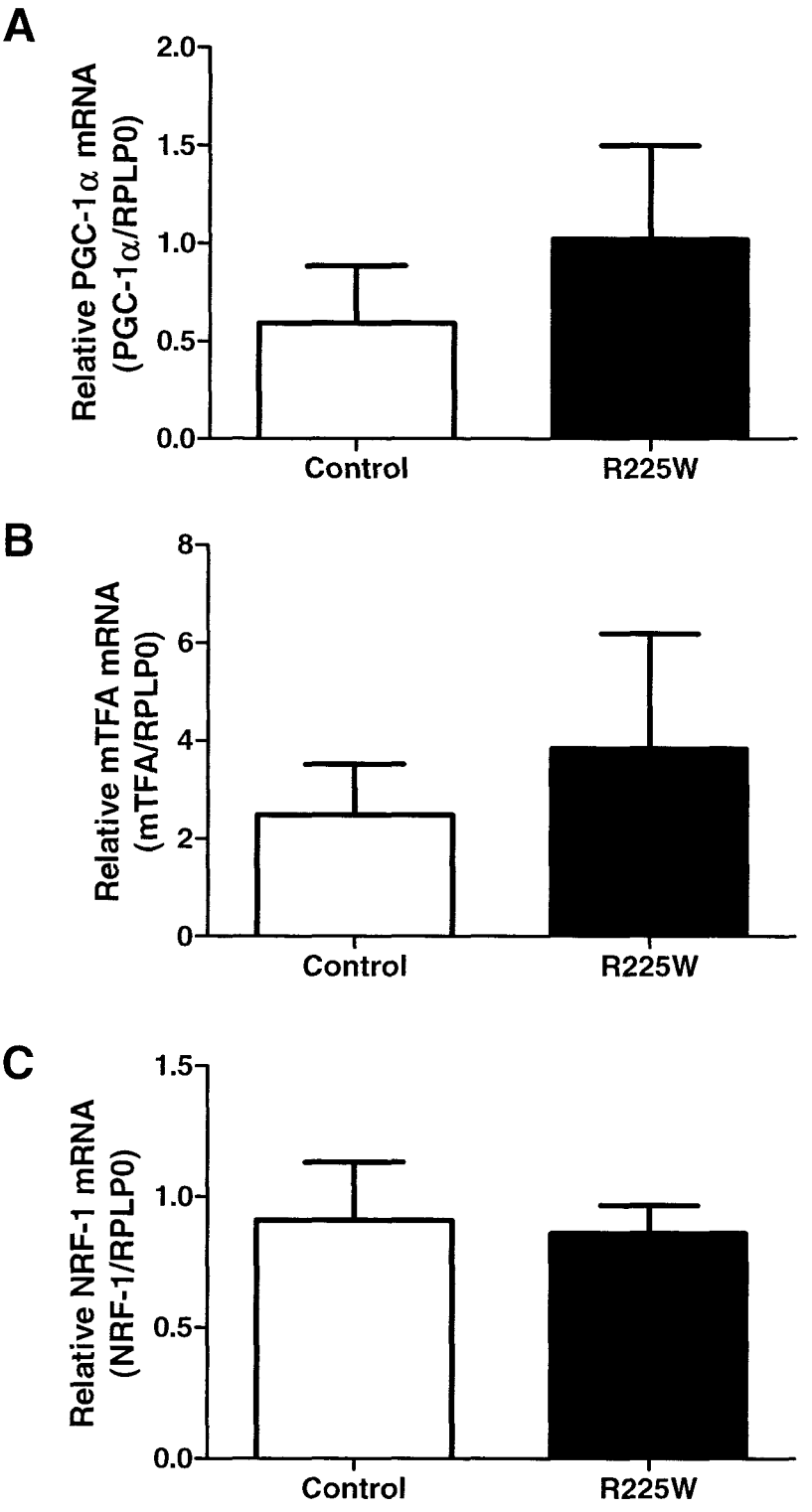

significant differences were observed in PGC-1α, mTFA or NRF-1 mRNA, as the inter-subject variability in these genes was much greater than any clear difference between groups.

Western Blotting

As expected, there was a a strong trend towards increased levels of AMPK phosphorylation, as assessed by the ratio of P-AMPK to AMPK, in myotubes of R225W carriers compared to matched controls (Figure 2-14). However, the expression of the catalytic alpha subunit of AMPK was found to be significantly lower in the R225W myotubes, suggesting an important feedback inhibition pathway in the regulation of AMPK. Cytochrome c oxidase expression was also found to be ~2.5-fold higher in myotubes from R225W carriers, consistent with the increase in cytochrome c oxidase activity as well as the increase in mitochondrial content (Figure 2-15; $p<0.05$). No significant differences were observed in the expression of the transcription factor, PGC1-α, or the expression of the mitochondrial reactive oxygen species scavenger, mnSOD, between R225W carriers and matched controls (Figure 2-16Figure 2-17)

Figure 2-14: Phospho-AMPK (p-AMPK) and AMPK α1 content(A) Representative Western blots of phospho-AMPK α1/α2 and AMPK α1 expression in control and R225W myotubes; (B) densitometry of phospho-AMPK normalized to AMPK; (C) densitometry of AMPK expression normalized to β-actin, means ± SEM, paired student's t-test, *$p<0.05$

Figure 2-14: Phospho-AMPK (p-AMPK) and AMPK α1 content

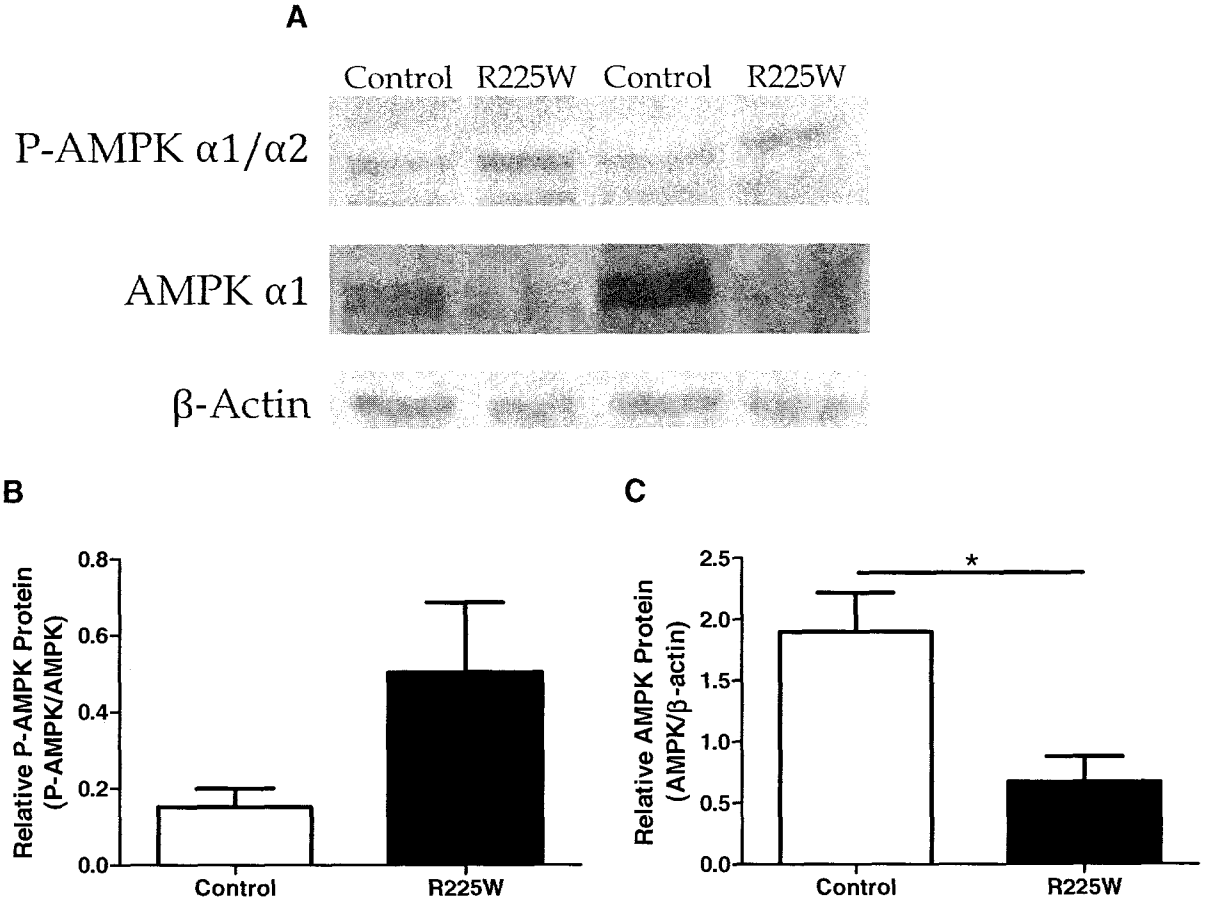

Figure 2-15: Cytochrome c Oxidase (COX-1) Content (A) Representative Western blot of cytochrome c oxidase expression in control and R225W myotubes; (B) densitometry of cytochrome c oxidase normalized to β-actin, means ± SEM, paired student's t-test, *$p<0.05$

Figure 2-15: Cytochrome c oxidase (COX-1) content

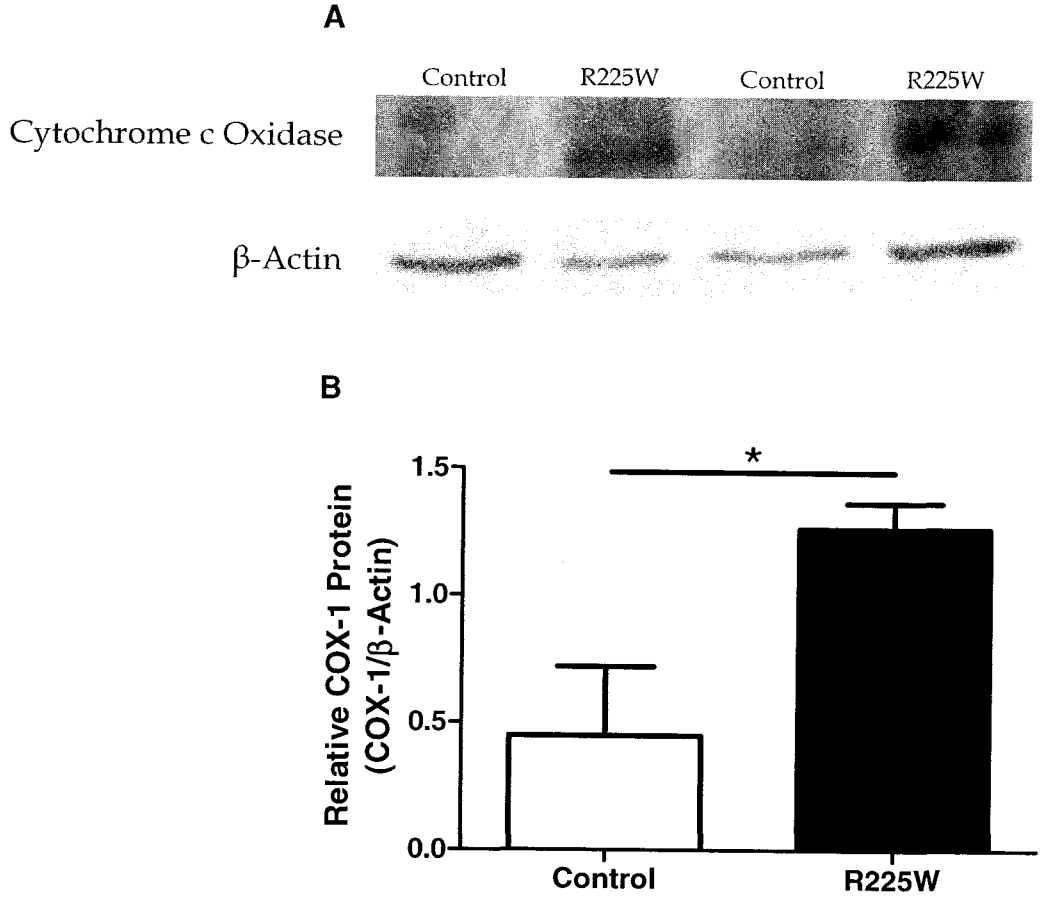

Figure 2-16: PPARγ co-activator1α (PGC-1α) Content (A) Representative Western blot of PGC-1α expression in control and R225W myotubes; (B) densitometry of PGC-1α normalized to β-actin, means ± SEM, paired student's t-test, NS

Figure 2-16: PPARγ co-activator1α (PGC-1α) Content

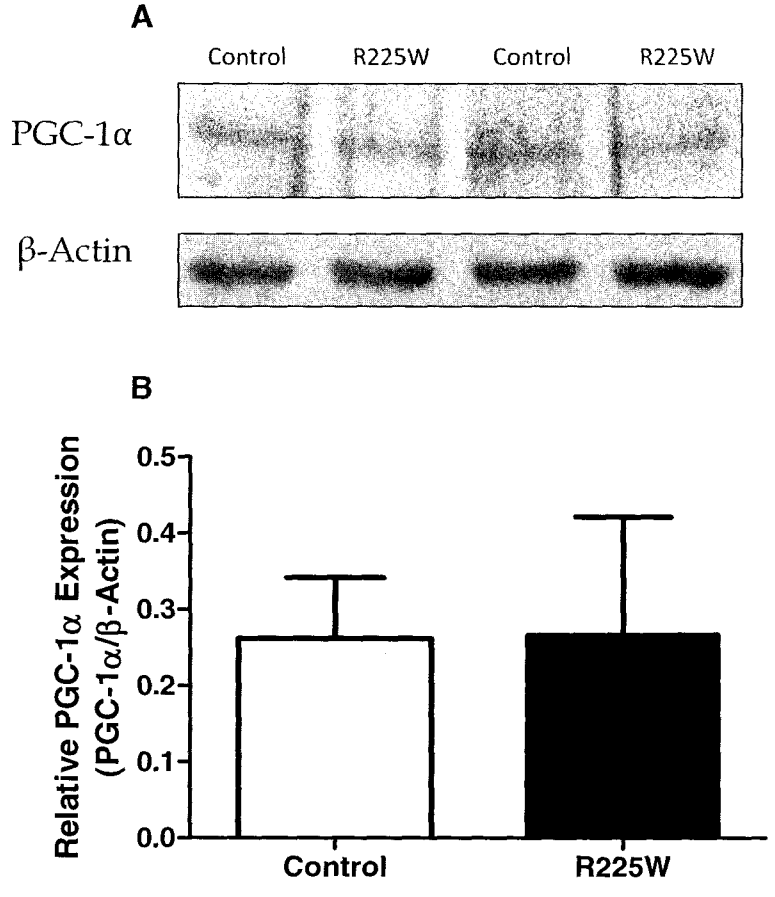

Figure 2-17: Manganese superoxide dismutase content. (A) Representative Western blot of mnSOD expression in control and R225W myotubes; (B) densitometry of mnSOD normalized to β-actin (C) densitometry of mnSOD normalized to succinate dehydrogenase (SDH), means ± SEM, paired student's t-test, NS

Figure 2-17: Manganese superoxide dismutase content

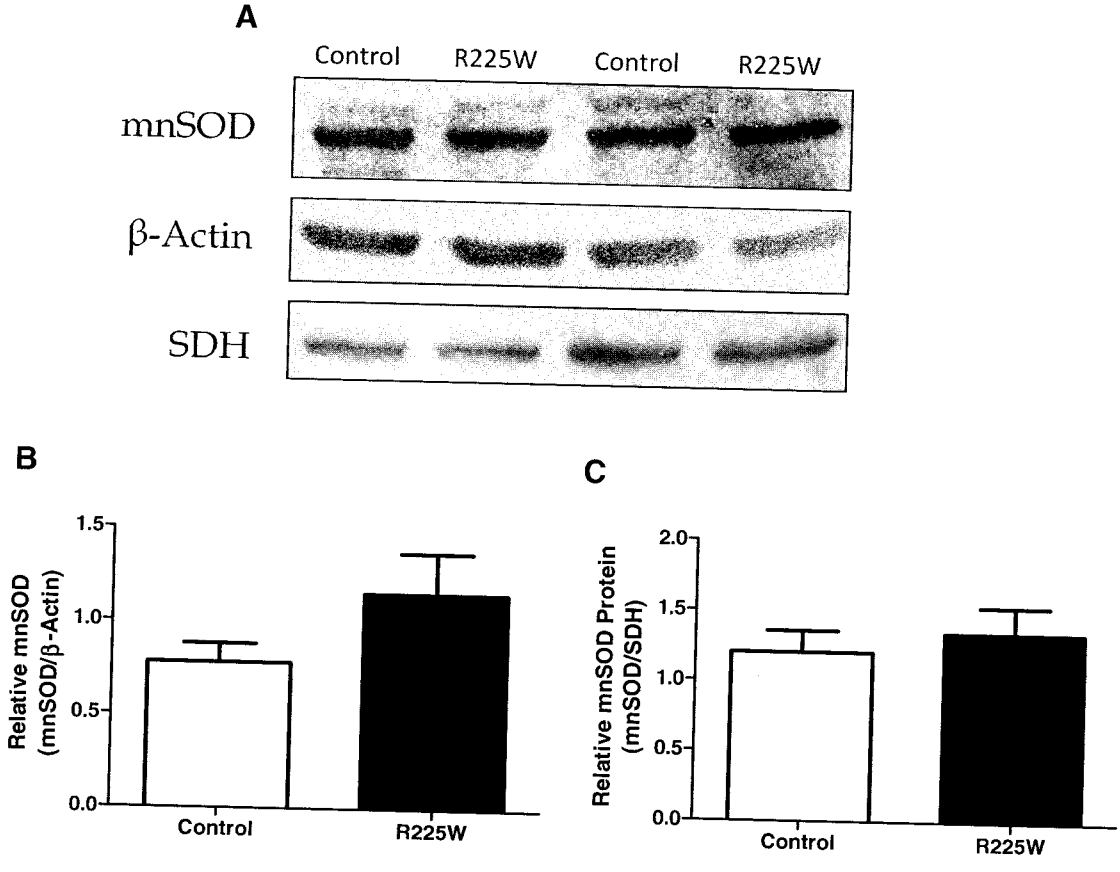

DISCUSSION

It is widely accepted that AMPK is an important regulator of cellular energy metabolism. Despite extensive characterization of acute AMPK activation in several models including mice and humans, the metabolic effects of chronic AMPK activation, especially in humans, are poorly understood. Our laboratory previously identified the AMPKγ3 R225W mutation in two probands within the Ottawa region and demonstrated a 2-fold increase in both the basal and AMP-stimulated AMPK activity in primary cultured myotubes from carriers of the R225W mutation compared to matched controls (33). *Ex vivo* histological analyses showed that R225W carriers had a 90% increase in skeletal muscle glycogen and a 30% decrease in intramuscular triglyceride (IMTG) stores compared to matched controls (33). The current study was designed to further characterize the skeletal muscle metabolism of these subjects both *in vivo* and *in vitro.*

While previous studies have documented enhanced glucose uptake in response to acute activation of AMPK either through exercise or treatment with the AMP mimetic, AICAR, in animal and cell culture models (38, 49, 50), these effects have not been previously evaluated *in vivo.* In this study, we sought to look at the effects of the AMPKγ3 R225W mutation on *in vivo* glucose uptake in both the resting and exercised quadriceps. Two of three R225W carriers exhibited a significantly larger volume of muscle actively taking up glucose (1.3-fold) as well as a trend for increased total glucose uptake in the exercised quadriceps. The remaining carrier of the AMPKγ3 R225W mutation exhibited extremely low levels of glucose uptake. This low level of glucose uptake is likely due, at least in part, to

abnormally elevated levels of serum cortisol, a potent inhibitor of skeletal muscle glucose uptake (51). This subject was not an outlier in any of the *in vitro* assays or in the muscular fatigue evaluations, suggesting that the increase in cortisol is a stress-related response to the PET scanning procedure.

No differences were observed in the resting leg. Levels of glucose uptake in fasted resting skeletal muscle are relatively low and PET scanning may not in fact be sensitive enough to detect potential low level changes in glucose uptake. The observed increase in plasma fatty acid mobilization during exercise in R225W carriers may indicate a more rapid transition to fatty acid oxidation, thereby blunting the observed glucose uptake in both the exercised and resting leg. Alternatively the increase in circulating fatty acids may be due to a normal mobilization of fatty acids (e.g., from adipose tissue stores), but a blunted increase in fatty acid uptake in muscle, stemming in turn from a greater proportional reliance on glucose and glycogen fuel stores in muscle of R225W subjects during fasting.

The mechanism behind the observed increase in glucose uptake in the R225W carriers during exercise is likely the result of elevated skeletal muscle GLUT4 expression, which has been previously demonstrated in mice chronically treated with AICAR (32). However, it is also possible that the observed increase in glucose is the result of the recruitment of a larger number of contractile fibers, as indicated by the increased volume of muscle actively taking up glucose. These results were further corroborated by the *in vitro* analysis of glucose uptake and glycogen synthesis in primary human myotubes. Differentiated myotubes from R225W carriers had 2-fold higher rates of glucose uptake as well glycogen-

synthesis relative to matched controls. There were no differences in insulin sensitivity as assessed by the absolute change in the rate of glucose uptake following insulin stimulation. These results suggest that AMPK-mediated glucose uptake is occurring through an insulin-independent pathway.

Paradoxical to the traditionally observed role of AMPK in the inhibition of anabolic pathways such as glycogen synthesis, carriers of the R225W mutation have increased intracellular glycogen stores. However, further AMPK activation through acute AICAR stimulation resulted in a decrease in glycogen levels in myotubes from both control and R225W carriers. The reduction in cellular glycogen content in both the controls and R225W carriers following acute AICAR treatment is likely the result of the direct phosphorylation of glycogen synthase kinase (52) by AMPK resulting in the inhibition of glycogen synthesis. The observed increase in basal glycogen storage on the other hand, is consistent with the increased rates of glycogen synthesis discussed above. During chronic AMPK activation, AMPK-stimulated glucose uptake may override AMPK's inhibition of glycogen synthase, resulting in enhanced glycogen storage. Similar effects of glycogen super-compensation have been previously observed in AICAR treated and endurance trained mice (32).

In vitro analysis of IMTG stores in differentiated myotubes from R225W carriers revealed a trend for a slight decrease in the total IMTG, which paralleled similar decreases in matched control subjects following acute AMPK activation with AICAR. This trend observed in differentiated human myotubes is consistent with previous *ex vivo* histological analyses of these subjects (33). In addition, acute activation of AMPK has been shown to result in the

phosphorylation and inactivation of acetyl CoA carboxylase (ACC), a key enzyme regulating the balance between fatty acid biosynthesis and oxidation (25, 53). ACC is the rate-limiting step in the synthesis of malonyl CoA, which is both a potent inhibitor of fatty acid oxidation and a key precursor in fatty acid synthesis. Inactivation of ACC leads to a decrease in fatty acid synthesis and a concomitant increase in fatty acid oxidation, which results in the depletion of IMTG stores (54, 55).

Consistent with AMPK's reported role in mitochondrial biogenesis through the induction of PGC-1α (23, 31), mitochondrial content and oxidative capacity was found to be significantly higher in the myotubes of R225W carriers than in myotubes of matched control subjects. While a trend for increased PGC-1α mRNA was observed in myotubes of R225W carriers, there were no differences in PGC-1α protein expression. However, despite no changes in protein expression, the activity of PGC-1α may be indirectly activated by AMPK. Jäger *et al.* showed that AMPK activation results in the phosphorylation of PGC-1α (23) and Canto *et al.* demonstrated that AMPK acts through the NAD^+ dependent deacetylase, SIRT1, to deacetylate and activate PGC-1α (56). Interestingly, while carriers of the R225W mutation expressed higher levels of AMPK phosphorylation relative to matched controls, expression of the catalytic alpha sub-unit was significantly down-regulated in the affected subjects. The observed down-regulation of AMPK in response to chronic activation suggests an important negative feedback mechanism involved in the regulation of AMPK.

Interestingly, the activity of citrate synthase per mitochondrion was increased in R225W carriers, suggesting enhanced TCA cycle capacity. While quantification of various TCA cycle

metabolites revealed a trend for a slight increase in the level of cellular citrate, there were no statistically significant changes in the levels of any of the analyzed TCA cycle metabolites. It is still reasonable to hypothesize that the elevated glucose uptake in myotubes of R225W subjects may be responsible for the increases in TCA cycle activity (e.g., to handle the influx of energy substrate). However, the lack of a corresponding increase in electron transport chain activity suggests that these metabolites are being diverted to alternative pathways. To further assess this question, future studies will need to examine the specific activities of additional TCA cycle enzymes and possibly glucose oxidation and fatty acid oxidation as well. One could also trace the flux of metabolites using universally labeled 13-C-glucose with mass spectrometry and NMR spectroscopy (57).

Carriers of the R225W mutation were shown to exhibit dramatically reduced rates of muscular fatigue, which is consistent with previous reports of increases in the time to 50% fatigue in mice with the analogous R225Q mutation (58). This increased capacity for endurance exercise is likely due to a combination of the increased glycogen content, glycogen synthesis rate and oxidative capacity (mitochondrial content etc) observed in R225W carriers. In fact, the increase in mean frequency of contraction observed in these individuals may also suggest that these individuals are recruiting additional contractile fibers to maintain this level of intense force output.

As a whole these results are consistent with the idea that the AMPKγ3 R225W mutation is largely beneficial to overall health and exercise performance capabilities of affected subjects. Findings demonstrate enhanced glucose uptake, oxidative capacity, and a delayed

onset of muscular fatigue. As a direct result of this mutation, these individuals likely have an enhanced capacity for endurance exercise. However, possibly of more importance is the protection from the development of T2DM that this mutation may confer through the enhancement of skeletal muscle glucose uptake in conjunction with increased mitochondrial content and oxidative capacity. These results suggest that the γ_3 subunit of AMPK may indeed make a suitable tissue-specific target for the treatment of T2DM.

REFERENCES

1. Hardie, D.G. 2008. AMPK: a key regulator of energy balance in the single cell and the whole organism. *Int J Obes (Lond)* 32 Suppl 4:S7-12.

2. Hawley, S.A., M. Davison, A. Woods, S.P. Davies, R.K. Beri, D. Carling, and D.G. Hardie. 1996. Characterization of the AMP-activated protein kinase kinase from rat liver and identification of threonine 172 as the major site at which it phosphorylates AMP-activated protein kinase. *J Biol Chem* 271:27879-27887.

3. Hudson, E.R., D.A. Pan, J. James, J.M. Lucocq, S.A. Hawley, K.A. Green, O. Baba, T. Terashima, and D.G. Hardie. 2003. A novel domain in AMP-activated protein kinase causes glycogen storage bodies similar to those seen in hereditary cardiac arrhythmias. *Curr Biol* 13:861-866.

4. Polekhina, G., A. Gupta, B.J. Michell, B. van Denderen, S. Murthy, S.C. Feil, I.G. Jennings, D.J. Campbell, L.A. Witters, M.W. Parker, B.E. Kemp, and D. Stapleton. 2003. AMPK beta subunit targets metabolic stress sensing to glycogen. *Curr Biol* 13:867-871.

5. McBride, A., S. Ghilagaber, A. Nikolaev, and D.G. Hardie. 2009. The glycogen-binding domain on the AMPK beta subunit allows the kinase to act as a glycogen sensor. *Cell Metab* 9:23-34.

6. Townley, R., and L. Shapiro. 2007. Crystal structures of the adenylate sensor from fission yeast AMP-activated protein kinase. *Science* 315:1726-1729.

7. Yeh, L.A., K.H. Lee, and K.H. Kim. 1980. Regulation of rat liver acetyl-CoA carboxylase. Regulation of phosphorylation and inactivation of acetyl-CoA carboxylase by the adenylate energy charge. *J Biol Chem* 255:2308-2314.

8. Davies, S.P., N.R. Helps, P.T. Cohen, and D.G. Hardie. 1995. 5'-AMP inhibits dephosphorylation, as well as promoting phosphorylation, of the AMP-activated protein kinase. Studies using bacterially expressed human protein phosphatase-2C alpha and native bovine protein phosphatase-2AC. *FEBS Lett* 377:421-425.

9. Sanders, M.J., P.O. Grondin, B.D. Hegarty, M.A. Snowden, and D. Carling. 2007. Investigating the mechanism for AMP activation of the AMP-activated protein kinase cascade. *Biochem J* 403:139-148.

10. Wojtaszewski, J.F., J.B. Birk, C. Frosig, M. Holten, H. Pilegaard, and F. Dela. 2005. 5'AMP activated protein kinase expression in human skeletal muscle: effects of strength training and type 2 diabetes. *J Physiol* 564:563-573.

11. Birk, J.B., and J.F. Wojtaszewski. 2006. Predominant alpha2/beta2/gamma3 AMPK activation during exercise in human skeletal muscle. *J Physiol* 577:1021-1032.

12. Mahlapuu, M., C. Johansson, K. Lindgren, G. Hjalm, B.R. Barnes, A. Krook, J.R. Zierath, L. Andersson, and S. Marklund. 2004. Expression profiling of the gamma-subunit isoforms of AMP-activated protein kinase suggests a major role for gamma3 in white skeletal muscle. *Am J Physiol Endocrinol Metab* 286:E194-200.

13. Wright, D.C., K.A. Hucker, J.O. Holloszy, and D.H. Han. 2004. Ca2+ and AMPK both mediate stimulation of glucose transport by muscle contractions. *Diabetes* 53:330-335.

14. Canto, C., A.V. Chibalin, B.R. Barnes, S. Glund, E. Suarez, J.W. Ryder, M. Palacin, J.R. Zierath, A. Zorzano, and A. Guma. 2006. Neuregulins mediate calcium-induced glucose transport during muscle contraction. *J Biol Chem* 281:21690-21697.

15. Hawley, S.A., D.A. Pan, K.J. Mustard, L. Ross, J. Bain, A.M. Edelman, B.G. Frenguelli, and D.G. Hardie. 2005. Calmodulin-dependent protein kinase kinase-beta is an alternative upstream kinase for AMP-activated protein kinase. *Cell Metab* 2:9-19.

16. Hawley, S.A., J. Boudeau, J.L. Reid, K.J. Mustard, L. Udd, T.P. Makela, D.R. Alessi, and D.G. Hardie. 2003. Complexes between the LKB1 tumor suppressor, STRAD alpha/beta and MO25 alpha/beta are upstream kinases in the AMP-activated protein kinase cascade. *J Biol* 2:28.

17. Sakamoto, K., A. McCarthy, D. Smith, K.A. Green, D. Grahame Hardie, A. Ashworth, and D.R. Alessi. 2005. Deficiency of LKB1 in skeletal muscle prevents AMPK activation and glucose uptake during contraction. *EMBO J* 24:1810-1820.

18. Carling, D., P.R. Clarke, V.A. Zammit, and D.G. Hardie. 1989. Purification and characterization of the AMP-activated protein kinase. Copurification of acetyl-CoA carboxylase kinase and 3-hydroxy-3-methylglutaryl-CoA reductase kinase activities. *Eur J Biochem* 186:129-136.

19. Ferrer, A., C. Caelles, and F.G. Hegardt. 1987. Reaction of 5'-p-fluorosulfonylbenzoyladenosine with the catalytic and AMP allosteric sites of microsomal HMG-CoA reductase kinase. *Biochem Biophys Res Commun* 148:1009-1016.

20. Shaw, R.J., M. Kosmatka, N. Bardeesy, R.L. Hurley, L.A. Witters, R.A. DePinho, and L.C. Cantley. 2004. The tumor suppressor LKB1 kinase directly activates AMP-activated kinase and regulates apoptosis in response to energy stress. *Proc Natl Acad Sci U S A* 101:3329-3335.

21. Hardie, D.G. 2007. AMP-activated/SNF1 protein kinases: conserved guardians of cellular energy. *Nat Rev Mol Cell Biol* 8:774-785.

22. Suwa, M., H. Nakano, and S. Kumagai. 2003. Effects of chronic AICAR treatment on fiber composition, enzyme activity, UCP3, and PGC-1 in rat muscles. *J Appl Physiol* 95:960-968.

23. Jager, S., C. Handschin, J. St-Pierre, and B.M. Spiegelman. 2007. AMP-activated protein kinase (AMPK) action in skeletal muscle via direct phosphorylation of PGC-1alpha. *Proc Natl Acad Sci U S A* 104:12017-12022.

24. Koistinen, H.A., D. Galuska, A.V. Chibalin, J. Yang, J.R. Zierath, G.D. Holman, and H. Wallberg-Henriksson. 2003. 5-amino-imidazole carboxamide riboside increases glucose transport and cell-surface GLUT4 content in skeletal muscle from subjects with type 2 diabetes. *Diabetes* 52:1066-1072.

25. Corton, J.M., J.G. Gillespie, and D.G. Hardie. 1994. Role of the AMP-activated protein kinase in the cellular stress response. *Curr Biol* 4:315-324.

26. Foretz, M., D. Carling, C. Guichard, P. Ferre, and F. Foufelle. 1998. AMP-activated protein kinase inhibits the glucose-activated expression of fatty acid synthase gene in rat hepatocytes. *J Biol Chem* 273:14767-14771.

27. Foretz, M., N. Ancellin, F. Andreelli, Y. Saintillan, P. Grondin, A. Kahn, B. Thorens, S. Vaulont, and B. Viollet. 2005. Short-term overexpression of a constitutively active form of AMP-activated protein kinase in the liver leads to mild hypoglycemia and fatty liver. *Diabetes* 54:1331-1339.

28. Leclerc, I., A. Kahn, and B. Doiron. 1998. The 5'-AMP-activated protein kinase inhibits the transcriptional stimulation by glucose in liver cells, acting through the glucose response complex. *FEBS Lett* 431:180-184.

29. Leclerc, I., C. Lenzner, L. Gourdon, S. Vaulont, A. Kahn, and B. Viollet. 2001. Hepatocyte nuclear factor-4alpha involved in type 1 maturity-onset diabetes of the young is a novel target of AMP-activated protein kinase. *Diabetes* 50:1515-1521.

30. Woods, A., D. Azzout-Marniche, M. Foretz, S.C. Stein, P. Lemarchand, P. Ferre, F. Foufelle, and D. Carling. 2000. Characterization of the role of AMP-activated protein kinase in the regulation of glucose-activated gene expression using constitutively active and dominant negative forms of the kinase. *Mol Cell Biol* 20:6704-6711.

31. Garcia-Roves, P.M., M.E. Osler, M.H. Holmstrom, and J.R. Zierath. 2008. Gain-of-function R225Q mutation in AMP-activated protein kinase gamma3 subunit increases mitochondrial biogenesis in glycolytic skeletal muscle. *J Biol Chem* 283:35724-35734.

32. Holmes, B.F., E.J. Kurth-Kraczek, and W.W. Winder. 1999. Chronic activation of 5'-AMP-activated protein kinase increases GLUT-4, hexokinase, and glycogen in muscle. *J Appl Physiol* 87:1990-1995.

33. Costford, S.R., N. Kavaslar, N. Ahituv, S.N. Chaudhry, W.S. Schackwitz, R. Dent, L.A. Pennacchio, R. McPherson, and M.E. Harper. 2007. Gain-of-function R225W mutation in human AMPKgamma3 causing increased glycogen and decreased triglyceride in skeletal muscle. *PLoS ONE* 2:e903.

34. Milan, D., J.T. Jeon, C. Looft, V. Amarger, A. Robic, M. Thelander, C. Rogel-Gaillard, S. Paul, N. Iannuccelli, L. Rask, H. Ronne, K. Lundstrom, N. Reinsch, J. Gellin, E. Kalm, P.L. Roy, P. Chardon, and L. Andersson. 2000. A mutation in PRKAG3 associated with excess glycogen content in pig skeletal muscle. *Science* 288:1248-1251.

35. Arad, M., D.W. Benson, A.R. Perez-Atayde, W.J. McKenna, E.A. Sparks, R.J. Kanter, K. McGarry, J.G. Seidman, and C.E. Seidman. 2002. Constitutively active AMP kinase mutations cause glycogen storage disease mimicking hypertrophic cardiomyopathy. *J Clin Invest* 109:357-362.

36. Gollob, M.H., J.J. Seger, T.N. Gollob, T. Tapscott, O. Gonzales, L. Bachinski, and R. Roberts. 2001. Novel PRKAG2 mutation responsible for the genetic syndrome of ventricular preexcitation and conduction system disease with childhood onset and absence of cardiac hypertrophy. *Circulation* 104:3030-3033.

37. Gollob, M.H., M.S. Green, A.S. Tang, T. Gollob, A. Karibe, A.S. Ali Hassan, F. Ahmad, R. Lozado, G. Shah, L. Fananapazir, L.L. Bachinski, and R. Roberts. 2001. Identification of a gene responsible for familial Wolff-Parkinson-White syndrome. *N Engl J Med* 344:1823-1831.

38. Mu, J., J.T. Brozinick, Jr., O. Valladares, M. Bucan, and M.J. Birnbaum. 2001. A role for AMP-activated protein kinase in contraction- and hypoxia-regulated glucose transport in skeletal muscle. *Mol Cell* 7:1085-1094.

39. Lochhead, P.A., I.P. Salt, K.S. Walker, D.G. Hardie, and C. Sutherland. 2000. 5-aminoimidazole-4-carboxamide riboside mimics the effects of insulin on the expression of the 2 key gluconeogenic genes PEPCK and glucose-6-phosphatase. *Diabetes* 49:896-903.

40. Fryer, L.G., A. Parbu-Patel, and D. Carling. 2002. The Anti-diabetic drugs rosiglitazone and metformin stimulate AMP-activated protein kinase through distinct signaling pathways. *J Biol Chem* 277:25226-25232.

41. Kubota, N., Y. Terauchi, T. Kubota, H. Kumagai, S. Itoh, H. Satoh, W. Yano, H. Ogata, K. Tokuyama, I. Takamoto, T. Mineyama, M. Ishikawa, M. Moroi, K. Sugi, T. Yamauchi, K. Ueki, K. Tobe, T. Noda, R. Nagai, and T. Kadowaki. 2006. Pioglitazone ameliorates insulin resistance and diabetes by both adiponectin-dependent and -independent pathways. *J Biol Chem* 281:8748-8755.

42. Ronnett, G.V., S. Ramamurthy, A.M. Kleman, L.E. Landree, and S. Aja. 2009. AMPK in the brain: its roles in energy balance and neuroprotection. *J Neurochem* 109 Suppl 1:17-23.

43. Nissen, S.E., S.J. Nicholls, K. Wolski, D.C. Howey, E. McErlean, M.D. Wang, E.V. Gomez, and J.M. Russo. 2007. Effects of a potent and selective PPAR-alpha agonist in patients with atherogenic dyslipidemia or hypercholesterolemia: two randomized controlled trials. *JAMA* 297:1362-1373.

44. Hardie, D.G. 2008. Role of AMP-activated protein kinase in the metabolic syndrome and in heart disease. *FEBS Lett* 582:81-89.

45. Folch, J., M. Lees, and G.H. Sloane Stanley. 1957. A simple method for the isolation and purification of total lipides from animal tissues. *J Biol Chem* 226:497-509.

46. McIntyre, E.A., R. Halse, S.J. Yeaman, and M. Walker. 2004. Cultured muscle cells from insulin-resistant type 2 diabetes patients have impaired insulin, but normal 5-amino-4-imidazolecarboxamide riboside-stimulated, glucose uptake. *J Clin Endocrinol Metab* 89:3440-3448.

47. Wensaas, A.J., A.C. Rustan, K. Lovstedt, B. Kull, S. Wikstrom, C.A. Drevon, and S. Hallen. 2007. Cell-based multiwell assays for the detection of substrate accumulation and oxidation. *J Lipid Res* 48:961-967.

48. Steinberg, G.R., S.L. Macaulay, M.A. Febbraio, and B.E. Kemp. 2006. AMP-activated protein kinase--the fat controller of the energy railroad. *Can J Physiol Pharmacol* 84:655-665.

49. Hayashi, T., M.F. Hirshman, E.J. Kurth, W.W. Winder, and L.J. Goodyear. 1998. Evidence for 5' AMP-activated protein kinase mediation of the effect of muscle contraction on glucose transport. *Diabetes* 47:1369-1373.

50. Kurth-Kraczek, E.J., M.F. Hirshman, L.J. Goodyear, and W.W. Winder. 1999. 5' AMP-activated protein kinase activation causes GLUT4 translocation in skeletal muscle. *Diabetes* 48:1667-1671.

51. Curry, D.L., and L.L. Bennett. 1973. Dynamics of insulin release by perfused rat pancreases: effects of hypophysectomy, growth hormone, adrenocorticotropic hormone, and hydrocortisone. *Endocrinology* 93:602-609.

52. Horike, N., H. Sakoda, A. Kushiyama, H. Ono, M. Fujishiro, H. Kamata, K. Nishiyama, Y. Uchijima, Y. Kurihara, H. Kurihara, and T. Asano. 2008. AMP-activated protein kinase activation increases phosphorylation of glycogen synthase kinase 3beta and thereby reduces cAMP-responsive element transcriptional activity and phosphoenolpyruvate carboxykinase C gene expression in the liver. *J Biol Chem* 283:33902-33910.

53. Henin, N., M.F. Vincent, H.E. Gruber, and G. Van den Berghe. 1995. Inhibition of fatty acid and cholesterol synthesis by stimulation of AMP-activated protein kinase. *FASEB J* 9:541-546.

54. Velasco, G., M.J. Geelen, and M. Guzman. 1997. Control of hepatic fatty acid oxidation by 5'-AMP-activated protein kinase involves a malonyl-CoA-dependent and a malonyl-CoA-independent mechanism. *Arch Biochem Biophys* 337:169-175.

55. Brusq, J.M., N. Ancellin, P. Grondin, R. Guillard, S. Martin, Y. Saintillan, and M. Issandou. 2006. Inhibition of lipid synthesis through activation of AMP kinase: an additional mechanism for the hypolipidemic effects of berberine. *J Lipid Res* 47:1281-1288.

56. Canto, C., Z. Gerhart-Hines, J.N. Feige, M. Lagouge, L. Noriega, J.C. Milne, P.J. Elliott, P. Puigserver, and J. Auwerx. 2009. AMPK regulates energy expenditure by modulating NAD+ metabolism and SIRT1 activity. *Nature* 458:1056-1060.

57. Fan, T.W., M. Kucia, K. Jankowski, R.M. Higashi, J. Ratajczak, M.Z. Ratajczak, and A.N. Lane. 2008. Rhabdomyosarcoma cells show an energy producing anabolic metabolic phenotype compared with primary myocytes. *Mol Cancer* 7:79.

58. Barnes, B.R., S. Glund, Y.C. Long, G. Hjalm, L. Andersson, and J.R. Zierath. 2005. 5'-AMP-activated protein kinase regulates skeletal muscle glycogen content and ergogenics. *FASEB J* 19:773-779.

General Discussion

The prevalence of metabolic diseases including obesity and T2DM is increasing worldwide at an unprecedented pace. With 1.7 billion overweight or obese people and 176 million people suffering from T2DM, the fundamental understanding of the molecular mechanisms underlying these diseases is essential to the development of new therapeutics and treatment strategies (1, 2). As obesity is the primary risk factor for T2DM and 85% of individuals with T2DM are overweight or obese, the relationship between obesity and T2DM is of particular interest. Nevertheless it is important to note that only ~35% of overweight or obese individuals have T2DM (3, 4). Extensive research over the last decade has dramatically improved our understanding of the mechanisms underpinning T2DM. However, the defects in molecular metabolism that may predispose obese individuals to the development of T2DM are still poorly understood.

Metabolic Deficits – A Genetic Predisposition to Type 2 Diabetes Mellitus

To better understand the mechanistic association between obesity and T2DM, we compared the skeletal muscle metabolism of subjects with or without a history of obesity-associated T2DM. One of the primary deficits observed in primary myotubes from individuals with a history of obesity-associated diabetes was the inability of myotubes to undergo mitochondrial biogenesis in response to conditions of high glucose and insulin (HGI). Previous studies have demonstrated lower mitochondrial content concurrent with elevated levels of IMTG in the skeletal muscle of individuals with T2DM and their insulin-resistant offspring (5-8). However, the presence of reduced mitochondrial biogenesis in

subjects with a history of T2DM in the absence of elevated IMTG content lends support to the hypothesis that defects in mitochondrial function precede the accumulation of IMTG in skeletal muscle.

Myotubes from post-DM individuals also exhibited increased oxidative damage under hyperglycemic conditions. Moreover, expression of the mitochondrial ROS scavenger, mnSOD, was higher in Post-DM myotubes compared to Non-DM myotubes in the both basal state and under HGI conditions. The elevation in basal mnSOD expression in Post-DM individuals suggests elevated production of reactive oxygen species. However, when subjected to the stress of HGI, the cellular antioxidant mechanisms in Post-DM myotubes were not able to cope with the additional production of ROS, resulting in increased oxidative damage in these individuals. Interestingly, despite the oxidative damage generated in Post-DM cells, it appears as though this signal is not able to activate UCP3 to affect a lower membrane potential and ultimately decrease ROS production.

While both mitochondrial content and oxidative stress have been closely associated with insulin resistance and T2DM in skeletal muscle, this study demonstrated for the first time that impaired metabolism can be re-elicited in skeletal muscle cells from subjects with history of obesity-associated T2DM, despite the resolution of the clinical symptoms of T2DM through weight loss. These results provide further insight into the metabolic mechanisms and deficits that may predispose individuals to the development of T2DM; however, it remains to be determined whether the observed metabolic characteristics are genetic or whether they are acquired epigenetically during the development of T2DM (9).

Future studies will need to further characterize the mechanisms underlying the high glucose and insulin mediated mitochondrial biogenesis, in order to begin to understand the molecular defect that prevents individuals with a history of type 2 diabetes from undergoing similar mitochondrial biogenesis. In addition, further investigations will also need to characterize the potential role of UCP3 in mitigating the high glucose and insulin induced oxidative damage through the reduction of membrane potential.

AMP-Activated Protein Kinase as a Pharmaceutical Target

Currently, the American Diabetes Association guidelines for the treatment of T2DM recommend the screening and treatment of individuals at high risk for the development of diabetes through a combination of weight loss, physical activity, and in some cases, the initiation of anti-hyperglycemic pharmaceutical agents (10). While the most effective treatment remains lifestyle modification, delaying or preventing the onset of T2DM through weight loss and physical activity has become increasingly difficult for many individuals (11). Weight loss has proven to be very effective in improving glucose uptake and restoring insulin sensitivity (12); however, the ready availability of calorie-dense foods and the sedentary culture that has become so prevalent in Western society make weight loss a challenge for many individuals.

The rapid increase in the prevalence of obesity and T2DM over the last several decades and the aforementioned difficulties in the treatment of T2DM through lifestyle intervention have created a pressing need for safe and effective pharmacological therapies. Current pharmacological treatment options for T2DM include metformin, sulfonylureas, DPP-4

inhibitors, PPARγ agonists, α-glucosidase inhibitors, insulin, and GLP-1 analogs. However, many of these drugs have not only efficacy and durability issues, but also side effects including hypoglycemia, weight gain, edema, fractures, lactic acidosis, and gastrointestinal intolerance (reviewed in (13, 14)). In the last several years, AMPK has emerged as a prime pharmacological target for the treatment of T2DM. Of the current anti-hyperglycemic agents available, it is thought that metformin indirectly activates AMPK through its upstream kinase LKB1 (15-17), whereas the PPARγ agonists rosiglitazone and pioglitazone activate AMPK primarily through the induction of adiponectin release (18-20). Adiponectin induces the phosphorylation and activation of AMPK in target tissues including liver and skeletal muscle (21, 22). However, metformin and the TZDs are systemic activators of AMPK and may lead to undesirable side effects through the chronic activation of AMPK in tissues such as the hypothalamus, heart and gastrointestinal tract (reviewed in (14)).

The negative effects associated with chronic systemic AMPK activation make the development of tissue-specific AMPK agonists an attractive alternative. As discussed previously, AMPK's role in suppressing hepatic glucose output while increasing skeletal muscle glucose uptake and fatty acid oxidation make liver and skeletal muscle the two tissues that would likely contribute the most to the suppression of plasma glucose levels and the restoration of insulin sensitivity (reviewed in (13)). The current study examined the metabolic effects of a naturally occurring gain-of-function mutation in the γ3 subunit of AMPK in humans, which is of special interest due to its almost exclusive expression in skeletal muscle.

The AMPKγ3 R225W mutation resulted in significantly increased skeletal muscle glucose uptake *in vitro* in primary myotubes as well as a trend for increased glucose uptake *in vivo*. Additionally, this increase in glucose uptake appeared to be mediated through an insulin-independent pathway as the effect of insulin on glucose uptake appeared to be additive. Myotubes from these subjects also exhibited significantly elevated levels of glycogen, consistent with the chronically enhanced glucose uptake in these subjects. While there was a small trend for decreased IMTG *in vitro*, carriers of the R225W mutation exhibited a greater relative increase in plasma fatty acids during exercise compared with matched controls. This increase in FFA could be the result of decreased skeletal muscle fatty acid uptake or it could be the result of an increased mobilization of fatty acids from adipose tissue.

Of most interest, however, were the increases in oxidative capacity observed in primary myotubes from carriers of the R225W mutation. R225W carriers exhibited increased maximal cytochrome c oxidase and citrate synthase activity as well as increased maximal oxygen consumption. Mitochondrial dysfunction is one of the most likely candidates in the development of insulin resistance in skeletal muscle. As discussed previously, reduced mitochondrial content has been observed in individuals with T2DM, as well as in lean insulin-resistant offspring of individuals with T2DM (5-8). It is likely that these mitochondrial defects contribute to incomplete fatty acid oxidation, increased IMTG, increased ROS damage, and ultimately the development of insulin resistance.

While future studies will be needed to further evaluate other metabolic aspects of this mutation, including determinations of fatty acid oxidation and metabolic flexibility, the human AMPKγ3 R225W mutation has proven to be an excellent model for the evaluation of chronic AMPK activation in skeletal muscle. In addition, the current results suggest that the γ_3 subunit of AMPK may indeed make a suitable tissue-specific target for the treatment of T2DM. Two of the most important traits of an effective pharmaceutical agent for the treatment of T2DM are the ability to reliably and effectively reduce circulating glucose levels while enhancing insulin-sensitivity. We have demonstrated that the AMPKγ_3 R225W mutation enhances both glucose uptake and mitochondrial biogenesis. The stimulation of AMPKγ_3 may therefore lead to improved glycemic control in individuals with T2DM.

REFERENCES

1. James, P.T., N. Rigby, and R. Leach. 2004. The obesity epidemic, metabolic syndrome and future prevention strategies. *Eur J Cardiovasc Prev Rehabil* 11:3-8.

2. Wild, S., G. Roglic, A. Green, R. Sicree, and H. King. 2004. Global prevalence of diabetes: estimates for the year 2000 and projections for 2030. *Diabetes Care* 27:1047-1053.

3. Control, C.f.D. 2004. National Health and Examination Survey. *CDC*

4. Finkelstein, M.M. 2008. The prevalence of diabetes among overweight and obese individuals is higher in poorer than in richer neighbourhoods. *Canadian Journal of Diabetes* 32:190.

5. Morino, K., K.F. Petersen, S. Dufour, D. Befroy, J. Frattini, N. Shatzkes, S. Neschen, M.F. White, S. Bilz, S. Sono, M. Pypaert, and G.I. Shulman. 2005. Reduced mitochondrial density and increased IRS-1 serine phosphorylation in muscle of insulin-resistant offspring of type 2 diabetic parents. *J Clin Invest* 115:3587-3593.

6. Petersen, K.F., S. Dufour, D. Befroy, R. Garcia, and G.I. Shulman. 2004. Impaired mitochondrial activity in the insulin-resistant offspring of patients with type 2 diabetes. *N Engl J Med* 350:664-671.

7. Kelley, D.E., J. He, E.V. Menshikova, and V.B. Ritov. 2002. Dysfunction of mitochondria in human skeletal muscle in type 2 diabetes. *Diabetes* 51:2944-2950.

8. Ritov, V.B., E.V. Menshikova, J. He, R.E. Ferrell, B.H. Goodpaster, and D.E. Kelley. 2005. Deficiency of subsarcolemmal mitochondria in obesity and type 2 diabetes. *Diabetes* 54:8-14.

9. Levin, B.E. 2008. Epigenetic influences on food intake and physical activity level: review of animal studies. *Obesity (Silver Spring)* 16 Suppl 3:S51-54.

10. 2008. Standards of medical care in diabetes--2008. *Diabetes Care* 31 Suppl 1:S12-54.

11. Orchard, T.J., M. Temprosa, R. Goldberg, S. Haffner, R. Ratner, S. Marcovina, and S. Fowler. 2005. The effect of metformin and intensive lifestyle intervention on the metabolic syndrome: the Diabetes Prevention Program randomized trial. *Ann Intern Med* 142:611-619.

12. Hoecker, C., M. Nelle, B. Beedgen, J. Rengelshausen, and O. Linderkamp. 2006. Effects of a divided high loading dose of caffeine on circulatory variables in preterm infants. *Arch Dis Child Fetal Neonatal Ed* 91:F61-64.

13. Zhang, B.B., G. Zhou, and C. Li. 2009. AMPK: an emerging drug target for diabetes and the metabolic syndrome. *Cell Metab* 9:407-416.

14. Nathan, D.M., J.B. Buse, M.B. Davidson, E. Ferrannini, R.R. Holman, R. Sherwin, and B. Zinman. 2009. Medical management of hyperglycemia in type 2 diabetes: a consensus algorithm for the initiation and adjustment of therapy: a consensus statement of the American Diabetes Association and the European Association for the Study of Diabetes. *Diabetes Care* 32:193-203.

15. Zhou, G., R. Myers, Y. Li, Y. Chen, X. Shen, J. Fenyk-Melody, M. Wu, J. Ventre, T. Doebber, N. Fujii, N. Musi, M.F. Hirshman, L.J. Goodyear, and D.E. Moller. 2001. Role of AMP-activated protein kinase in mechanism of metformin action. *J Clin Invest* 108:1167-1174.

16. Shaw, R.J., K.A. Lamia, D. Vasquez, S.H. Koo, N. Bardeesy, R.A. Depinho, M. Montminy, and L.C. Cantley. 2005. The kinase LKB1 mediates glucose homeostasis in liver and therapeutic effects of metformin. *Science* 310:1642-1646.

17. Musi, N., M.F. Hirshman, J. Nygren, M. Svanfeldt, P. Bavenholm, O. Rooyackers, G. Zhou, J.M. Williamson, O. Ljunqvist, S. Efendic, D.E. Moller, A. Thorell, and L.J. Goodyear. 2002. Metformin increases AMP-activated protein kinase activity in skeletal muscle of subjects with type 2 diabetes. *Diabetes* 51:2074-2081.

18. LeBrasseur, N.K., M. Kelly, T.S. Tsao, S.R. Farmer, A.K. Saha, N.B. Ruderman, and E. Tomas. 2006. Thiazolidinediones can rapidly activate AMP-activated protein kinase in mammalian tissues. *Am J Physiol Endocrinol Metab* 291:E175-181.

19. Ye, J.M., N. Dzamko, A.J. Hoy, M.A. Iglesias, B. Kemp, and E. Kraegen. 2006. Rosiglitazone treatment enhances acute AMP-activated protein kinase-mediated muscle and adipose tissue glucose uptake in high-fat-fed rats. *Diabetes* 55:2797-2804.

20. Kubota, N., Y. Terauchi, T. Kubota, H. Kumagai, S. Itoh, H. Satoh, W. Yano, H. Ogata, K. Tokuyama, I. Takamoto, T. Mineyama, M. Ishikawa, M. Moroi, K. Sugi, T. Yamauchi, K. Ueki, K. Tobe, T. Noda, R. Nagai, and T. Kadowaki. 2006. Pioglitazone ameliorates insulin resistance and diabetes by both adiponectin-dependent and -independent pathways. *J Biol Chem* 281:8748-8755.

21. Yamauchi, T., J. Kamon, Y. Minokoshi, Y. Ito, H. Waki, S. Uchida, S. Yamashita, M. Noda, S. Kita, K. Ueki, K. Eto, Y. Akanuma, P. Froguel, F. Foufelle, P. Ferre, D. Carling, S. Kimura, R. Nagai, B.B. Kahn, and T. Kadowaki. 2002. Adiponectin stimulates glucose utilization and fatty-acid oxidation by activating AMP-activated protein kinase. *Nat Med* 8:1288-1295.

22. Andreelli, F., M. Foretz, C. Knauf, P.D. Cani, C. Perrin, M.A. Iglesias, B. Pillot, A. Bado, F. Tronche, G. Mithieux, S. Vaulont, R. Burcelin, and B. Viollet. 2006. Liver adenosine monophosphate-activated kinase-alpha2 catalytic subunit is a key target for the control of hepatic glucose production by adiponectin and leptin but not insulin. *Endocrinology* 147:2432-2441.